

## CHAPTER 2 TOPOGRAPHY AND GEOLOGY IN PILOT REGION

### 2.1 Kabupaten Jember

#### 2.1.1 Landform of Kabupaten Jember

The following mountains are located in Kabupaten Jember: the Argopuro mountain (highest point of altitude 3,072m) in the north, and the Raung mountain (highest point of altitude 3,328m) to the northeast, while in the south the South-eastern Mountains (highest point of altitude 1,223m) extend east to west. The lowlands are spread in the southwest of the province, surrounded by Argopuro mountain, Raung mountain and the Southern Mountains.

Kabupaten Jember can be divided into 4 landforms (Figure 2.1.1). The characteristics of each landform province are given below.

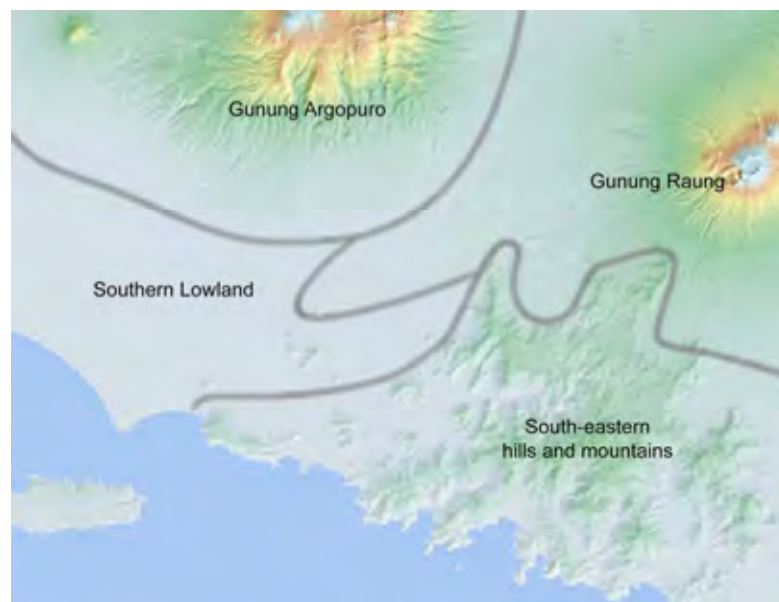


**Figure 2.1.1 Geomorphological Divisions in Jember**

##### 1) South-eastern lowland

The lowlands extend through the central west of Kabupaten Jember at an elevation 0-50m above sea level.

The fluvial plain in the central area is made up of the Bedadung river and its tributaries. The western area is comprised of a fluvial plain of sediment from the Malang and Bondoyudan rivers that flow down from Argopuro mountain. Many tributaries and irrigation channels branch out from the river mid-downstream.

The Bedadung river that runs along the central part of Jember city is mixed with edifice collapse deposits from Raung mountain and Argopuro mountain, (see below), and debris from the dissected valleys. This deep valley profile across the Bedadung river and a 7~8m high erosion plane from the riverbed was formed from a portion of the surrounding plateau where a large number of homes have been built.

On the ocean side of the coastal plane, one sees sand dunes of approximately 10 m in height, and further inland is a sand bar of approximately 5 to 9m in elevation. The sand dunes form a virtual chain from Pugur to Paseban.

## **2) Raung mountain slope**

The western slope of the Raung mountain is part of Kabupaten Jember. A large, horseshoe shaped edifice collapse slope is featured on the western face of Raung mountain, with several mounds at its base. The mounds (Gemuk) that are distributed at the western base of Raung mountain are known as the Ten thousand hills, or Bukit Sepuluh Ribu. The western-most mound (Gemuk) is Kecamatan Balung, which lies approximately 40km from the summit of Raung mountain.

Mount Panjungan (2,367m) is a conical volcano that was formed at the top of the edifice collapse slope, from which the volcanic ejecta is deposited in the vicinity at 400m above sea-level (near Sumberjambe).

## **3) Argopuro mountain slope**

The southern slope of Argopuro mountain is part of Kabupaten Jember. The summit of Argopuro mountain features 5 distinct cones; the southern slope is the old volcano slope. The southeast slope of Argopuro mountain is dissected by several valleys so one can see the collapsed slope and deep valley. A representative valley is being devastated by the Karangbayat river, Klatakan river, Kali Putih river, and Kemiri (Jompo) river from the west, which all produce a large amount of deposits forming an alluvial fan at the foot of the volcano and a debris flow terrace.

Old alluvial fans surrounding the Argopuro mountain slope are the hills at an elevation of 400~500m.

## **4) South-eastern mountains “Meru Betiri Mountains”**

A hill and mountain range stretches across the southern part of Kabupaten Jember and Kabupaten Banyuwangi at 50~1,200m above sea-level. The mountain range itself reaches 50km across east to west, or 90km including the distant hills. It is approximately 40km in length from north to south. The ridge, which extends irregularly, is a lineament resembling a fault landform and is hardly visible. The north and west sections of the southeastern mountains are buried in volcanic ejecta. In addition, the southern part faces directly with the sea forming the Rias coast. Nusabarong island is a karst plateau which consists of limestone at an altitude of 200~300m.

## 2.1.2 Geology of Kabupaten Jember

The stratigraphy of this region is a unit from the Holocene period to Late Oligocene.

Table 2.1.1 shows the geology of Kabupaten Jember.

**Table 2.1.1 Geology of Kabupaten Jember**

Geologic Age	Geology	Rock Type and Stratigraphy
Quaternary	Alluvial Deposits	Fluvial deposit
		Marine deposit
		Debris flow deposit
	Volcanic Products	Volcanic ash and thick Laterite
		Edifice collapse deposit of Raung volcano
		Pyroclastic rock of Raung volcano
Tertiary		Pyroclastic rock of Argopuro volcano
		Mandalika formation
		Puger formation
		Granodiorite and Dioraite
		Limestone member of Merubetiri formation
		Sukumade formation
		Merubetiri formation
	Batuampar formation	

The oldest geology of this region is tertiary sedimentary rock which is distributed at 200~1200m in elevation in the southeastern mountains. Here one also finds deposits from Oligocene to Miocene of clay stone, sandstone, tuffaceous sand, and limestone. The stones are consolidated, but weathering of the surface is advanced.

Following the sedimentary rocks of the south-eastern mountains is volcanic ejecta of Argopuro mountain. The periods differ according to the distribution area of the volcanic ejecta of Argopuro mountain. As for the volcanic body, the west side is old and the foot of the mountain is also dissected by a small valley, and thick latosol has formed. On the east side of the mountain body lava and pyroclastic material are exposed parallel along the valley. Several deep valleys have formed at the southern slope of Argopuro mountain, and debris and clay from the valley has formed an old alluvial fan. Since a large-scale alluvial fan is part of the Kalatakan river, thick alluvial fan sediment has been distributed.

Raung mountain is newer than Argopuro volcano, and is presently active. On the west side slope on the side of Kabupaten Jember, one may observe the continuity of the edifice collapse deposit which runs parallel to the Bedadung river through central Jember. The edifice collapse deposit is approximately 15m thick with andesite rounded particles of 20cm~50cm and a matrix of lithic sand from the riverbed. Also, boulders that exceed 3m in diameter can be seen in the riverbed. The outcrop conditions are hardly favorable, as the sediment is disorderly, and the bedding structure is difficult to see.

The volcanic ash source latosol covers the ground at the base of Raung mountain and Argopuro mountain. The thickness of the latosol is over 5m. When latosol is dried, it is relatively hard, but when water is included, it becomes loose and easily deteriorates.



**Photo 2.1.1      Latosol at Kecamatan Panti**

### **2.1.3    Ground Type Classification and Soil Types**

#### **1)    Collection of related data**

Topography maps (1:25,000 scale), aerial photos (1:50,000 scale, 1993), geological maps (1:100,000 scale) and borehole data have been collected for the topography/geological analysis. The borehole data was collected via PU, and thus all data is according to bridge construction.

**Table 2.1.2      Collected Borehole Data**

Map Number and Map Name	Number of Sites	Number of Boreholes
1607-523 Kencong	2	4
1607-542 Tanggul	2	4
1607-552 Getem	2	4
1607-631 Rampipuji	3	6
1607-632 Jember	3	6

#### **2)    Ground Condition Mapping**

Ground Condition Map is used for seismic hazard mapping and sediment related disaster hazard mapping. These are different from usual geological survey maps as they consider the soil and geological features, assess the type and likelihood of a disaster and are suitably classified. There

were 18 classifications of ground type in Kabupaten Jember. Of the 18 ground types, tertiary rocks are counted as one group for ground movement estimations so that 13 types are considered.

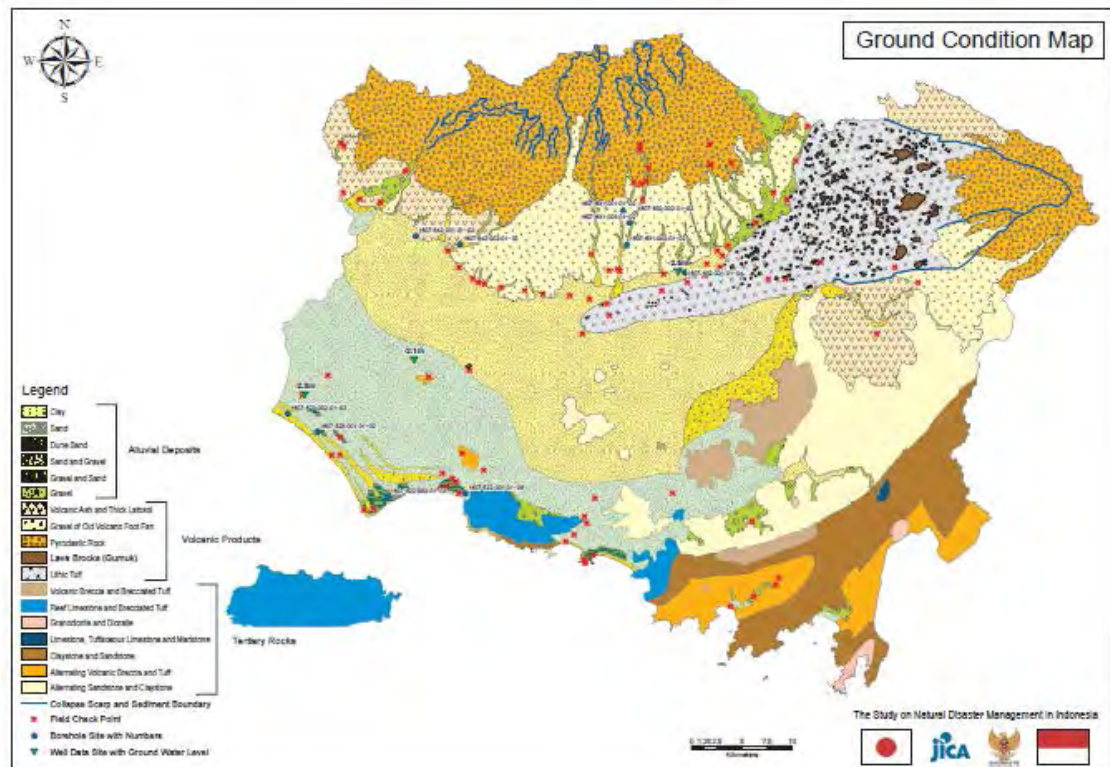
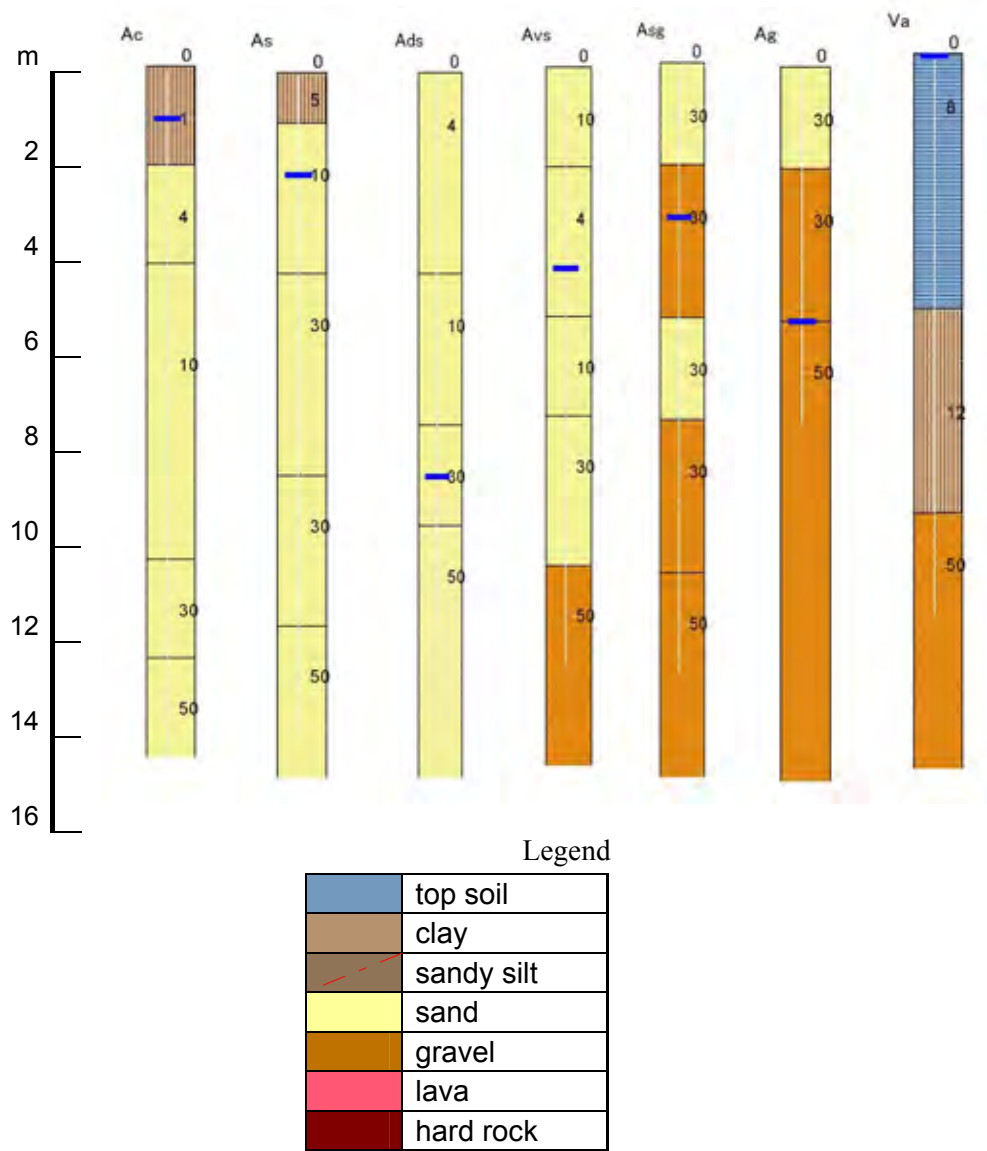


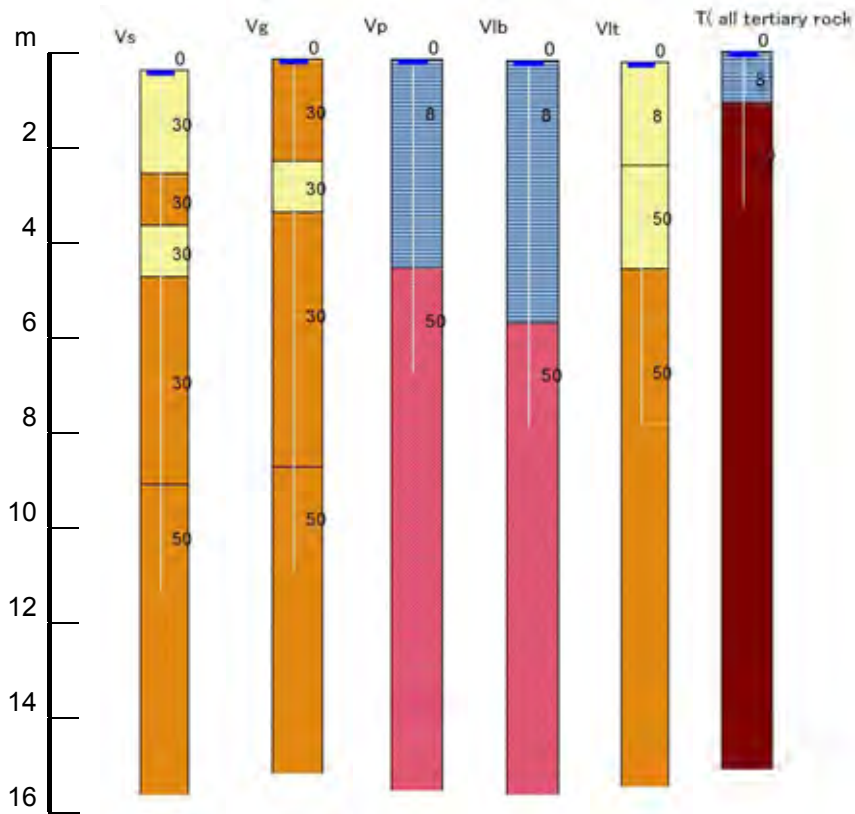
Figure 2.1.2 Ground Condition Map

### 3) Creation of Simplified Geologic Column

To estimate earthquake ground motion, we examined the simplified geologic columns of the above-mentioned 13 ground types and physical properties of each soil and geological feature respectively. The results of the Standard Penetration Test were shown in the borehole data that was collected, and based on that and using case examples from Japan, we estimated the Average Standard Penetration Test Value, density, and S-wave velocity.



**Figure 2.1.3 Simplified Geologic Column for Seismic Analysis (1)**



Legend

	top soil
	clay
	sandy silt
	sand
	gravel
	lava
	hard rock

Number : Value of Standard Penetration Test

**Figure 2.1.4 Simplified Geologic Column for Seismic Analysis (2)**

**Table 2.1.3 Physical Values of Soil and Rock Type**

Geological time		Soil and Geology	Symbol	Physical Value			
				Range of Standard penetration test value	Average Standard penetration test value	Density (g/cm <sup>3</sup> )	S-wave velocity (m/s)
Quaternary	Recent	Clay	Ac1	0 to 3	1	1.5	120
			Ac2	3 to 10	5	1.6	180
		Sand	As1	1 to 8	4	1.7	150
			As2	8 to 20	10	1.8	190
			As3	20 and more	30	1.8	250
		Gravel	Ag	10 to 50	30	2.0	270
	Latosol	Lm	5 to 10	8	1.6	190	
	Pleistocene	Clay	Dc1	2 to 8	4	1.6	190
			Dc2	8 to 20	12	1.7	250
			Dc3	20 and more	25	1.8	320
		Sand	Ds1	1 to 15	8	1.8	200
			Ds2	15 to 50	30	1.8	250
			Ds3	More than 50	50	1.9	400
		Gravel	Dg1	Less than 50	30	2.0	350
			Dg2	More than 50	50	2.1	500
		Volcanic gravel	Vg	More than 50	50	2.1	500
		Recent and Pleistocene	Lava	Lv	More than 50	50	2.1
	Tertiary	Hard rock	T	More than 50	50	2.2	1500

### 2.1.4 Target Earthquakes in Kabupaten Jember

We examined target earthquakes from the historical earthquake disaster record, past seismic activity, and tectonic background. In the Java Island sea, subduction of the Indian Ocean-Australian plate under the Eurasia plate is continuing at a relative speed of approximately 6~7cm/yr. In the Java Island sea, the asymmetry of the plate boundaries according to the relative movement between the plates is cancelled out by non seismic slip or any earthquake of M7~8, so that even looking back at the historical earthquake disaster record, interplate earthquakes exceeding M8 have been unknown.

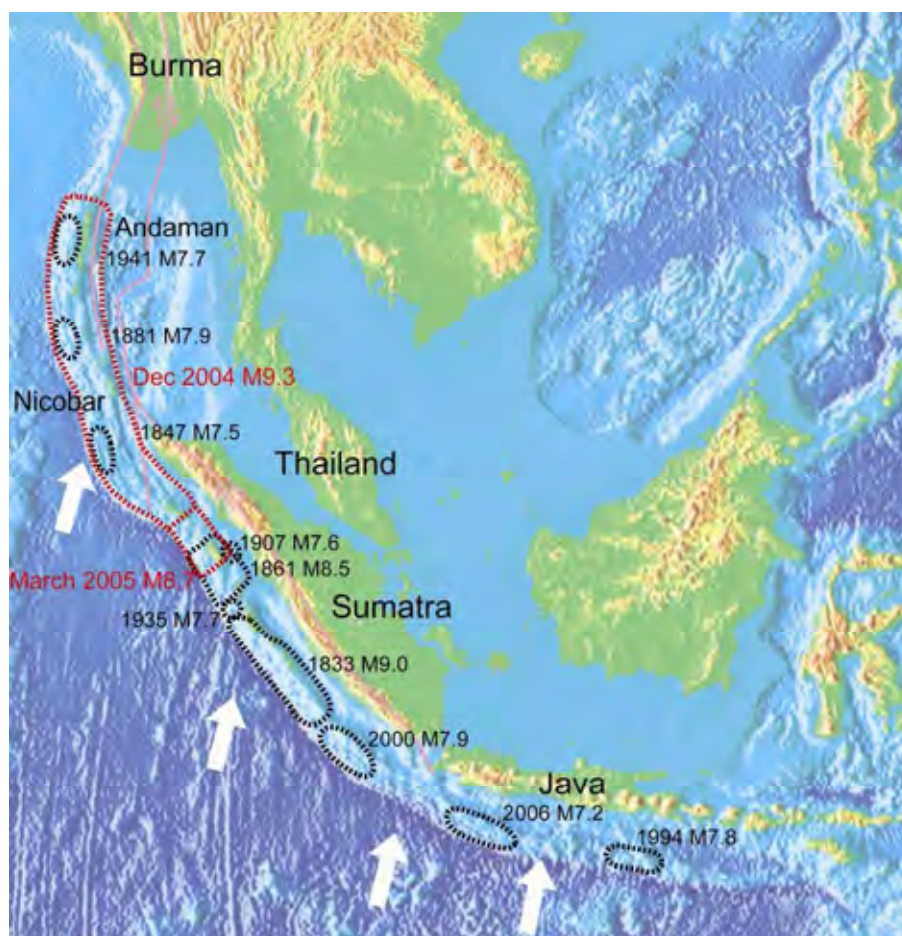


**Figure 2.1.5 Tectonic Background and Past Earthquake Rupture Zones  
on Andaman-Sunda Arc**

**(Thick white arrows indicate the direction of Indian Ocean-Australian plate movement)**

### 1) Interplate Earthquakes

In the Java Island sea, destructive M7.5~M8 class earthquakes occur near the trench axis inside the Indian Ocean-Australian plate, as happened in 1921 (Ms7.5) and 1977 (Ms7.9). It is believed that the maximum magnitude of interplate and intraplate earthquakes is the same. Recently, an interplate earthquake (Mw7.6) occurred in the Java Island sea on 2 June 1994, and an intraplate earthquake occurred on 17 July 2006.

Under these conditions, the target earthquake of Kabupaten Jember is believed to be an interplate earthquake which would occur offshore Kabupaten Jember.

The fault parameter definition is given in Figure 2.1.6, and the fault parameter which exerts an effect on Kabupaten Jember is shown in Table 2.1.4.

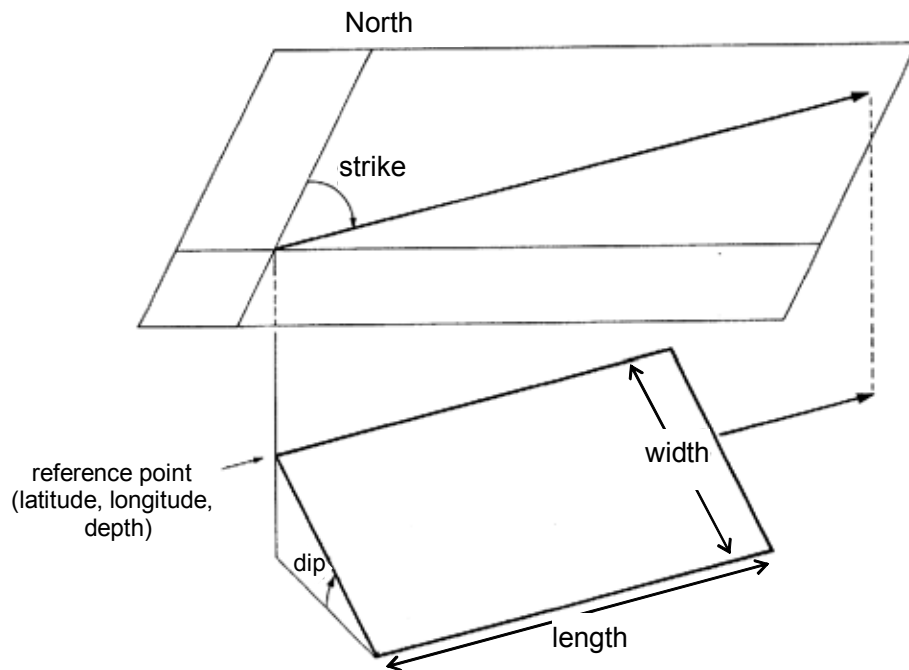


**Figure 2.1.6 Elements of Fault Parameter**

**Table 2.1.4 Fault Parameter of Target Earthquake  
(Interplate Earthquake at Kabupaten Jember offshore)**

Mw	Latitude(D)	Longitude(D)	Depth	Length	Width	Strike	Dip
8.0	-10.780	113.905	0 km	126 km	61 km	284°	12°

**2) Inland Earthquakes**

There is also a possibility in Kabupaten Jember that inland active faults or active faults yet unknown could cause an earthquake, such as the central Java earthquake on 27 June 2006. However, this is not understood from the topography or surface layer geology because of the thick volcanic deposits (volcanic ejecta and alluvial fan deposits) that cover the land and under which a fault could be buried.

It is difficult to speculate on an inland hypocenter from the fact there is no active fault seen inland which could become an earthquake source fault and, in addition, precision crustal movement observation is not carried out. Therefore, it is justified to assume an inland target earthquake could happen anywhere inside Kabupaten Jember.

## 2.2 Kabupaten Padang Pariaman

### 2.2.1 Landform of Kabupaten Padang Pariaman

West Sumatra Province is a mountainous district nearly 3,000 meters in elevation made of Paleozoic sedimentary rock and Igneous rock that extends from the active row of volcanoes to the east. The Great Sumatran Fault divides the center of the province—the fault topography clearly visible—in a North-northwest (NNW) to South-southeast (SSE) direction. The stretch of land between the central mountain range and the shore is made of volcanic uplands and pyroclastic flow uplands with a narrow coastal plain distributed along the seacoast.

Towering above the eastern side (i.e. the mountain side) of Kabupaten Padang Pariaman are two large volcanoes; Gunung Tandikat standing at 2,347m and its twin volcano Gunung Singgalang at 2,877m. Lake Maninjau, located at the north end of Kabupaten Padang Pariaman, is a caldera lake measuring 20 kilometers north-south and 8 kilometers east-west which formed after a large volcanic eruption 52,000 years ago. The volcanic products from this giant eruption are scattered over a wide area in the north-central area of Kabupaten Padang Pariaman. Today, these volcanic products are seen as pyroclastic flow uplands and low relief hills.

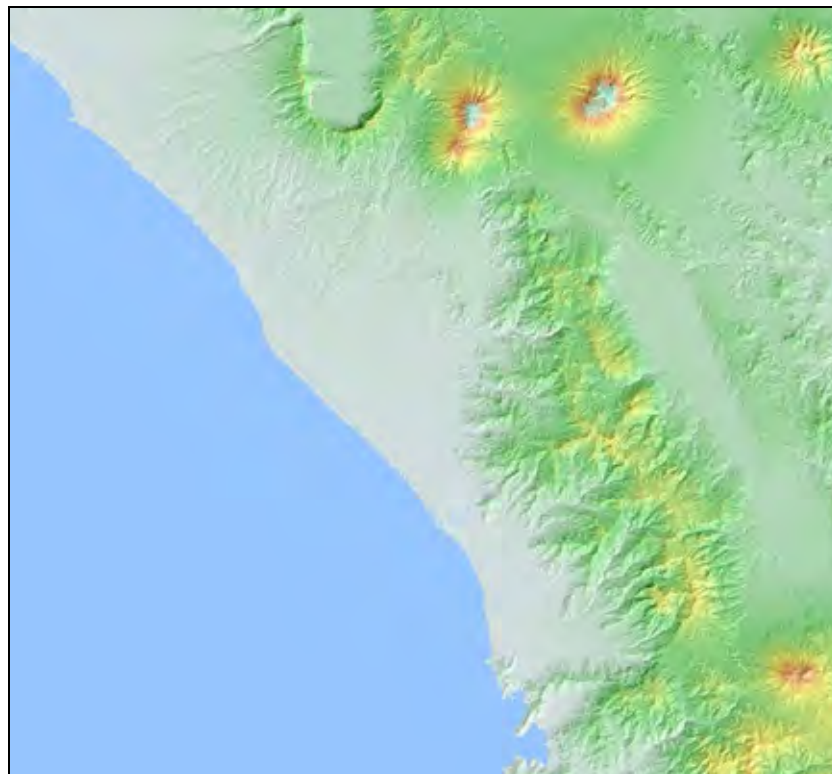


**Figure 2.2.1** Topographic Overview of West Sumatra Region

Volcano and pyroclastic flow upland formed from the giant eruption that formed the Maninjau caldera 52,000 years ago accounts for the wide area of northwest Kabupaten Padang Pariaman. The area consists largely of unconsolidated pumiceous sand and gravel and is prone to slope failure.

The lowland is divided into a fluvial plain and coastal plain. The fluvial plain was formed by the flooding of some of the largest rivers, the Batang Andi, Batang Ulakan and Batang Mangau. There are three narrow segments clearly visible in the Batang Andi mid-upper stream. These have a great effect on changing the river's topology. The narrow segments at the lower end, downstream from BT. Tinjaulaut are striking meandering water channels. This meander belt and flood plain are prone to flooding.

The central and western river basin is mostly pyroclastic flow upland and low relief hills (mostly made up of pyroclastic flow deposits), although both the basin area and channel length are relatively small. Among those rivers, there are the wide basins of Batang Ulakan and Batang Mangau in the south, and the meander trace can be seen at downstream.

Shared by a number of rivers, the river mouths are blocked by sand bars, beach ridges and sand dunes that line the coast, causing poor drainage and forming a marsh.

Kabupaten Padang Pariaman has a straight seacoast that changes little, lined with a string of sand bars, beach ridges and sand dunes. These sit at an elevation of 3 or 4 meters, with even the highest sand dunes at around 5 meters.

Between these elevated areas is inter-levee lowland, part of which is marsh and paddy fields.

The Geomorphological Map legend and results are given in Table 2.2.1 and Figure 2.2.2.

**Table 2.2.1 Geomorphological Map Legend of Kabupaten Padang Pariaman**

Landform Group	Landform type	State of landform
Lowland	Artificial land	Distribute mainly, at Minang Kabau International Airport
	Sand bar, Beach ridge and Sand dune	High place along the coast
	Coastal plain	The plain along the coast
	Meander belt	Flood plain with clear meander trace
	Alluvial fan	Flat lowland from mountain area to the coast consist of fluvial deposits
	Valley plain	Flat lowland in the valley
	Flood plain	Flat lowland by sequential floods
	Back marsh	Marsh behind the river channel
Terrace	River terrace	Fluvial terrace
Volcano	Tandikat volcano	Tandikat volcano
	Low relief hill	Low relief hills formed by Maninjau Caldera eruption. Because of the fine materials, many small valleys are developed.
	Pyroclastic flow upland	Pyroclastic flow upland formed by Maninjau Caldera eruption. Flat surface remains more than low relief hills .
	Old Maninjau volcano	Old Maninjau volcano slope
Mountain	Talus	The landform produced by slope failure debris
	Lithic tuff (QTt)	Mountain slope with Lithic tuff
	Andesite (Qtp)	Mountain slope with Andesite
	Miocene granite (Tmgr)	Mountain slope with Miocene granite
	Quartzite member of Permian (Pq)	Mountain slope with Quartzite member of Permian
	Undifferentiated rock (QTau)	Mountain slope with undifferentiated rock
Additional landform	Fault and lineament	Active faults and suspicious landform
	Slope failure	Old slope failure

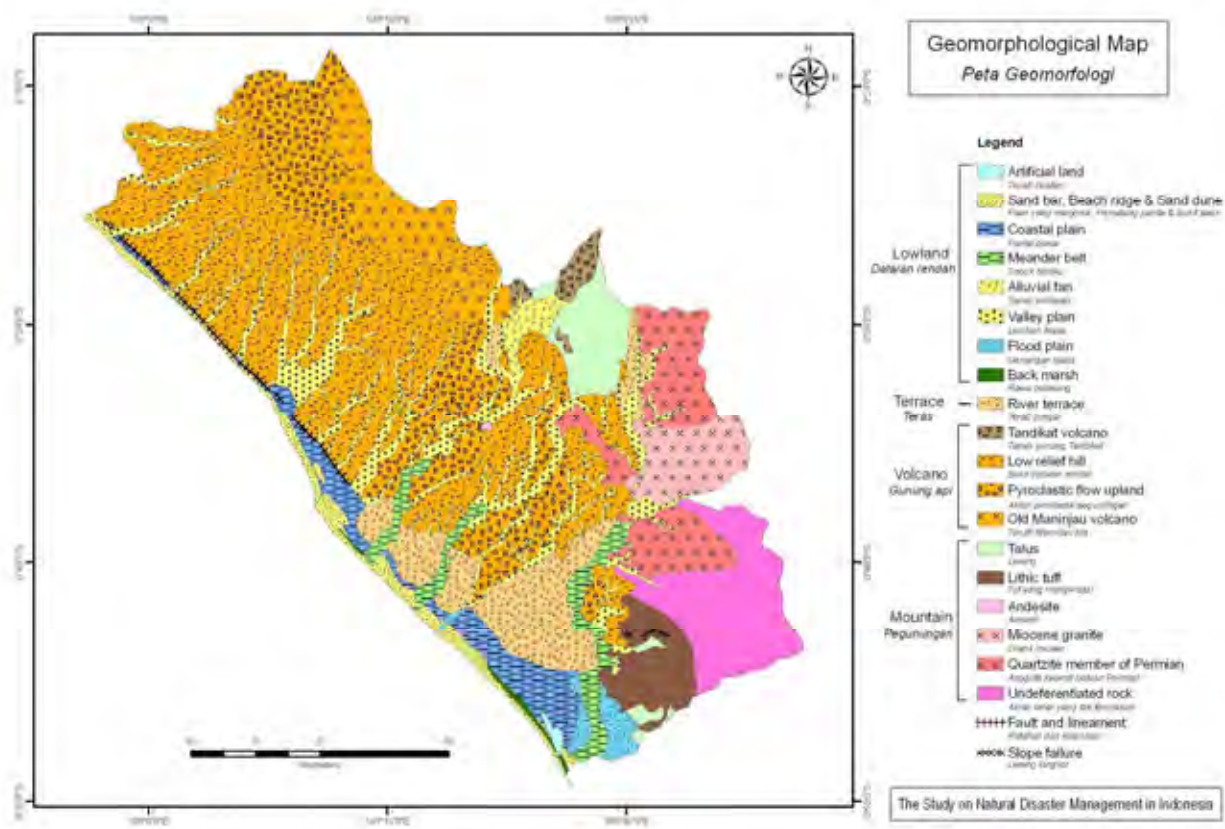


Figure 2.2.2 Geomorphological Map of Kabupaten Padang Pariaman

## 2.2.2 Geology of Kabupaten Padang Pariaman

The stratigraphy of this region is a unit from the Recent period to Permian Paleozoic.

Table 2.2.2 shows the geology of Kabupaten Padang Pariaman.

**Table 2.2.2 Geology of Kabupaten Padang Pariaman**

Geologic Age	Geology	Rock Type and Stratigraphy
Quaternary	Alluvial Deposits	Eolian deposit
		Fluvial deposit
		Marine deposit
		Debris flow deposit
	Volcanic Products	Volcanic ash
		Edifice collapse deposit of Tandikat volcano
		Volcanic Products of Tandikat volcano
		Pyroclastic rock and pyroclastic flow deposit from the Old Maninjau volcano
	Volcanic Rock	Lithic tuff
Andesite		
Tertiary	Igneous Rock	Miocene Granite rock
Paleozoic	Igneous Rock	Permian Quarzite

### - Alluvial Deposits

There are a large amount of alluvial deposits that can be divided into fluvial deposits and marine deposits. The Batang Andi basin consists of fluvial deposits widespread over eastern and southern Kabupaten Padang Pariaman. With the mountains encroaching upon the plains, the main sediment is coarse fragments, while near the estuary the main feature is sandy sediments. The layers are an alternation of beds of clay and gravel. The main sediment of the fluvial deposit of northwest Kabupaten is pumiceous sand.

Marine deposits are found in a long, narrow strip along the seashore. The sand bars, beach ridges and sand dunes that line the coast form a sand bed made of uniform grain size that exceeds 5 meters in depth. The inter-levee lowland features marshy, argilliferous sediment.

### - Quaternary Volcanic Products

There are a variety of volcanic products dated from recent to early Quaternary. New volcanic products are lava and pyroclastic products from the Tandikat volcano, and products from the Old Maninjau volcano which consists mostly of a large number of pyroclastic deposits from the great eruption 52,000 years ago that formed the Maninjau caldera. Most of the area of Kabupaten Padang Pariaman is pumiceous sand, however, the Maninjau caldera is pyroclastic flow deposit. Pyroclastic flow deposits that appear in plateau cliffs are at least 30 m thick.

Found in the southeast mountains are blocks of slightly old Lithic tuff (QTt).

- Tertiary Igneous rocks and Paleozoic rocks

The eastern part of Kabupaten Padang Pariaman consists of Tertiary igneous rocks and Paleozoic rocks. The Tertiary igneous rocks, granite and quartz diorite, are found in large clusters. Paleozoic Permian was slightly metamorphosed to green schist, and faulted vertically.

Miocene granite is contained in the neck, and topographically makes up the ridge in many areas. The north and east are covered by volcanic products, and buried beneath the new volcanic products are these consolidated Tertiary igneous rocks and Paleozoic rocks.

### 2.2.3 Ground type classification and amplification analysis

Only a small amount of materials could be gathered on boring this time, and the area was limited to southern Kabupaten, so this was not suitable to expand to all of Kabupaten. Thereupon, the geology and ground conditions were estimated based on the geomorphological map.

A recommendation can be found in the Cabinet Office, Japan (2005) “The manual of making earthquake disaster prevention maps” for producing shaking potential maps based on empirical methods. In this material, suggestions for methods to produce a simple estimate of the shaking potential based on geomorphic maps are given in cases where ground information is unavailable or insufficient. Due to the lack of materials in this instance, the amplification ratio between subsurface and ground surface was recognized using the empirical methods in the Cabinet Office, Japan (2005).

Prior to seeking the amplification ratio, the landform types were grouped to match the classifications in “The manual of making earthquake disaster prevention maps”, and a Ground Condition Map produced. The relationship between landform type and ground condition type is shown in Table 2.2.3.

The relationship between landform types and AVS30 in “The manual of making earthquake disaster prevention maps” is as shown below:

$$\text{Log AVS30} = a + b \text{LogH} + c \text{LogD} \pm \sigma$$

Here, AVS30 signifies estimated Average Velocity of S-wave in 30m of subsurface materials, H signifies elevation (m), D signifies distance from major river (km), a (micro landform), b (elevation) and c (distance from major river) signify coefficient of each micro landform type,  $\sigma$  signifies standard deviation.

Considerations for elevation and distance from major rivers were ignored in this study. The topography that appeared is included in the following six groups.

The relational expression between AVS30 and amplification G is as follows:

$$\text{Log G} = 1.83 - 0.66 \text{LogAVS30} \pm 0.16$$

Here, AVS30 signifies estimated Average Velocity of S-wave in 30m of subsurface materials, whereas,  $100\text{m/s} < \text{AVS30} < 1500 \text{ m/s}$ , G signifies

Amplification ratio between the base of 600m/s S-wave maximum velocity and that of the ground surface

**Table 2.2.3 The index of Landform type, Ground condition type and Shaking potential**

Ground condition type	Landform type	a	b	c	Log G	G (Amplification ratio)
1 Hard rock	Paleozoic, Mesozoic and Paleogene Rock Mountain	2.75	0	0	0.015	1.035
2 Unconsolidated sediments	Volcano slope	2.35	0	0	0.279	1.901
3 Unconsolidated sand, gravel and pyroclastic flow deposit	Gravel upland and Hills	2.34	0	0	0.286	1.930
4 Alluvium (gravel and sand)	Alluvial fan and Valley plain	2.39	0	0	0.253	1.789
5 Alluvium (sand and silt, reclaimed fill)	Sand bar and Sand dune	2.19	0	0	0.385	2.424
6 Alluvium (clay, silt and sand)	Coastal plain and Back marsh	2.10	0	0	0.444	2.780

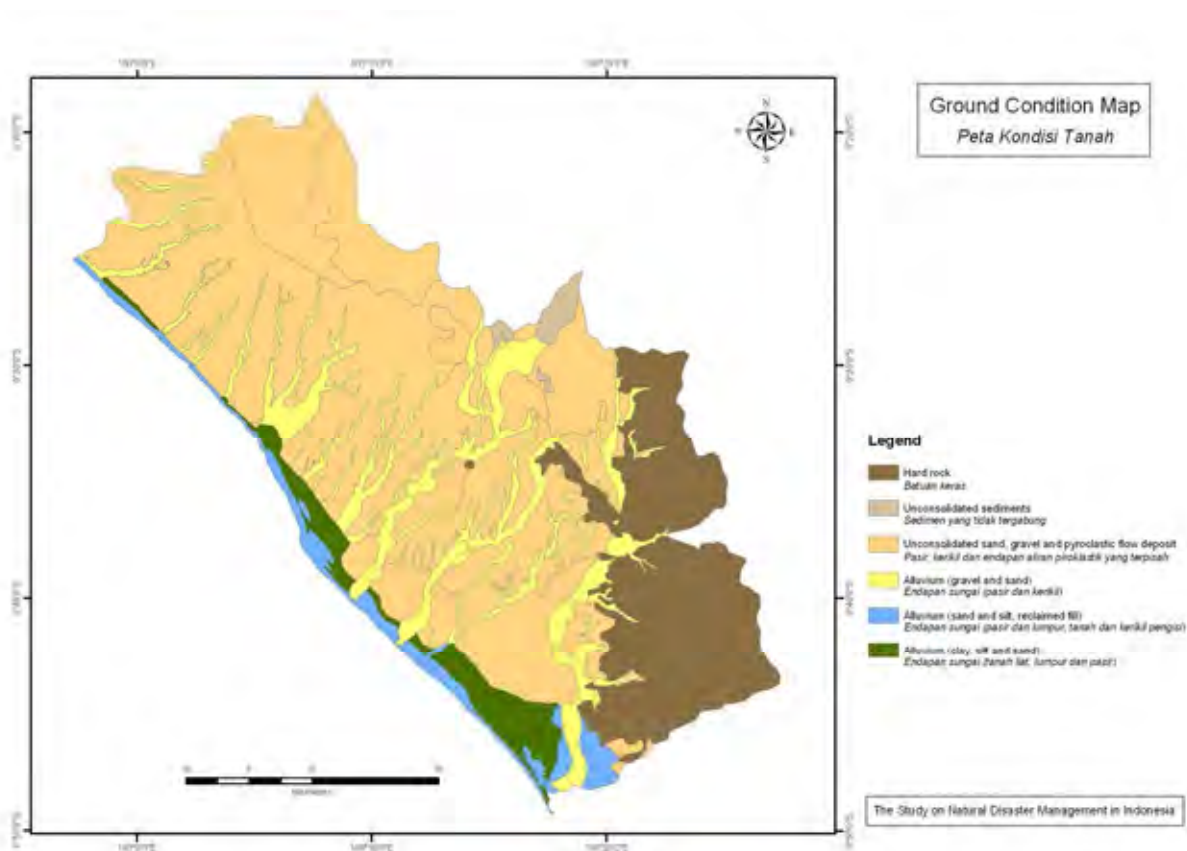


**Figure 2.2.3 Ground Condition Map**

Concerning landform type and liquefaction potential, in order to carry out liquefaction potential evaluation, the results from the subsurface geology and well water level observation were matched with the manual for liquefaction zoning published by the National Land Agency, Japan (1999).

The relation among landform type, subsurface geology, ground condition, well water level and liquefaction potential are shown in Table 2.2.4. Also, the Liquefaction Potential Map is given in Figure 2.2.4.

**Table 2.2.4 Landform type, subsurface geology, ground condition, well water level and liquefaction potential**

Landform Group	Landform type	Subsurface Geology	Ground Condition type	Water Level (GL.)	Liquefaction Potential
Lowland	Artificial land	Sand and Gravel	5	-1m~-3m	High
	Sand bar, Beach ridge and Sand dune	Sand	5	-1.5m~-3m	High
	Coastal plain	Sand and Gravel	6	-0.5m~-2m	High
	Meander belt	Sand and Gravel	4	-1m~-2m	Middle
	Alluvial fan	Gravel	4	-2m~-4m	Low
	Valley plain	Gravel	4	-1m~-3m	Low
	Flood plain	Sand and Gravel	5	-1m~-2m	Low
	Back marsh	Clay and Sand	6	0m~-0.5m	Middle
Terrace	River terrace	Gravel and Sand	3	-1m~-2m	Low
Volcano	Tandikat volcano	Volcanic ash, Pyroclastic rock and Lava	2	-	Not occur
	Low relief hill	Pyroclastic flow deposit and Volcanic ash	3	-	Not occur
	Pyroclastic flow upland	Pyroclastic flow deposit and Volcanic ash	3	-	Not occur
	Old Maninjau volcano	Volcanic ash, Pyroclastic rock and Lava	3	-	Not occur
Mountain	Talus	Gravel	3	-	Not occur
	Lithic tuff (QTt)	Rock and Weathered material	1	-	Not occur
	Andesite (Qtp)	Rock and Weathered material	1	-	Not occur
	Miocene granite (Tmgr)	Rock and Weathered material	1	-	Not occur
	Quartzite member of Permian (Pq)	Rock and Weathered material	1	-	Not occur
	Undifferentiated rock (QTau)	Rock and Weathered material	1	-	Not occur

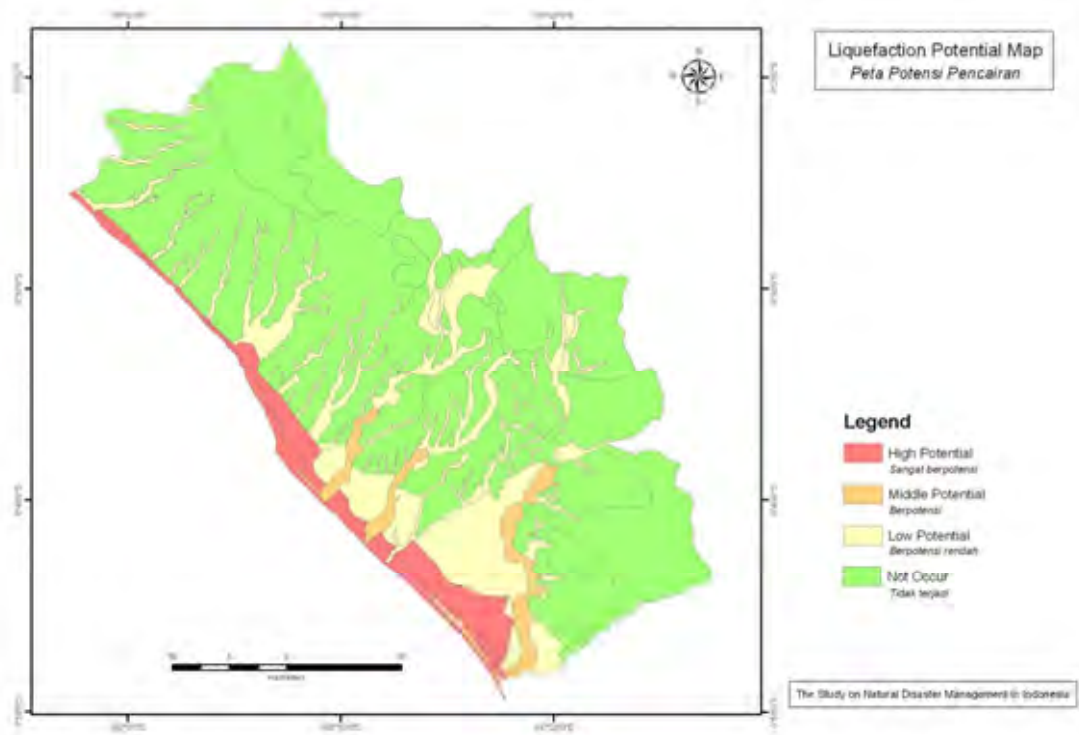


Figure 2.2.4 Liquefaction Potential Map

## 2.2.4 Investigation of Target Earthquake

In Kabupaten Padang Pariaman, the record of earthquakes shows two types:

1. Major earthquakes along the Sunda Trench west of the island of Sumatra
2. Earthquakes along the Great Sumatran fault

Major earthquakes along the Sunda Trench west of Sumatra include the Mw9.1 Andaman earthquake of December 26, 2004 and the Mw8.4 Bengkulu earthquake of September 12, 2007, and in Kabupaten Padang Pariaman it is predicted that similar quakes will occur west of Siberut and Sipura islands.

Recent earthquakes that have occurred along the Great Sumatran Fault, which cuts across Sumatra, are the series of quakes of March 6, 2007 measuring Mw6.4 and the Mw6.3 earthquake in the vicinity of Singkalak lake, which occurred in eastern Kabupaten Padang Pariaman.

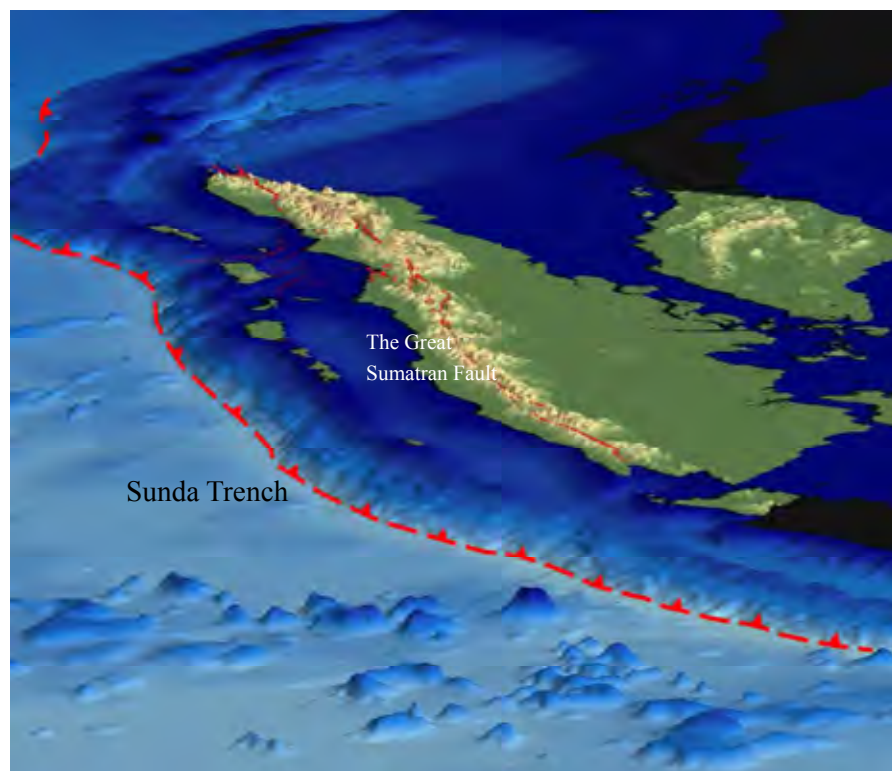


**Figure 2.2.5 Major tectonic situation around Sumatra island**

The record of earthquakes along the Sunda trench on the western coast of Sumatra was carefully analyzed by K. R. Newcom and W. R. Macann (1987). Analysis of earthquakes over the past 300 years, between 1661 and the early 1980s, showed two massive earthquakes: the Mw8.75 quake of 1833 and Mw8.25-8.5 quake of 1861. This revealed a high potential for a future interplate

earthquake to occur in the sea near Sumatra. After the December 2004 quake, there was a rapid influx of research, most of which predicted a succession of earthquakes in the sea near Sumatra. Following, in March 2005, an Mw8.7 earthquake with its epicenter near Nias Island, and the Mw8.4 Bengkulu earthquake on September 12, 2007 occurred, which closed up a layer of the Kabupaten Padang Pariaman offshore seismic gap.

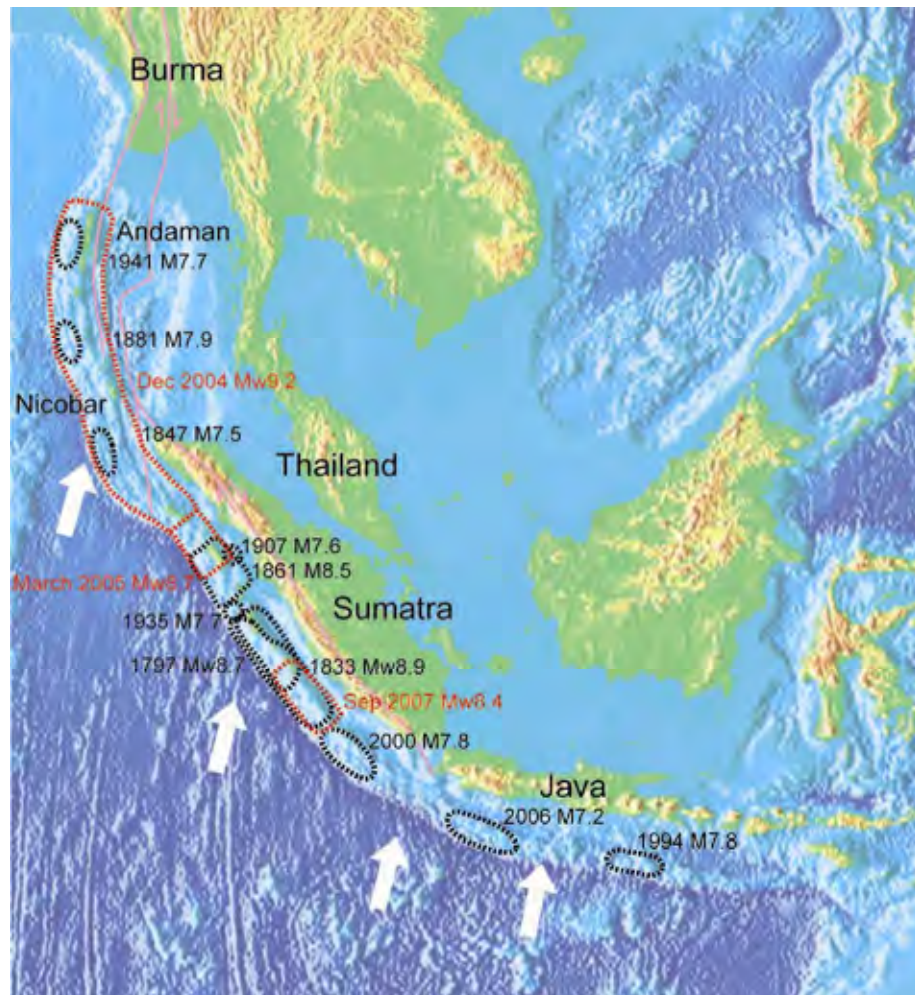


**Figure 2.2.6 Tectonic Background and Past Earthquake Rapture Zones on Andaman-Sunda Arc**

**(Thick white arrows indicate the direction of Indian Ocean-Australian plate movement)**

With the seismic gap in the offshore Kabupaten Padang Pariaman, there are areas that have not seen any remarkable earthquakes since those that occurred in 1797 and 1833. The locked patches located in the offshore Kabupaten Padang Pariaman are shown in Figure 2.2.7

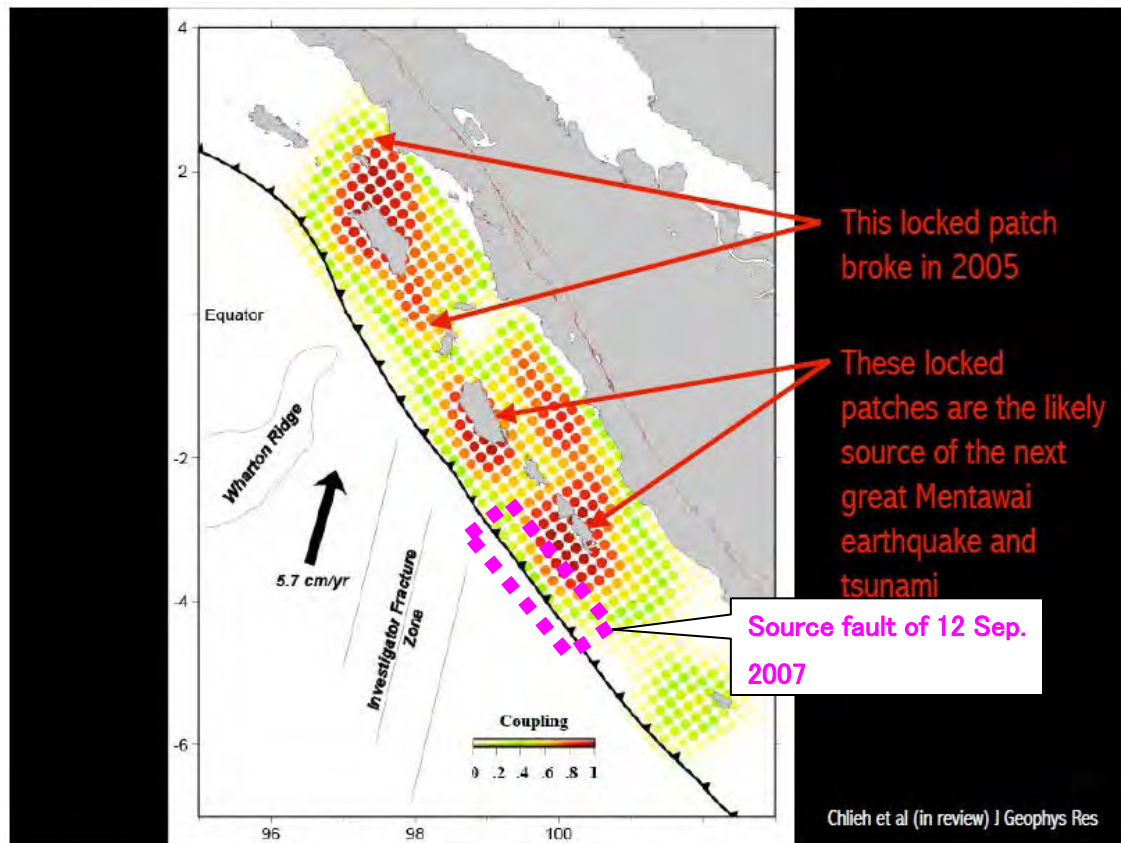


**Figure 2.2.7** Locked patches offshore Kabupaten Padang Pariaman (Sieh, 2007)

The fault model of 1797 and 1833, according to updip/downdip data by Natawidjaja et al. (2006), is estimated based on annual growth bands of microatoll, a type of coral (Figure 2.2.8).

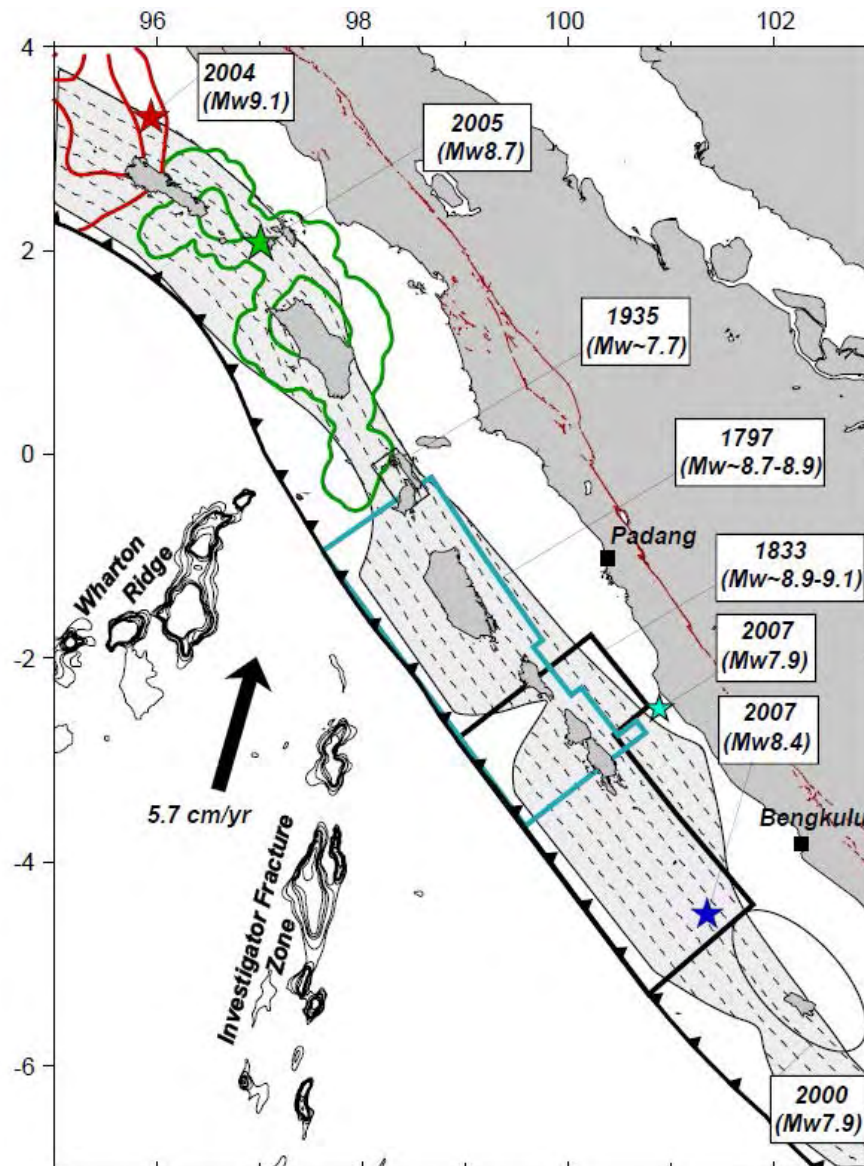


**Figure 2.2.8 Comparison of Interseismic Coupling along the Megathrust with the Rupture Areas of the Great 1797, 1833, 2005 and 2007 Quakes**

In this project, it is estimated that an earthquake would destroy a layer of the fault which includes part of the source fault of the September 12, 2007 earthquake, the largest to have occurred in this region since 1797 and 1833.

The parameter of the fault is as shown in Table 2.2.5. The values for the fault slope, depth and so on were taken from Natawidjaja et al. (2006).

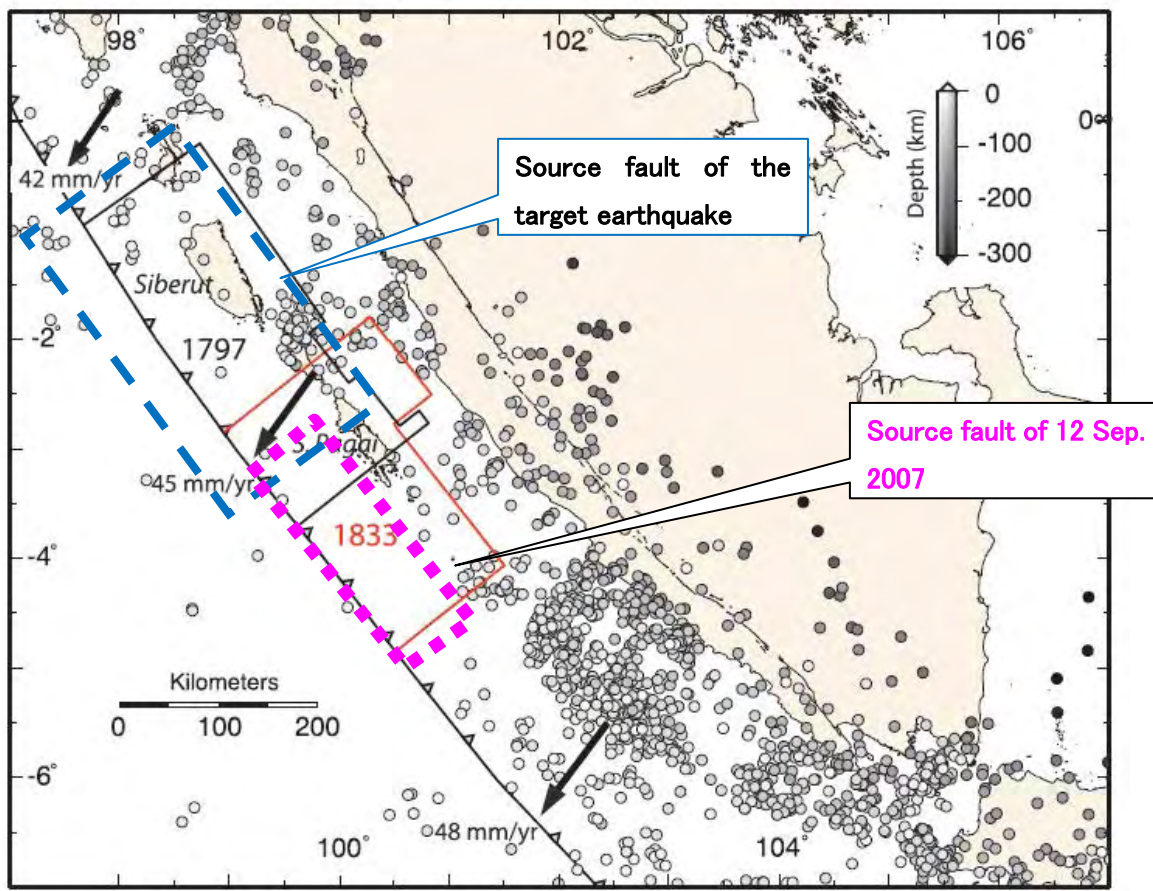


Figure 2.2.9 The Estimated 1797, 1833 and 2007 Fault Model and the Forecast Earthquake (Revision of the Figure from Natawidjaja et al., 2006)

Table 2.2.5 Fault Parameter: Interplate Earthquakes (offshore Kabupaten Padang Pariaman)

Mw	Lat. (degree)	Lon. (degree)	Depth (km)	Length (km)	Width (km)	Strike (deg)	Slope (degree)
8.4	-3.6	99.5	0	360	190	324	15

## **CHAPTER 3 DISASTER CHARACTERISTICS OF EARTHQUAKE AND COUNTERMEASURES IN PILOT REGIONS**

### **3.1 Disaster Characteristics of Earthquake and Countermeasures in Kabupaten Jember**

#### **3.1.1 Disaster Characteristics of Earthquake in Kabupaten Jember**

##### **1) Earthquake Disaster in the past**

A history of previous disasters can offer effective lessons for mitigation because comparatively large earthquake disasters occur periodically. In fact, the earthquake is a phenomenon which happens together with the movement of the lithospheric plate. There is some periodicity in the occurrences of large earthquakes although the movement speed of lithospheric plate is nearly constant. The return period of large earthquakes, which may have a big influence, is considerably long compared to human life (i.e. 200~1000 years). Therefore, even a person who lives in one region for a long time can hardly experience such a large seismic hazard. There are few documented historical facts or study's findings obtained by archaeological survey regarding the earthquake in Indonesia. However, this tendency does not mean that big earthquakes do not occur in that region. Plate tectonic surroundings and the past occurrences of earthquakes needs to be discussed widely to ensure accurate understanding of frequency and magnitude of seismic hazard. Actually, the earthquake hazard in Indonesia is more frequent than that of Japan if we count only the earthquake by which 100 lives or more were lost using "Utsu Database" or "USGS Database". Of course, the total human damage due to the earthquake is discussed here. Damage due to tremor is not discussed separately from damage due to seismic sea wave.

**Table 3.1.1 Earthquake by Which 100 Lives or More were Lost in Indonesia (1/2)**

(Web:[http://iisee.kenken.go.jp/utsu/utsuweq\\_bak.html](http://iisee.kenken.go.jp/utsu/utsuweq_bak.html))

Year	Month	day	Latitude	Longitude	Depth	M	Death	Injured	Remarks
1716	9	10	-1.0	120.2	--	--	many	--	Indonesia(Java/Sumatra)
1874	2	12	-3.5	128.2	--	--	2342	--	Indonesia(Moluccas) Amboina
1792	2	12	--	--	--	--	300	--	Indonesia(Sumatra) Padang
1815	11	27	-8	115.2	--	--	10253	--	Indonesia(Bali)
1820	12	29	-7	119	--	7.5	400	--	Indonesia(Sulawesi) Makassar, Sumbawa
1820	12	29	-2	121	--	--	many	--	Indonesia(Sulawesi) Macassar, Bona, Lombok(I=9)
1835	11	1	-3.4	128.1	--	--	149	--	Indonesia(Moluccas) Amboina, Haruku, Saparua(I=9)
1846	2	14	0.5	127.3	--	--	many	--	Indonesia(Moluccas) Ternate, Is.
1856	3	2	3.5	125.5	--	--	3000	--	Indonesia(Great Sanga(Volcanic))
1861	2	16	0.5	97.5	--	8.4	great	--	Indonesia(Sumatra) Lagundi, Padang, Batu I, Nias I.
1861	3	9	0	98	--	7	750	--	Indonesia(Sumatra) Padang, Batu Is., Simuk D=200
1864	5	23	-3	135	*	--	250	--	Indonesia(Irian Jaya) Geelvink Bay
1867	6	10	-7.8	110.5	--	--	327	--	Indonesia(Java) Djokjoharta, Soerakarta(I=9)
1871	3	2	0	120	--	--	400	--	Indonesia(Moluccas) Tagulandang Is., Ouhlas
1883	8	27	-5.8	106.3	--	--	Several tens of thousand ds	--	Indonesia(Krakatoa)
1890	12	12	-6.4	111	--	--	many	--	Indonesia(Java) Djoewana(I=8) D=500
1896	4	10	-8.3	126	--	--	250	--	Indonesia(Timer/Alor)(I=8)
1899	9	29	-3	120.5	--	7.4	3064	--	Indonesia(Moluccas) Ceram(south coast) 7.15
1907	1	4	2	96.3	9	7.8	400	--	Indonesia(Sumatra) Gunung Sibol(Nias) 7.55
1909	6	3	-2.5	101.5	--	7.5	200	--	Indonesia(Sumatra) Korint, Djambi 7.35
1914	6	25	-4	102.5	--	8.1	many	--	Indonesia(Sumatra) Benkulen, D=11/20 7.65
1917	1	21	-8	115.4	--	6.5	15000	--	Indonesia(Bali)
1924	11	12	-7.2	109.5	--	--	609	--	Indonesia(Java) Wonosobo D=many/60
1924	12	2	-7.3	109.9	--	--	115	--	Indonesia(Java) Wonosobo
1924	12	22	--	--	--	--	113	--	Indonesia(Java) Wonosobo
1926	6	28	-0.5	100.5	--	6.8	222	--	Indonesia(Sumatra) Padang Highlands 新層
1926	6	29	--	--	--	--	400	--	Indonesia(Sumatra)
1928	8	4	-8.3	121.7	--	--	226	--	Indonesia(Palawan) Is. (Rokatinda Volcano)
1943	7	23	-9.5	110	90	8.1	213	--	Indonesia(Java) Jayakarta 7.6B
1964	1	4	-1.9	102.3	33	6.7	110	479	Indonesia(Sumatra)
1964	4	2	5.8	95.7	132	7	110	479	Indonesia(Sumatra)
1968	8	14	0.16	119.78	23	7.4	392	--	Indonesia(Sulawesi) D=200 7.35
1969	2	23	-3.12	118.87	13	6.9	600	--	Indonesia(Sulawesi) D=64 H=97
1976	6	25	-4.6	140.09	33	7.1	6000	--	Indonesia(Irian Jaya) D=422
1976	7	14	-8.17	114.89	40	6.5	563	2300	Indonesia(Bali)
1976	10	29	-4.52	139.92	33	7.2	6000	--	Indonesia(Irian Jaya) D=108/133(I=8)
1977	8	19	-11.09	118.46	33	7.9	189	75	Indonesia(Sumbawa Is. EQ)
1981	1	19	-4.58	139.23	33	6.7	1300	--	Indonesia(Irian Jaya) Jayawijaya Mts. D=261 6.6W
1989	8	1	-4.51	139.02	14	5.8	120	125	Indonesia(Irian Jaya) Kurima D=90 6.1W
1992	12	12	-8.48	121.9	28	7.5	1740	2144	Indonesia(Flores) Maumere, Babi Is. D=2080 7.7W
1994	2	15	-4.97	104.3	23	7	207	2000	Indonesia(Sumatra) Liew(Lampung Prov.) 6.9W
1994	6	2	-10.48	112.84	18	7.2	277	423	Indonesia(SE coast of Java) Bali
1996	2	17	-0.89	136.95	33	8.1	166	423	Indonesia(Irian Jaya) Blak, Supiori 8.2W
2000	6	4	-4.72	102.09	33	8	103	2585	Indonesia(Sumatra) Bengkulu D=90 I=2174 7.9W
2004	12	26	3.3	95.98	30	8.8	Several tens of thousand ds	Several tens of thousand ds	Indonesia(Sumatra)(I=9)landslide, mud volcano 9.0W

**Table 3.1.2 Earthquake by Which 100 Lives or More were Lost in Indonesia (2/2)**

(Web:<http://infotrek.er.usgs.gov/>)

Year	Mnth	Day	Time	Longitude	Latitude	Depth	Magnitude	Tsunami	Death	Injured	Damage	Note
1988	5	28	1327J	-2.91	139.32	65	7.7	--	--	--	limi	Indonesia(Irian Jaya) 7.2B
1988	8	10	0207J	1.42	126.22	33	7.6	T	--	--	limi	Indonesia(Molucca Passage) 7.5S
1988	8	14	2214J	0.18	119.78	23	7.4	T	392	--	seve	Indonesia(Sulawesi) D=200 7.3S
1989	1	30	1029J	4.81	127.44	70	7.9	--	--	--	--	Indonesia(Taloud) 7.1B
1971	1	10	0717J	-3.13	139.7	33	8.1	--	--	--	made	Indonesia(Irian Jaya) Djapuna, Sentani 7.9S
1971	2	4	1333J	0.65	96.84	33	7.1	--	--	--	limi	Indonesia(Sumatra) Nias, Sibolga, Tarutung, Pasaman
1972	6	11	1841J	3.94	124.32	325	7.5	--	--	--	--	Indonesia(Celebes) Sea 7.4B
1976	6	25	1918J	-4.6	140.09	33	7.1	--	8000	--	seve	Indonesia(Irian Jaya) D=422 Mission-9 F 6.8S
1976	10	29	0251J	-4.52	139.92	33	7.2	--	8000	--	caru	Indonesia(Irian Jaya) D=108/133(I=8)
1977	8	19	0803J	-11.09	118.46	33	7.9	T	189	75	made	Indonesia(Sumbawa Is. EQ) 8.1S 8.3W
1979	9	12	0317J	-1.68	136.04	5	7.9	T	15	many	seve	Indonesia(Irian Jaya) Yapan 7.7S 7.5W
1984	11	17	0649J	0.2	96.03	33	7.2	--	0	1	limi	Indonesia(D. H. W. Sumatra) Nias Is. D=1 7.1W
1985	11	17	0940J	-1.54	134.91	10	7.1	--	0	0	limi	Indonesia(Irian Jaya) Mandowari 7.1W
1990	4	18	1339J	1.19	122.85	26	7.4	--	3	25	some	Indonesia(Sulawesi) Bolaang-Garontara area 7.8W
1991	6	20	0318J	1.2	122.79	31	7.7	--	0	--	limi	Indonesia(Sulawesi) Garontara(Minahassa Pen.) 7.5W
1992	12	12	0329J	-8.48	121.9	28	7.5	T	1740	2144	seve	Indonesia(Flores) Maumere, Babi Is. D=2080 7.7W
1994	1	21	0224J	1.02	127.73	20	7.2	--	7	40	made	Indonesia(Halmahera) Kou area 7.0W
1994	2	15	1707J	-4.97	104.3	23	7	--	207	2000	caru	Indonesia(Sumatra) Liew(Lampung Prov.) 6.9W
1994	6	2	1817J	-10.48	112.84	18	7.2	T	277	423	caru	Indonesia(SE coast of Java) Bali Tsunami 7.7W
1995	3	21	2353J	-4.18	135.11	33	7.1	--	0	0	limi	Indonesia(Irian Jaya) Ayam, Fakfak, Nabire 6.9W
1996	1	10	0803J	0.73	119.83	24	7.6	T	10	--	some	Indonesia(Sulawesi) Minahasa Pen. 7.9W
1996	2	17	0359J	-0.89	136.95	33	8.1	T	186	423	caru	Indonesia(Irian Jaya) Blak, Supiori 8.2W
1996	2	17	1459L	-0.89	136.95	33	8.1	T	0	0	D1	Indonesia Chichijima 103m, Shionan 24686cm 8.2W
1996	11	29	1410J	-2.07	124.89	33	7.7	--	41	161	caru	Indonesia(Ceram Sea) Mangale, Talisabu, Mansada 7.7W
2000	5	4	0421J	-1.11	123.57	26	7.5	T	46	264	caru	Indonesia(Sulawesi) Luwuk, Banggai, Peleng 7.8W
2000	6	4	1828J	-4.72	102.09	33	8	--	103	2585	caru	Indonesia(Sumatra) Bengkulu D=90 I=2174 7.9W
2002	10	10	1050J	-1.76	134.3	10	7.7	T	8	数百	caru	Indonesia(Irian Jaya) Fault, Slope Failure 7.8W
2002	11	20	129J	2.62	96.09	30	7.6	--	3	85	made	Indonesia(Simeulu) 7.4W
2003	5	26	1923J	2.35	128.85	31	7.1	--	1	7	limi	Indonesia(Halmahera) Elerebere 7.0W

Frequency and magnitude of earthquake must be discussed observing the characteristics of surrounding plate structure and past occurrence of big earthquakes. Indonesia has a plate boundary in southern part of Sumatra and Java Island. The oceanic plate subducts towards the bottom of the island. The subduction zone is located in Sunda Trench. A very big earthquake caused by reverse fault occurs in this subduction zone.

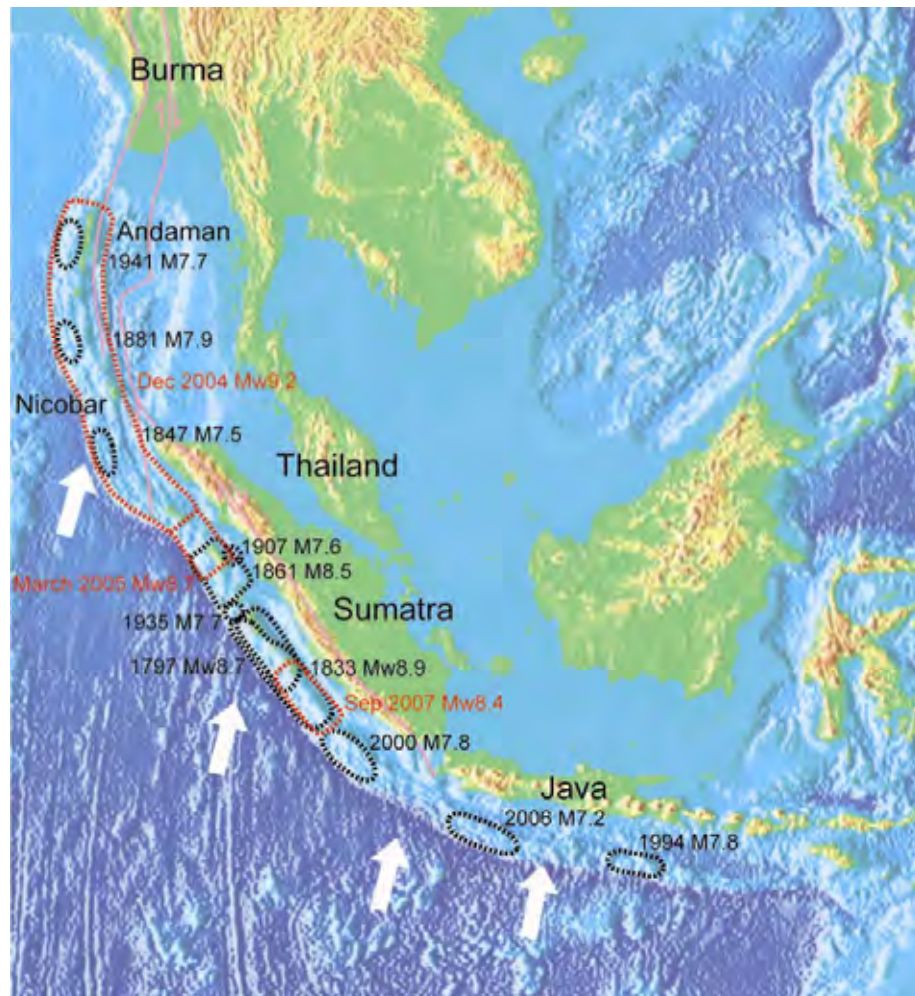


**Figure 3.1.1 Sunda Trench**

There was another example of near-field earthquake at Yogyakarta city (i.e, 27 May 2006 Yogya Earthquake M<sub>w</sub> 6.5). The relationship between damage and surface ground motion intensity in Kabupaten Bantul was referred to as a benchmark of the vulnerability function in this report.

The above-mentioned seismic circumstance is also very similar to Japanese circumstance, so Japan experiences regarding earthquake hazard needs to be used.

## 2) Factors for Damages due to Earthquake

Damage of earthquake disaster is divided into following three aspects:

1. Structure damage due to ground tremor
2. Damage due to capacity shortage of ground such as slope failure or liquefaction
3. Damage due to seismic sea wave

It is pointed that the aspects of above 1 and 2 tend to be forgotten after an earthquake because the damage due to seismic sea wave gives overwhelming impression to victims. The aspects of above 1 and 2 are absolutely different from the sea wave because we can have some leeway to mitigate damage due to seismic the sea wave. However structural damage due to ground tremor occurs quite suddenly. Any warning can not be effective. Only strengthening of structures done beforehand is effective to mitigate damage. Any effort done after earthquake can not be effective to reduce the number of human lives lost.

### 3.1.2 Earthquake Hazard Map in Kabupaten Jember

#### 1) Basis of Hazard Map Creation for Earthquake

The meaning of the word “Hazard” is defined as the cause of disaster. Therefore, regarding earthquake, only the distribution of the ground surface acceleration intensity must be shown in “Hazard Map”. No other aspect is necessary for Hazard Map for the above definition.

The ground surface acceleration intensity is described at each part of mesh in study area using the title of “Peak Ground Acceleration” (it is called as PGA here in after) or “Modified Mercalli Intensity scale” (it is called as MMI here in after).

Next topic, which is discussed in this chapter, is how to define the target value of the ground surface acceleration intensity. Generally there is a steady tendency of the relationship between the magnitude of earthquake and frequency of occurrence. So this means that small earthquake can occur frequently, but large earthquake rarely occur so frequently.

Figure 3.1.2 shows the relationship between the magnitude of earthquake and frequency of occurrence regarding earthquakes that occurred from 1629 to 2004 in Indonesia

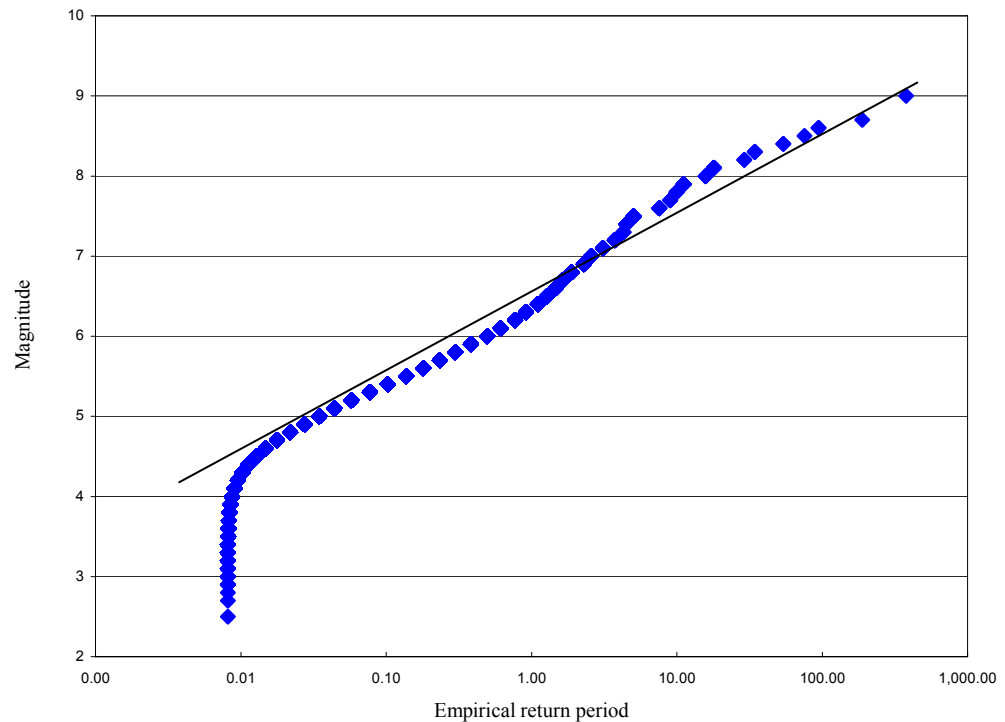


**Figure 3.1.2 Relation between Magnitude and Return Period**

Y axis means magnitude of the earthquake, and X axis means empirical return period  $T_E$ .

$$T_E = \frac{T_S}{m} \quad (\text{Eq. 3.1})$$

Where

$T_E$  : Empirical return period

$T_S$  : Sampling term

$m$  : Order when the sample is arranged in magnitude order

For example, the largest earthquake generated in this area is the 2004 earthquake with magnitude 9, then order  $m$  is the first, Sampling term  $T_S$  is 2004 minus 1629 equal to 375, Empirical return period  $T_E$  must be 375 years. The large one in second is the 1833 earthquake with magnitude 8.7, then order  $m$  is the second, Sampling term  $T_S$  is 375 years divided 2 equal to 187, Empirical return period  $T_E$  must be 187 years. When the relationship between magnitude and the empirical return period  $T_E$  of each recorded earthquake is plotted in the same manner, the plotted pattern tends to be almost on straight line on one-half of logarithm graph paper, but limited in range of more than magnitude 5. This finding is called the thesis of Gutenberg Richter or G-R formula. The angle  $b$  of this approximation line represents the difference between the occurrence frequency of big earthquake and that of small earthquake. If the surrounding of Indonesia is divided into some

domains, which has consistent condition of seismicity, the above mentioned angle  $b$  must be particular for each particular domain. If the occurrence of earthquakes is a spatially independent and independent timewise incident Poisson model can be applied to the analysis.

The peak acceleration value of the base rock at a certain point can be calculated utilizing attenuation formula. Attenuation formula is a kind of regression formula by which the peak acceleration value of the base rock is presumed from the magnitude of earthquake source and distance from earthquake source to a certain point.

In this computational procedure previously mentioned each domain must be further divided into small piece by utilizing polar coordinate system. In addition, an implicit method is needed in this procedure because the magnitude of earthquake source, which brings the peak acceleration value in a certain point, must be obtained in a computation step. Therefore a huge amount of the calculation is required in order to carry out this analysis. The computer program "EZFRISK" or "EQRISK" is used in an actual analysis. The peak acceleration value of the base rock at each part of Indonesia was calculated. Figure 3.1.3 shows the results of the above described procedure.

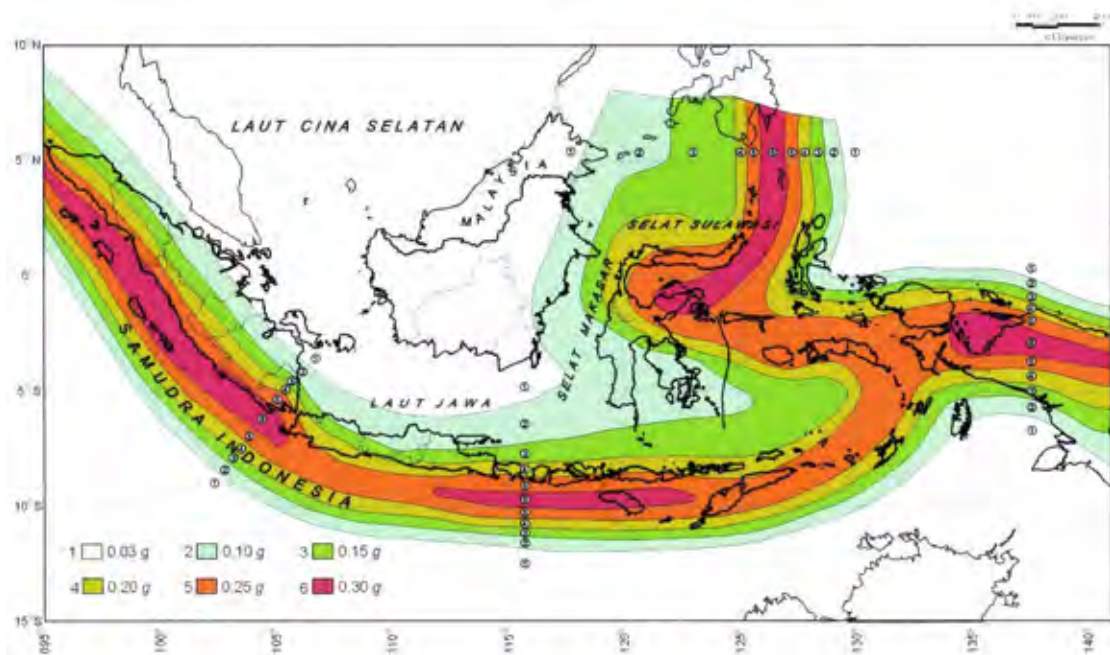


**Figure 3.1.3 Peak Acceleration Value of the Base Rock at Each Part of Indonesia (From SNI 03-1726-2002 the Indonesian code for seismic load)**

Each value shown in Figure 3.1.3 is the peak acceleration value of the base rock at each colored zone and corresponding to 500 years of return period. For instance, Kabupaten Jember belongs to Zone 4. Therefore the peak acceleration value of the base rock is 0.2g (the value of 0.2g means 0.2 times acceleration of gravity).

When concretely explaining the 500 years of return period, it means that the probability of exceedance is 10% for 50 years. For example, if a structure, which has 50 years of service time, is designed utilizing the design seismic load of 500 years of return period, the probability by which the structure will fall due to an unexpectedly large earthquake is 10%. Indeed 90% of incidents are comprised in this category. This setting is almost perfect in realistic meaning because 100% of safety can not be obtained using probability theory.

The above explained value is the peak acceleration value at the base rock that is defined as a base rock layer that is consisted of homogeneous material. The peak acceleration value at the base rock can be estimated utilizing attenuation function. However the value, which is needed for application of hazard map, must be the peak acceleration value at ground surface.

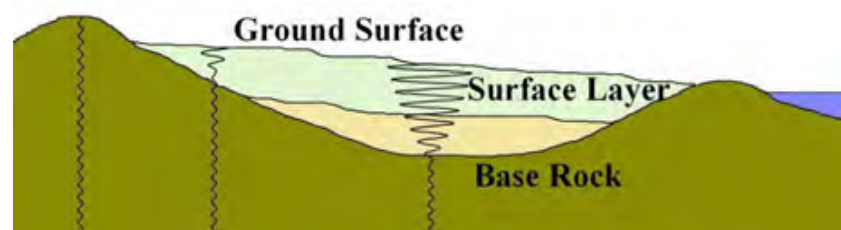


**Figure 3.1.4 Peak Acceleration Value of the Base Rock and Peak Acceleration Value of Ground Surface**

As explained in Figure 3.1.4 the ground tremor is amplified while it is propagated in the surface layer. In fact, the ground tremor at outcrop of base rock is usually small. On the other hand the ground tremor at the soft layer is usually large. Degree of amplification depends on characteristics of surface layer of the ground. Surface layer must be investigated in order to discuss this aspect. Geomorphological feature of surface layer around Kabupaten Jember is shown in Figure 3.1.5.

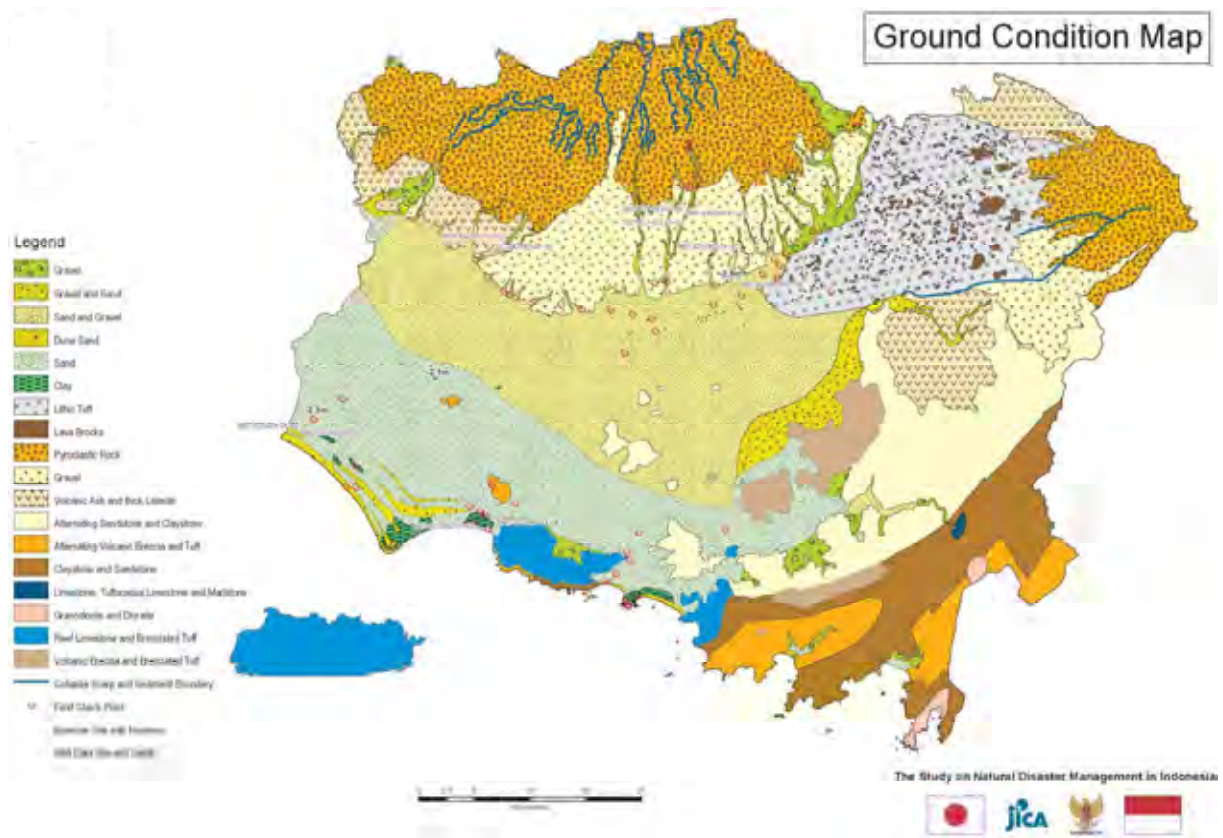


**Figure 3.1.5 Geomorphological Feature of Surface Layer around Kabupaten Jember**

Distribution of characteristics of surface layer at each Segment of the study area is shown in Figure 3.1.6.

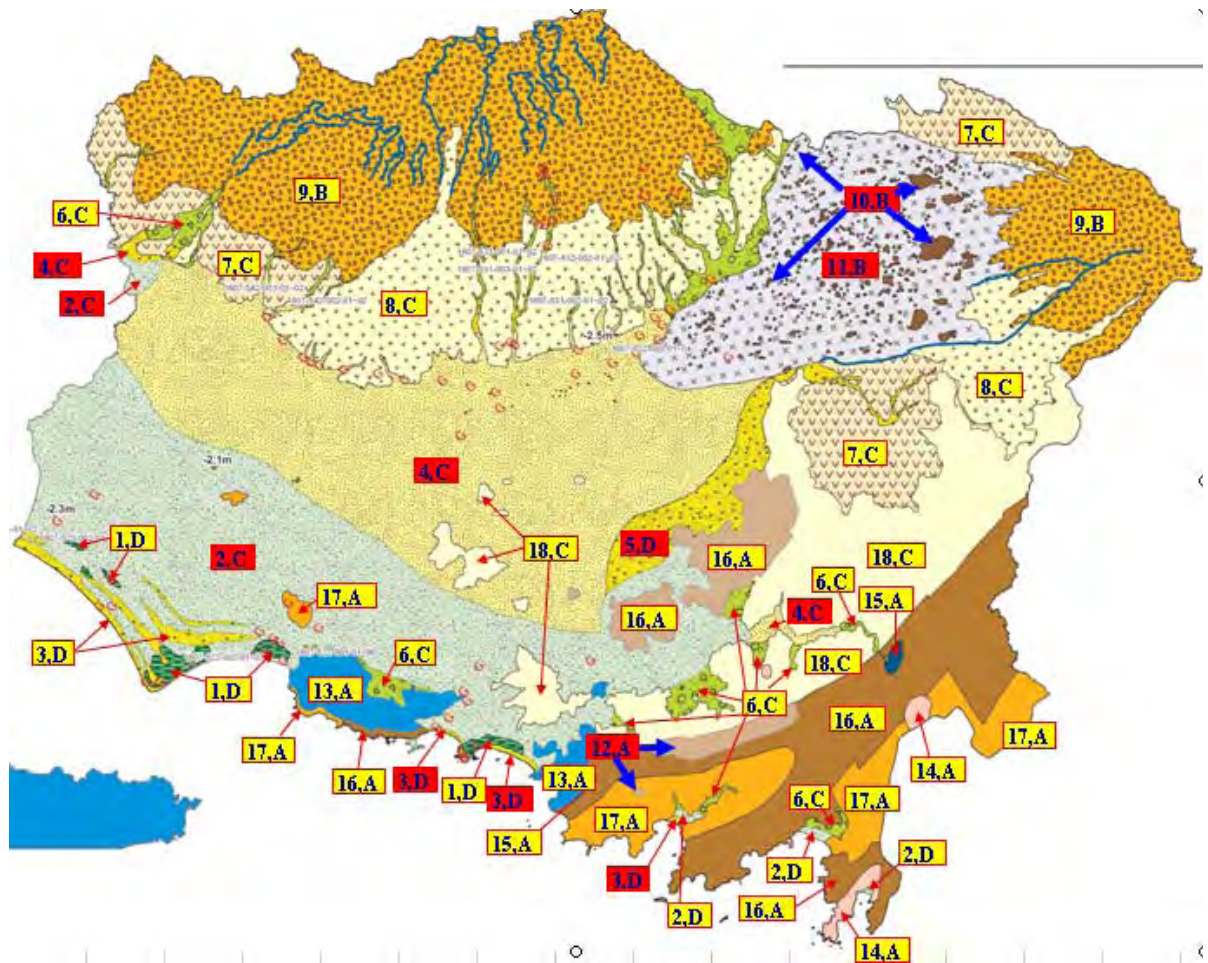


**Figure 3.1.6 Segmentation of Soil Class (classified according to stiffness of surface layer)**

Segmentation of soil class shown in Figure 3.1.6 is classified according to stiffness of surface layer. The classification is based on some speculations on geomorphological features given by geological map and field survey done by the expert in charge of geological features. However more accurate material that will given by borehole logging and PS logging must be referred if it is available. Moreover, continuous improving effort shall be made regarding accuracy of hazard mapping.

As explain here, the intensity of the surface ground motion at earthquake is estimated referring the zone classified in SNI 03-1726-2002 and the soil class. The surface ground motion is expressed by PGA and the response spectrum, shown in Figure 3.1.7. The value of vertical axis in the response spectrum means the acceleration response of the SDOF (Single degree of Freedom) model that has the natural period shown in the horizontal axis. Therefore the value on the extreme left correspond to PGA. This value of PGA shall be shown in the hazard map because these values represent the tremor of ground surface.

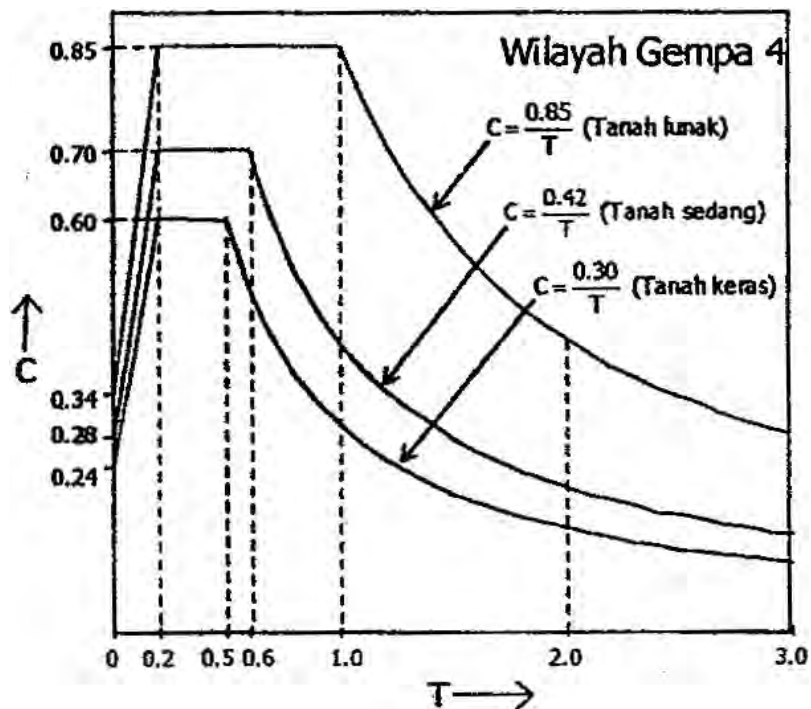
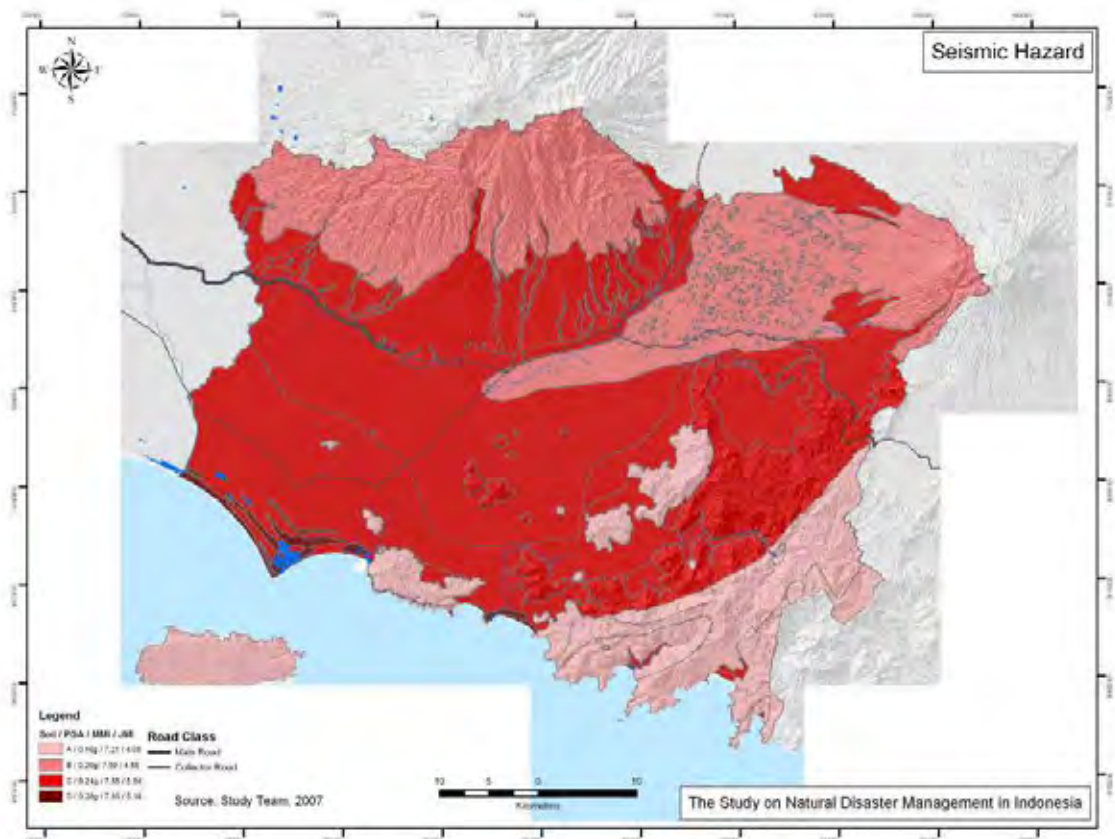


Figure 3.1.7 Response Spectrum Stipulated in 03-1726-2002

## 2) Earthquake Hazard Map in Kabupaten Jember

The expected value distribution of the ground surface acceleration intensity is shown in Figure 3.1.8. The ground surface acceleration intensity is described using the title of PGA and MMI. PGA is a value which will be obtained as the maximum value when the quake of the ground level is measured with accelerograph. The modified Mercalli intensity scale (MMI) divides earthquake intensity into 12 stages of evaluation, and each stage is defined by describing the incident through observation and sensing (for example; “Difficult to stand”). Therefore expression of MMI is a discrete number originally but one digit below the decimal point is written in this report in order to distinguish a detailed difference. The estimated MMI for Kabupaten Jember is about seven from 8 between 8 or more in the MMI display. This level of intensity corresponds to “5 or more” in Japan Meteorological Agency Seismic Intensity Scale (it is called as JMI hereafter). JMI also divides earthquake intensity into 10 stages of evaluation, and each stage is defined by describing the incident through observation and sensing. Some sort of slight damage is found when the earthquake of “5 or more” in JMI occurs in Japan but it is thought that considerably more serious damage may be generated by the same level of earthquake in Indonesia because earthquake resistant capacity of Indonesian buildings is poor comparing with that of Japan.



**Figure 3.1.8 Expected Value Distribution of Ground Surface Tremor**

### 3.1.3 Earthquake Risk Map in Kabupaten Jember

#### 1) Basis of Risk Map Creation for Earthquake

Earthquake risk is an abstract concept by itself. So some definition or physical understanding must be supplied. Earthquake disaster risk is the possibility of destruction that can be analyzed as a synergistic result of earthquake hazard and vulnerability of a facility. Every aspect of the magnitude in earthquake disaster, including human loss and economical loss, can be evaluated based on structural destruction. In an actual disaster situation, people are not killed by quake of ground but they are killed by collapsing of buildings. As shown in Figure 3.1.9, the majority cause of death in 1995 Great Hanshin Earthquake originated almost always in the collapse of the building. Therefore it can be said that it is indispensable to know how many buildings shall collapse when we discuss the risk of earthquakes.

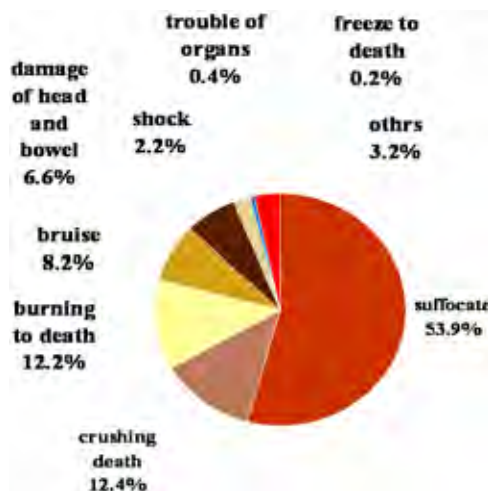


**Figure 3.1.9 Ratio of the Cause of Death at 1995 Great Hanshin Earthquake**

Therefore Earthquake risk is defined as the damage ratio  $P$  under the condition of assumed ground motion and characteristics of the buildings. The damage ratio  $P$  is defined by Eq. 3.2.

$$P = \frac{N_D}{N_T} \tag{Eq. 3.2}$$

Where,

- $N_D$  : Number of damaged building
- $N_T$  : Total number of existing building

In this context damaged buildings means the buildings that suffer equal or more “large damage” defined by Architectural Institute of Japan (AIJ). The damage grade “large damage” is strictly defined from the viewpoint of structure engineering. Generally, dead and injured are generated in the buildings that suffer equal or more “large damage”. That is why this grade was chosen for the target of this evaluation. This grade is also similar to “Grade 4 Very Heavy Damage” of European Macroseismic Scale (EMS).

The damage ratio  $P$  is assessed by utilizing the fragility function. The outline of the fragility function analysis utilized in this study is shown in Figure 3.1.10.

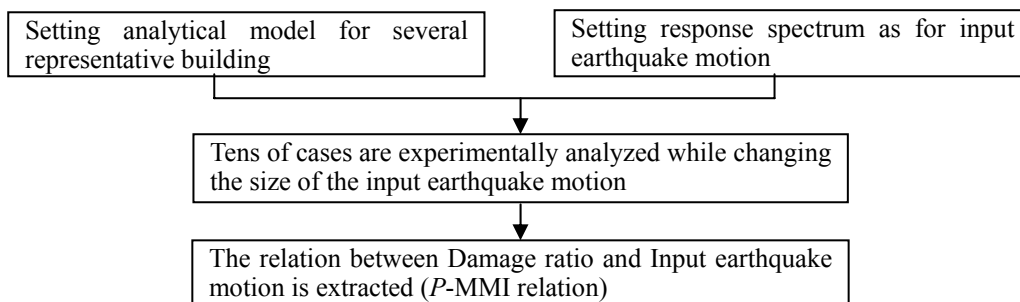


**Figure 3.1.10 Outline of Fragility Function Analysis**

The fragility function mainly depends on the characteristics of building structure. Therefore the buildings in the study area are divided into several building types and the typical building of each building type is modeled. Outline of building model is shown in Figure 3.1.11.

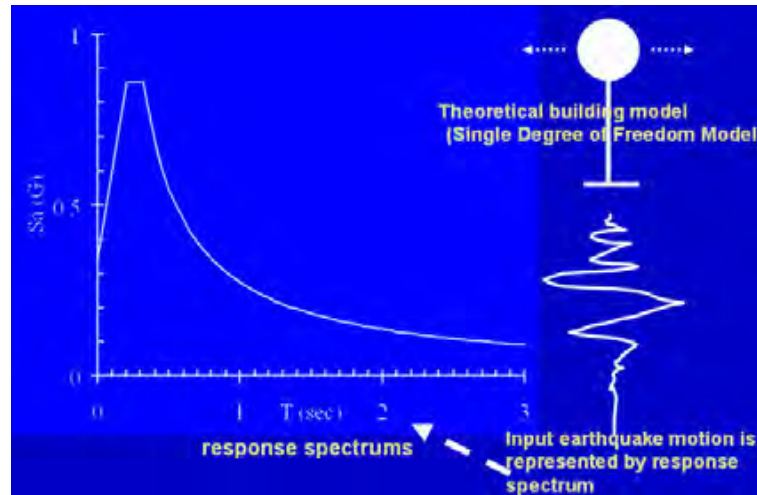


**Figure 3.1.11 Outline of Building Model**

Then a simplified dynamic analysis is carried out applying increasing earthquake input motion step by step. Then the relationship between MMI and the damage ratio  $P$  is obtained as a fragility function. The procedure to generate the relationship between MMI and the damage ratio  $P$  is common to the procedure done by committee of Japanese government and US Project “HAZUS” (see Appendix of this report).

A highly probable result can not be obtained when the sensitivity of the fragility function does not fit real earthquake resistance of the buildings in a corresponding study area. In this study some steps of calibration were carried out applying consideration through the research report of past earthquake disasters that occurred near the study area. The example of Yogyakarta city (i.e, 27 May 2006 Yogya Earthquake  $M_w$  6.5) was effective material to apply because a Japanese reconnaissance team reported the intensity of surface ground motion investigated through interview intended for the residents and some observation on damage state of the building in disaster area (Shiro Takada et. al “Strong Ground Motion and Lifeline Damage during the Java Jogjakarta Earthquake”).

The obtained relationship between MMI and the damage ratio  $P$  is shown in Figure 3.1.12. The fragility function is generated for each building type.

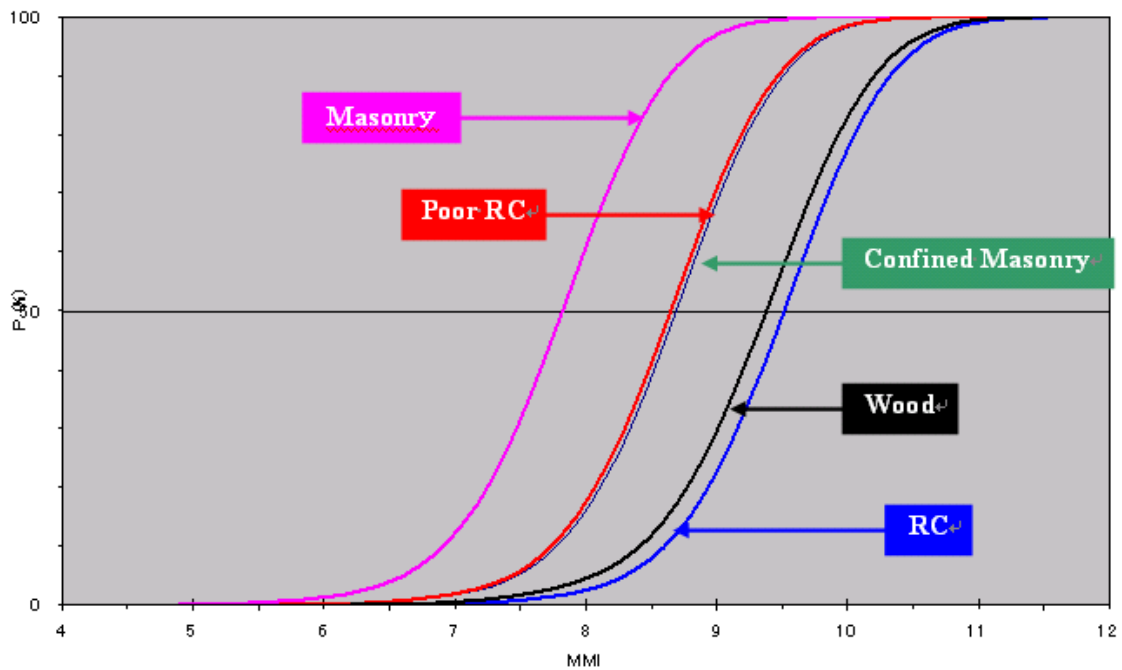


**Figure 3.1.12 Fragility Function (Relationship between MMI and the Damage Ratio  $P$ )**

On the other hand, the damage examples observed in Sumatra Island also need to be referred. Therefore some reports about 2004 Andaman earthquake and 2007 Solok earthquake were referred and it was confirmed that these observations do not contradict the fragility function.

In this report the hazard map shows the expected surface ground motion intensity of each point by MMI. So the value of the damage ratio  $P$  can be obtained by applying the fragility function and referring the value of MMI. By using a database and that indicates the number of each building type, the expected number of damaged buildings can be calculated by multiplying existing building number and the damage ratio  $P$ .

If above estimation is carried out based on enough grounds

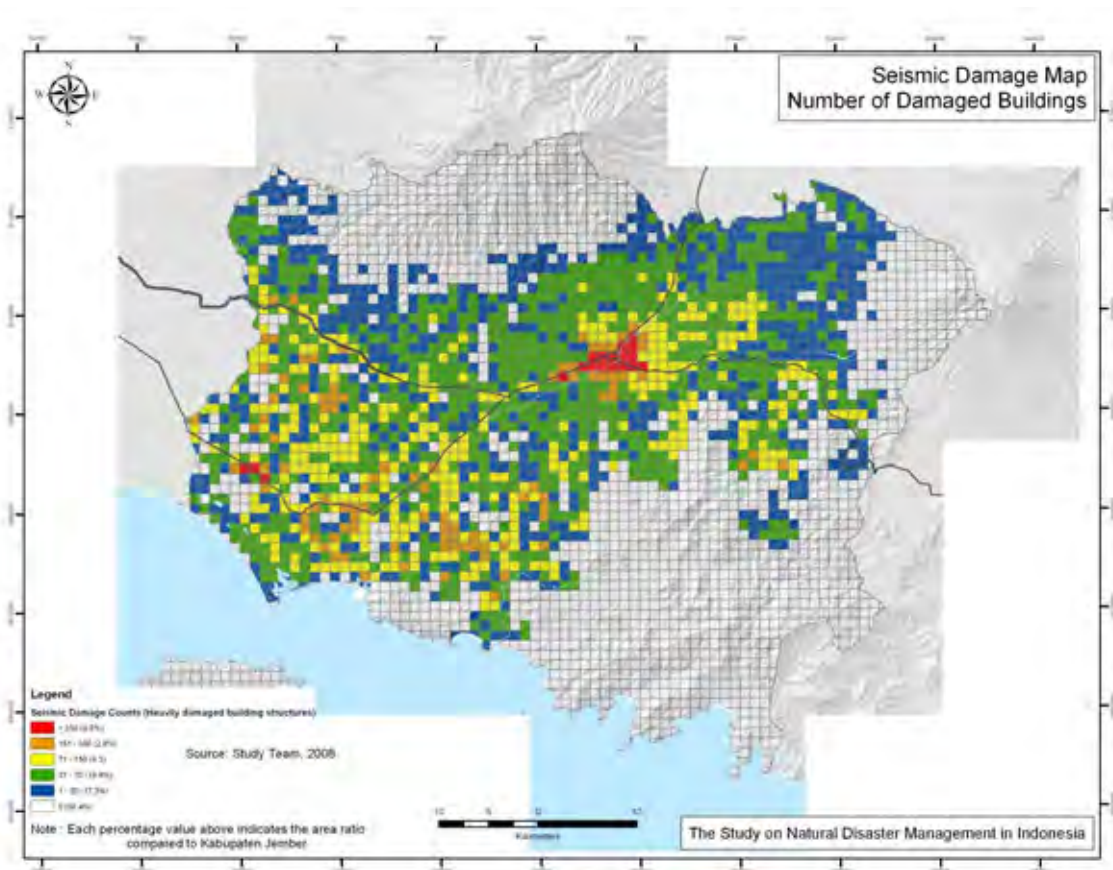
- It can be known how large project of building strengthening is needed for disaster mitigation viewpoint
- Expected number of dead and injured at earthquake can be estimated, and
- Scale of preparedness required for emergency aid can be estimated

However, in this study gaps in the database had to be filled by referring to some survey results and rough considerations because the database which was obtained now did not offer detailed information. The responsible Agency in Kabupaten Jember has to implement the building census from the structural viewpoint and improve the database in the future.

## 2) Earthquake Risk Map in Kabupaten Jember

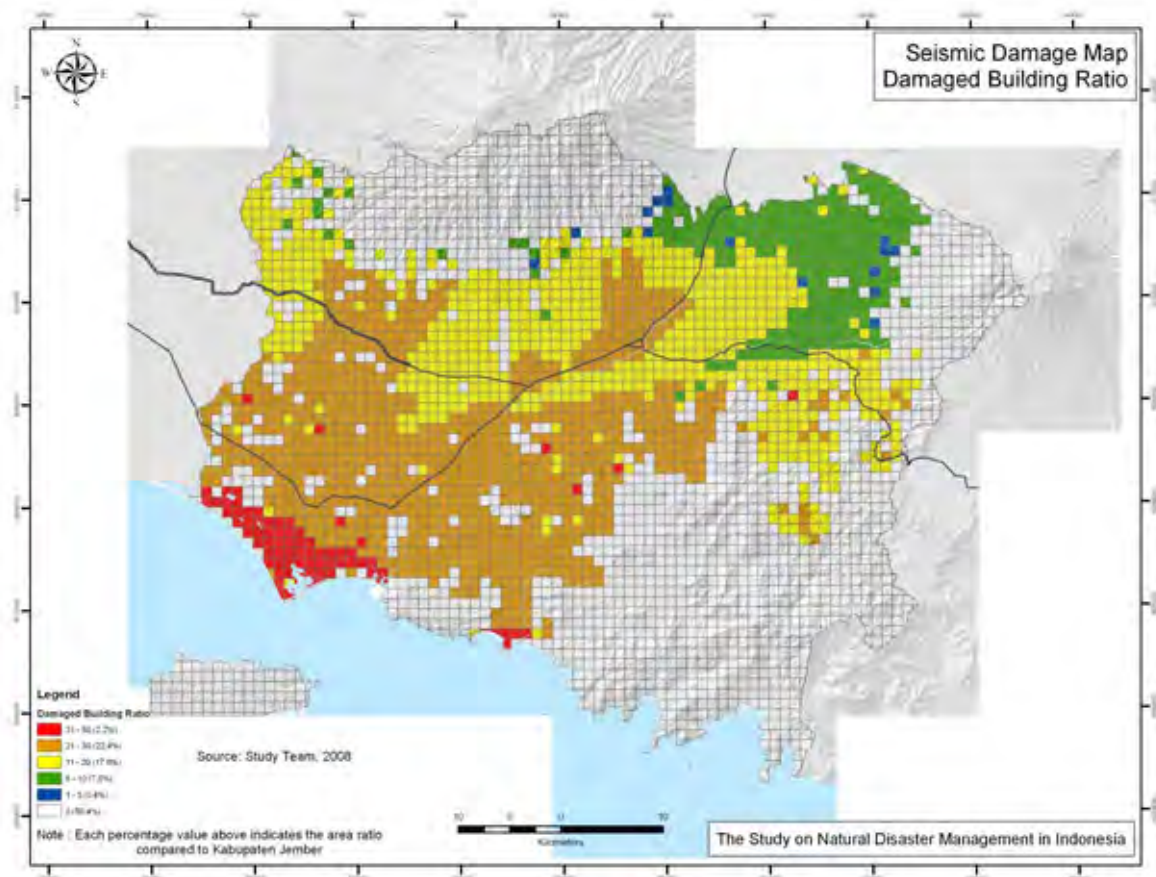
The intensity of surface ground motion differs according to the location. The vulnerability of the building also differs according to the building type. For instance, the reinforced concrete building, which was designed and constructed through modern design concepts, is sustainable with 10% or less of damage ratio even if the intensity of surface ground motion is equal to MMI 8 or more, but the unreinforced masonry building may suffer damage with near to 90% of damage ratio. There is some difficulty to wrap up the risk map to only one figure because of above situation.

Figure 3.1.13 shows the expected number of damaged buildings that are located in each grid square of  $1\text{km} \times 1\text{km}$ . The tendency of the distribution of damaged buildings that depends on vulnerability of existing buildings is shown. In a word, there is high risk at the location where vulnerable buildings exist.



**Figure 3.1.13 Building Damage Per Grid**

Figure 3.1.14 shows the value of the expected number of damaged buildings divided by the total number of existing buildings that is located in each grid of  $1\text{km} \times 1\text{km}$ . This indicates the average damage ratio for each grid and thus shows the tendency more clearly than previous Figure 3.1.13.



**Figure 3.1.14 Building Damage Ratio Per Grid**

It is felt strongly that the accuracy of building database is very important for this kind of study because above shown study results indicate that the difference of vulnerability in each building type is a dominant factor of damage distribution. Ratio of each building type is shown in Figure 3.1.15 These figures are shown in order to obtain an overview of the building data. Currently, the area of each survey unit is uneven. Some of them are corresponding to Kecamatan; some of them are corresponding to Nagari. Especially, the most northern survey unit is very large and built up areas are concentrated there. This kind of inconsistency of statistics data may skew the analysis. This is the reason why effort of data collection must be continued and improved.

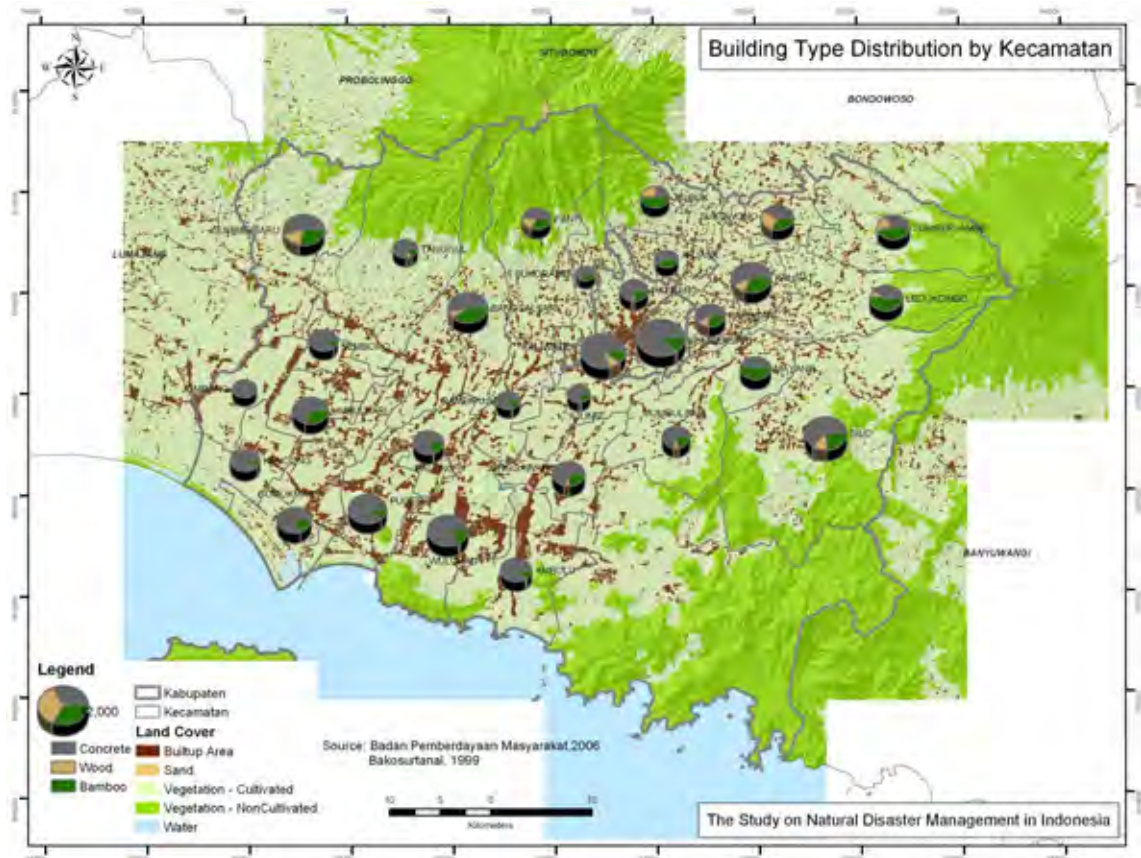


Figure 3.1.15 Number of Buildings in Each Survey Unit and Ratio of Each Building Type

There are some common points of building structure and distribution of building type in Indonesia. Aspects of building construction method and its variety are discussed below.

**(1) Timber made and Bamboo made**

This is a comparatively old type of construction method. There are some 100-year old buildings of this type in study area. Two types of structure are found: one is dressed timber made or elemental bamboo made frame structure, and the other consists of column and wall made of slim wood strings or bamboo strings grouted with lime or mortar. There are several types of structure details according to the region. Earthquake resistant capacity of these buildings is generally better than masonry and Confined masonry, but many examples with badly designed or deteriorated condition are found.



**Figure 3.1.16 Timber Made and Bamboo Made**

**(2) Brick Masonry**

The bearing wall thickness of most of brick masonry in this area is as much as one brick. Matters which should be obeyed on masonry construction are hardly paid attention to. There are problems of quality of brick and grout in many cases.



**Figure 3.1.17 Brick Masonry**

### (3) Cobble masonry

There are many cobble masonry buildings in the area far from the main street. Earthquake resistant capacity of this type is very poor because of lack in grip effect between each cobble and poor quality of grout.



**Figure 3.1.18 Cobble Masonry**

### (4) Confined masonry

This building type is becoming the major type in recent years. Regarding confined masonry bearing wall itself resists against load. RC made column, beam and lintel only give confinement effect to bearing wall. This is the difference between confined masonry and RC frame. Dimension of RC made members of confined masonry is smaller than that of RC frame. Earthquake resistant capacity of this type is better than unreinforced masonry, but considerably poorer than RC frame with modern design concepts.



**Figure 3.1.19 Confined Masonry**

**(5) Reinforced Concrete Moment Resisting Frame**

Buildings of Reinforced Concrete Moment Resisting Frame (RCMRF) resist against load by its frame consisting of column and beam, although its appearance is similar to confined masonry. Walls of most RCMRF buildings in this study area are made of brick. This kind of wall can not be a bearing wall, they are partition walls, because brick wall may lose its stiffness when the frame is deformed by inertia force caused by earthquake. Of course the wall can resist against inertia force caused by earthquake if it consists of Reinforced Concrete Shear Wall but effective shear walls can rarely be seen in this study area.



**Figure 3.1.20 Reinforced Concrete Moment Resisting Frame**

**(6) Combination of different kind construction method**

There are many buildings with combination of different kinds construction methods in this study area. Different kinds construction methods tend to be applied when the building is extended after some time interval. Serious destruction can start at the boundary of this kind combination when earthquake hits as was seen in examples damaged during 2007 Solok earthquake.



**Figure 3.1.21 Combination of Different Kinds of Construction Methods**

The following situation is seen in study area regarding building distribution

**(1) Building density**

Most buildings are concentrated in very limited area and other area is less-populated. Generally speaking, this tendency works advantageously during earthquake damage because interference between neighboring buildings under quake phenomenon does not happen easily. Empty space can be found to use as an urgent support center easily after an earthquake.

**(2) Building Type**

Comparatively modern building types like as RCMRF or confined masonry are dominant in the main street; on the other hand, old building types like as masonry, timber made and combination of different kind construction methods exceed modern building types in the areas far from main street. Especially cobble masonry, which can be seen a lot in the area far from main street, does not have sufficient earthquake resistant capacity.

**(3) Comparatively modern and old**

Confined Masonry building is becoming the majority in recent years. It is thought that this type of construction method can achieve almost sufficient earthquake resistant capacity if it is designed and constructed in a careful manner. At least it has greater capacity than stone masonry or brick unreinforced masonry. It is close to RC building capacity even though it is not equal. Actually some researchers offer the results of experiments and instructional books in order to obtain structural capacity. However there can be found a lot of examples that were constructed without sufficient attention in this study area.

The following points are found frequently:

- Bricks are not soaked in water before piling up (Sufficient water is needed for the hydration reaction of cement in grout)
- Situations in which a building is seen as a whole load path system are not present
- Opening in bearing wall is excessively large
- Dimension of confinement members is not sufficient
- Detail of reinforcing bar is not sufficient
- Compaction of concrete is not sufficient
- Inadequate aggregate (pumice stone)
- Stiffness and bearing capacity of foundation is not sufficient

### **3.1.4 Possible Countermeasures against Earthquake in Kabupaten Jember**

#### **1) Structure measure**

Only strengthening of structure done beforehand is effective to mitigate human damage because structural damage due to earthquake occurs quite suddenly, and we can not prepare any effective warning system. Any effort done after earthquake can not be effective to reduce the number of human lives lost. Rescue activity and supporting activity have to be done after earthquake occurrence, but those efforts hardly reduce lives lost.

Strengthening measures are as follows:

##### **(1) Consolidate building permission and supervising system**

In many cases, individually owned buildings are not built by a specialist, but rather by inexperienced amateurs or workmen who did not pass professional instruction.

Building permissioning and supervising system was established already, but not necessarily all permits were applied for. There have been a lot of application leakages. Even for investigation on structural issues is generally loose. In addition, most buildings are usually built without any public supervision. If these defects are not going to be solved, every earthquake with considerable size may cause a large number of casualties.

##### **(2) Consolidate diagnosis system for existing building**

##### **(3) Encourage earthquake strengthening in existing building**

There can not be the concept of “Existing nonqualified building” because building permission and supervising system is not functioning currently. However existing weak buildings have to be reconstructed if they are evaluated as “nonqualified” through the diagnosis. If it is not possible to reconstruct every building, the next best thing to do is to strengthen existing buildings. The fundamental principle of strengthening is to specify the weak point of the building and to improve capacity of that weak point. Dominant weak points found in this study area are as follows:

#### **A. Rigidity shortage of roof and floor**

There can be seen many one-story buildings, which do not have any lintel or roof slab, in this study area. As a result that building does not have sufficient rigidity in roof level so collapse because of twisting motion during earthquake is likely. As countermeasures, additional lintel or additional roof slab had better be set up.



**Figure 3.1.22 Building with no Lintel and Roof Slab**

### **B. Capacity shortage of brick masonry wall**

Brick masonry wall is weak to force in an out-of-plane direction.

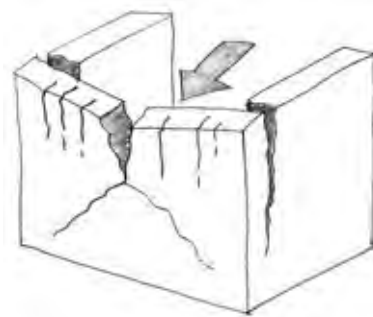


**Figure 3.1.23 Destruction by Force in Out-Of-Plane Direction**

Many kinds of reinforcement methods are proposed to prevent this type destruction. For instance, it is reported that reinforcement using meshed steel wire and cement mortar is effective as measures. However brick column or brick wall with small cross section can not have sufficient bearing capacity. This kind of member has to be changed to reinforce the concrete member.

### **C. Defect of connection part of combined building**

Serious kind of destruction can start at connection part of combined building.



**Figure 3.1.24 Example of Connection Part**

Even if the different kinds of construction methods are connected, the shape of each single construction part must be completed. However some kind of unfit end tends to be left at the connecting part. That kind of unfit may generate extraordinary concentration of force that causes decay. Demolishing and reconstruction is recommended when the effect of unfit shape is serious.

**(4) Encouragement of rebuilding**

Effort to make a financing system of the earthquake strengthening construction capital should be made for people who have a concrete plan of earthquake strengthening construction.

**(5) Education regarding earthquake resistance of building**

**2) Non structural measures**

It is not possible to reduce human casualties by implementing non structural measures, but still it is beneficial to make advance preparations toward emergency rescue, life support and relief. The preparation for that is as follows:

**(1) Securing temporary shelter place**

**(2) Preparing and Stock materials in emergency**

**(3) Mutual support agreement with the administrative organization in the vicinity**

**(4) Establishment Cooperation method with disaster prevention organization of central government**

**(5) Establishment of Post-Earthquake Temporary Risk Evaluation system**

**(6) Educate and hold drills for the organizations and the residents in the region**

## **3.2 Disaster Characteristics of Earthquake and Countermeasures in Kabupaten Padang Pariaman**

### **3.2.1 Disaster Characteristics of Earthquake in Kabupaten Padang Pariaman**

#### **1) Earthquake Disaster in the past**

A history of previous disasters can offer effective lessons for mitigation because comparatively large earthquake disasters occur periodically. In fact, the earthquake is a phenomenon which happens together with the movement of the lithospheric plate. There is some periodicity in the occurrences of large earthquakes although the movement speed of lithospheric plate is nearly constant. The return period of large earthquakes, which may have a big influence, is considerably long compared to human life (i.e. 200~1000 years). Therefore, even a person who lives in one region for a long time can hardly experience such as large seismic hazard. There are few documented historical facts or study's findings obtained by archaeological survey regarding the earthquake in Indonesia. However, this tendency does not mean that big earthquakes do not occur in that region. Plate tectonic surroundings and the past occurrences of earthquakes needs to be discussed widely to ensure accurate understanding of frequency and magnitude of seismic hazard. Actually, the earthquake hazard in Indonesia is more frequent than that of Japan if we count only the earthquake by which 100 lives or more were lost using "Uzu Database" or "USGS Database". Of course, the total human damage due to the earthquake is discussed here. Damage due to tremor is not discussed separately from damage due to seismic sea wave.

**Table 3.2.1 Earthquake by Which 100 Lives or More were Lost in Indonesia (1/2)**

(Web:[http://iisee.kenken.go.jp/utsu/utsuweq\\_bak.html](http://iisee.kenken.go.jp/utsu/utsuweq_bak.html))

Year	Month	day	Latitude	Longitude	Depth	M	Death	Injured	Remarks
1716	9	10	-1.0	120	--	--	many	--	Indonesia(Java/Sumatra)
1674	2	12	-3.5	128.2	--	--	2342	--	Indonesia(Moluccas) Amboina
1792	2	12	--	--	--	--	300	--	Indonesia(Sumatra) Padang
1815	11	27	-8	115.2	--	--	10254	--	Indonesia(Bali)
1820	12	29	-7	119	--	7.5	400	--	Indonesia(Sulawesi) Makassar, Bone, Lembang
1828	12	29	-2	121	--	--	many	--	Indonesia(Sulawesi) Macassar, Bone, Lembang
1835	11	1	-3.4	128.1	--	--	149	--	Indonesia(Moluccas) Amboina, Haruku, Saparua
1846	2	14	0.5	127.3	--	--	many	--	Indonesia(Moluccas) Ternate, Is.
1856	3	2	3.5	125.5	--	--	3000	--	Indonesia(Great Sangei Volcanic)
1861	2	16	0.5	97.5	--	8.4	great	--	Indonesia(Sumatra) Lagundi, Padang, Batu L. Nias I
1861	3	9	0	98	--	7	750	--	Indonesia(Sumatra) Padang, Batu Is., Simuk D=200
1864	5	23	-3	135	*	--	250	--	Indonesia(Irian Jaya) Geobink, Elay
1867	6	10	-7.8	110.5	--	--	327	--	Indonesia(Java) Djakarta, Soerakarta
1871	3	2	0	128	--	--	400	--	Indonesia(Moluccas) Tagulandang Is., Dublan
1883	8	27	-5.8	106.3	--	--	Several tens of thousands	--	Indonesia Krakatoa
1890	12	12	-6.4	111	--	--	many	--	Indonesia(Java) Djawana(Japara) D=100 D=some
1896	4	18	-8.3	126	--	--	250	--	Indonesia(Timor/Alor) D=80
1899	9	29	-3	128.5	--	7.4	3864	--	Indonesia(Moluccas) Ceram(south coast) 7.1S
1907	1	4	2	96.3	6	7.8	400	--	Indonesia(Sumatra) Gunung Sibol(Nias) 7.5S
1909	6	3	-2.5	101.5	--	7.5	200	--	Indonesia(Sumatra) Korint, Djambi 7.3S
1914	6	25	-4	102.5	--	8.1	many	many	Indonesia(Sumatra) Benkulen D=11/20 7.6S
1917	1	21	-8	115.4	--	6.5	18000	--	Indonesia(Bali)
1924	11	12	-7.2	109.5	--	--	609	--	Indonesia(Java) Wonosobo D=many/60
1924	12	2	-7.3	109.9	--	--	115	--	Indonesia(Java) Wonosobo
1924	12	22	--	--	--	--	113	--	Indonesia(Java) Wonosobo
1926	6	28	-0.5	100.5	--	6.8	222	--	Indonesia(Sumatra) Padang Highlands 新層
1926	6	29	--	--	--	--	400	--	Indonesia(Sumatra)
1928	8	4	-8.3	121.7	--	--	226	--	Indonesia(Palembang Is.(Bokandia Volcano)
1943	7	23	-9.5	110	90	8.1	213	--	Indonesia(Java) Yogyakarta 7.6S
1964	1	4	-1.9	102.3	33	6.7	110	479	Indonesia(Sumatra)
1964	4	2	5.8	95.7	132	7	110	479	Indonesia(Sumatra)
1968	8	14	0.16	119.78	23	7.4	392	--	Indonesia(Sulawesi) D=200 7.3S
1969	2	23	-3.12	118.87	13	6.9	600	--	Indonesia(Sulawesi) D=64 H=97
1976	6	25	-4.6	140.09	33	7.1	6000	--	Indonesia(Irian Jaya) D=422
1976	7	14	-8.17	114.89	40	6.5	563	2300	Indonesia(Bali)
1976	10	29	-4.52	139.92	33	7.2	6000	--	Indonesia(Irian Jaya) D=108/133(E=8)
1977	8	19	-11.09	118.46	33	7.9	189	75	Indonesia(Sumbawa Is. EQ)
1981	1	19	-4.58	139.23	33	6.7	1300	--	Indonesia(Irian Jaya) Jayawijaya Mts. D=261 6.6W
1989	8	1	-4.51	139.02	14	5.8	120	125	Indonesia(Irian Jaya) Kurima D=90 6.1W
1992	12	12	-8.48	121.9	28	7.5	1740	2144	Indonesia(Flores) Maumere, Babi Is. D=2080 7.7W
1994	2	15	-4.97	104.3	23	7	207	2000	Indonesia(Sumatra) Liew(Lampung Prov.) 6.9W
1994	6	2	-10.48	112.84	18	7.2	277	423	Indonesia(SE coast of Java/Bali)
1996	2	17	-8.89	136.95	33	8.1	166	423	Indonesia(Irian Jaya) Bink, Suptori 8.2W
2000	6	4	-4.72	102.09	33	8	103	2585	Indonesia(Sumatra) Bengkulu D=90 I=2174 7.9W
2004	12	26	3.3	95.98	30	8.8	Several tens of thousands	Several tens of thousands	Indonesia(Sumatra) D=90 Landslide, mud volcano 9.0W

**Table 3.2.2 Earthquake by Which 100 Lives or More were Lost in Indonesia (2/2)**

(Web:<http://infotrek.er.usgs.gov/>)

Year	Mnth	Day	Time	Longitude	Latitude	Depth	Magnitude	Tsunami	Death	Injured	Damage	Note
1986	5	28	1327J	-2.91	139.32	85	7.7	-	-	0	limi	Indonesia(Irian Jaya) 7.2E
1986	8	10	0207J	1.42	126.22	33	7.6	T	-	0	limi	Indonesia(Malucca Passage) 7.5S
1986	8	14	2214J	0.16	119.78	23	7.4	T	392	0	seve	Indonesia(Sulawesi) D=200 7.3S
1989	1	30	1029J	4.81	127.44	70	7.9	-	-	0	-	Indonesia(Talau) 7.1E
1971	1	10	0717J	-3.13	139.7	33	8.1	-	-	0	made	Indonesia(Irian Jaya) Djajapura, Sentani 7.9S
1971	2	4	1533J	0.65	98.84	33	7.1	-	-	0	limi	Indonesia(Sumatra) Ntal, Sibolga, Tarutung, Pasaman
1972	6	11	1841J	3.94	124.32	325	7.5	-	-	0	-	Indonesia(Celebes Sea) 7.4E
1976	6	25	1918J	-4.6	140.09	33	7.1	-	8000	0	seve	Indonesia(Irian Jaya) D=422 Missign=9千 6.8S
1976	10	29	0251J	-4.52	139.92	33	7.2	-	8000	0	cars	Indonesia(Irian Jaya) D=108/133(E=8)
1977	8	19	0808J	-11.09	118.46	33	7.9	T	189	75	made	Indonesia(Sumbawa Is. EQ) 8.1S 8.3W
1979	9	12	0517J	-1.68	136.04	5	7.9	T	15	many	seve	Indonesia(Irian Jaya) Yapan 7.7S 7.3W
1984	11	17	0849J	0.2	98.03	33	7.2	-	0	1	limi	Indonesia(D'ff W. Sumatra/Nias Is. D=1 7.1W
1985	11	17	0940J	-1.64	134.91	10	7.1	-	0	0	limi	Indonesia(Irian Jaya) Mandowai 7.1W
1990	4	18	1339J	1.19	122.85	26	7.4	-	3	25	some	Indonesia(Sulawesi) Bolaang-Garontara area 7.8W
1991	6	20	0518J	1.2	122.79	31	7.?	-	0	0	-	Indonesia(Sulawesi) Garontala(Minahassa Pen.) 7.5W
1992	12	12	0329J	-8.48	121.9	28	7.5	T	1740	2144	seve	Indonesia(Flores) Maumere, Babi Is. D=2080 7.7W
1994	1	21	0224J	1.02	127.73	20	7.2	-	7	40	made	Indonesia(Ialmahera) Kou area 7.0W
1994	2	15	1707J	-4.97	104.3	23	7	-	207	2000	cars	Indonesia(Sumatra) Liew(Lampung Prov.) 6.9W
1994	6	2	1817J	-10.48	112.84	18	7.2	T	277	423	cars	Indonesia(SE coast of Java/Bali) Tsunami 7.7W
1995	3	19	2353J	-4.18	135.11	33	7.1	-	0	0	limi	Indonesia(Irian Jaya) Ayam, Fakfak, Nabire 6.9W
1996	1	1	0803J	0.73	119.93	24	7.6	T	10	-	some	Indonesia(Sulawesi) Minahasa Pen. 7.9W
1996	2	17	0559J	-0.89	136.95	33	8.1	T	186	423	cars	Indonesia(Irian Jaya) Bink, Suptori 8.2W
1996	2	17	1459L	-0.89	136.95	33	8.1	T	0	0	0	Indonesia Chichijima 103cm, Shionomisaki 96cm 8.2W
1996	11	29	1410J	-2.07	124.89	33	7.7	-	41	161	cars	Indonesia(Ceram Sea) Mangale, Talabu(Manado) 7.7W
2000	5	4	0421J	-1.11	123.57	26	7.5	T	46	284	cars	Indonesia(Sulawesi) Luwuk, Banggai, Peleng 7.8W
2000	6	4	1828J	-4.72	102.09	33	8	-	103	2585	cars	Indonesia(Sumatra) Bengkulu D=90 I=2174 7.9W
2002	10	10	1050J	-1.76	134.3	10	7.7	T	8	many	cars	Indonesia(Irian Jaya) Faut, Slope Failure 7.6W
2002	11	20	128J	2.82	96.09	30	7.6	-	3	85	made	Indonesia(Simulu) 7.4W
2003	5	26	1923J	2.35	128.85	31	7.1	-	1	7	limi	Indonesia(Ialmahera) Erebere 7.0W

Frequency and magnitude of earthquake must be discussed observing the characteristics of surrounding plate structure and past occurrence of big earthquakes. Indonesia has a plate boundary in southern part of Sumatra and Java Island. The oceanic plate subducts towards the bottom of the island. The subduction zone is located in Sunda Trench. A very big earthquake caused by reverse fault occurs in this subduction zone.

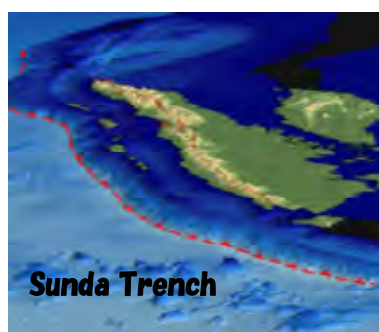


**Figure 3.2.1 Sunda Trench**

Recent impressive earthquakes generated in this zone are Andaman earthquake 26 Dec. 2004 M<sub>w</sub>9.1 and Bengkulu earthquake 12 Sep. 2007 M<sub>w</sub>8.4. Structure damage caused by tremor of this earthquake tended to be considered less serious because damage caused by seismic sea wave is so dominant. Certainly, the surface ground motion at these disaster areas is less than the value estimated considering magnitude of earthquake source. Two factors contribute to this tendency: one is rupture speed of these fault which is comparatively slow and the other is hypocentral distance from population concentration area which is long. However large damage is usually caused even by not so large earthquake motion because earthquake resistant capacity of residential buildings in this area is quite low.

Another dominant earthquake source is The Great Sumatran Fault that is located through the Sumatra Island. Mechanics of this fault are dextral strike-slip fault. Magnitude of earthquakes generated at this fault is slightly smaller than that of subduction zone, but the surface ground motion and damage can be seriously large if population concentration area is located near to the fault.

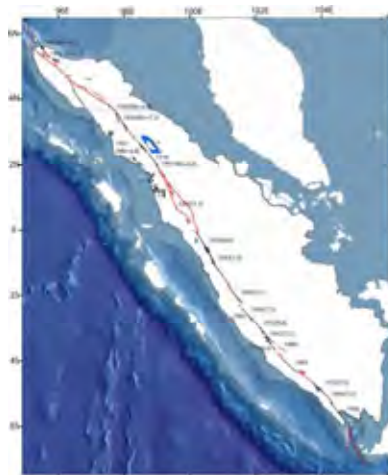


**Figure 3.2.2 The Great Sumatran Fault**

Recent impressive earthquakes generated in this fault are Solok earthquake 6 March 2007 6.4, and Mw 6.3. Two particular earthquakes were generated during 2 hours at south east side of Singkalak lake and north west side of it.

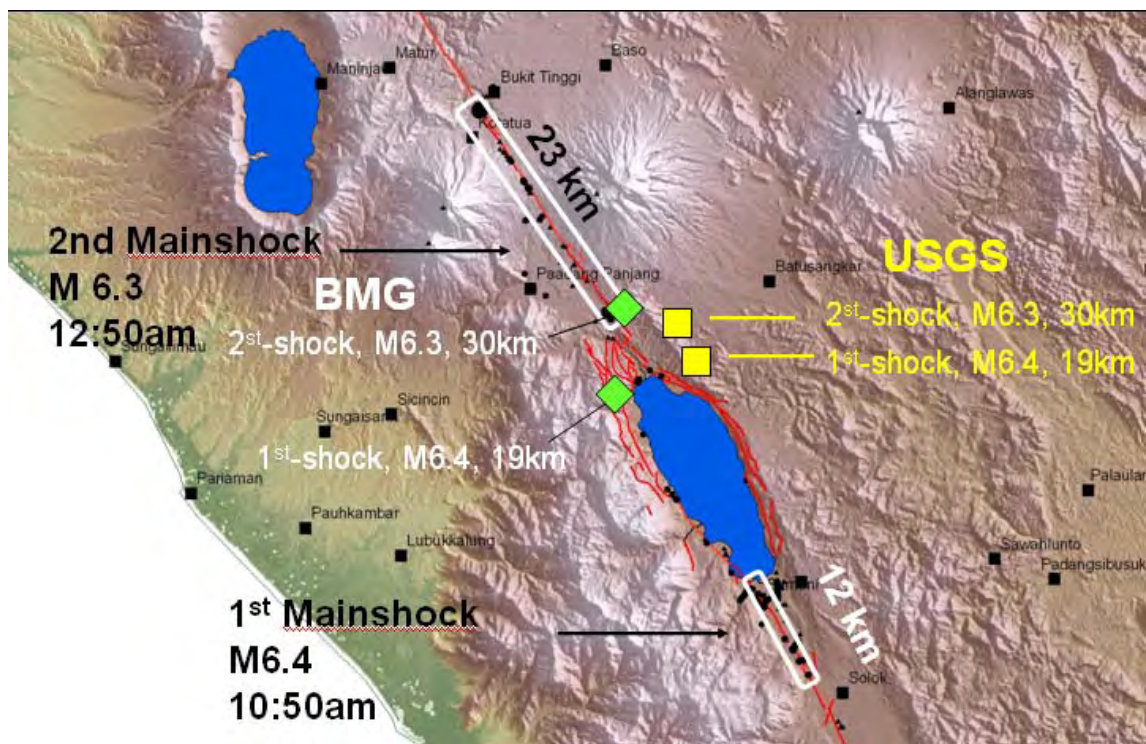


**Figure 3.2.3 Fault of Solok Earthquake 6 March 2007**

Source: (DANNY HILMAN NATAWIDJAJA, ADRIN TOHARI, EKO SUBOWO, AND MUDRIK R. DARYONO : A Review On The Sumatran Fault Zone And The 6 March 2007 Events (M 6.4 & 6.3) In Singkarak Lake, Central Sumatra, APRU/AEARU Research Symposium on Earthquake Hazards around the Pacific Rim June 21-22, Nikko Hotel, Jakarta, Indonesia) Geoteknologi LIPI

There was another example of near-field earthquake at Yogyakarta city (i.e, 27 May 2006 Yogya Earthquake  $M_w$  6.5). The relationship between damage and surface ground motion intensity in Kabupaten Bantul was referred to as a benchmark of the vulnerability function in this report.

The above-mentioned seismic circumstance is also very similar to Japanese circumstance, so Japan experiences regarding earthquake hazard needs to be used.

## **2) Factors for Damages due to Earthquake**

Damage of earthquake disaster is divided into following three aspects:

1. Structure damage due to ground tremor
2. Damage due to capacity shortage of ground such as slope failure or liquefaction
3. Damage due to seismic sea wave

It is pointed that the aspects of above 1 and 2 tend to be forgotten after an earthquake because the damage due to seismic sea wave gives overwhelming impression to victims. The aspects of above 1 and 2 are absolutely different from the sea wave because we can have some leeway to mitigate damage due to seismic the sea wave. However structural damage due to ground tremor occurs quite suddenly. Any warning can not be effective. Only strengthening of structure done beforehand is effective to mitigate damage. Any effort done after earthquake can not be effective to reduce the number of human lives lost.

### **3.2.2 Earthquake Hazard Map in Kabupaten Padang Pariaman**

#### **1) Basis of Hazard Map Creation for Earthquake**

The meaning of the word “Hazard” is defined as the cause of disaster. Therefore, regarding earthquake, only the distribution of the ground surface acceleration intensity must be shown in “Hazard Map”. No other aspect is necessary for Hazard Map for the above definition.

The ground surface acceleration intensity is described at each part of mesh in study area using the title of “Peak Ground Acceleration” (it is called as PGA here in after) or “Modified Mercalli Intensity scale” (it is called as MMI here in after).

Next topic, which is discussed in this chapter, is how to define the target value of the ground surface acceleration intensity. Generally there is a steady tendency of the relationship between the magnitude of earthquake and frequency of occurrence. So this means that small earthquake can occur frequently, but large earthquake rarely occur so frequently.

Figure 3.2.4 shows the relationship between the magnitude of earthquake and frequency of occurrence regarding earthquakes that occurred from 1629 to 2004 in Indonesia.

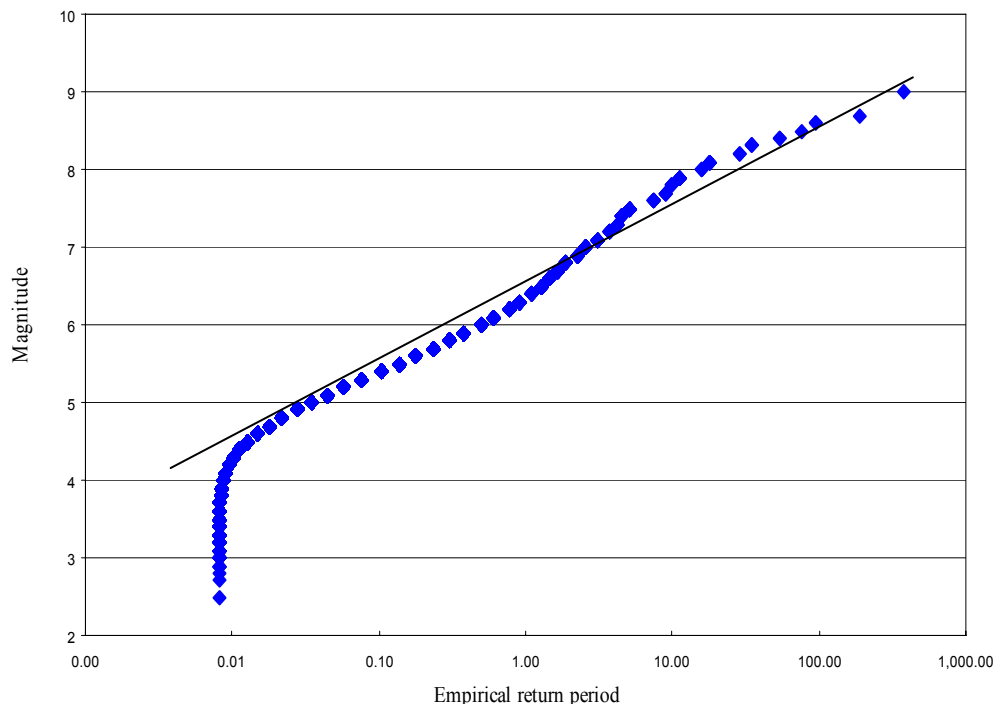


**Figure 3.2.4 Relation between Magnitude and Return Period**

Y axis means magnitude of the earthquake, and X axis means empirical return period  $T_E$ .

$$T_E = \frac{T_S}{m} \tag{Eq. 3.3}$$

Where

$T_E$  : Empirical return period

$T_S$  : Sampling term

$m$  : Order when the sample is arranged in magnitude order

For example, the largest earthquake generated in this area is the 2004 earthquake with magnitude 9, then order  $m$  is the first, Sampling term  $T_S$  is 2004 minus 1629 equal to 375, Empirical return period  $T_E$  must be 375 years. The large one in second is the 1833 earthquake with magnitude 8.7, then order  $m$  is the second, Sampling term  $T_S$  is 375 years divided 2 equal to 187, Empirical return period  $T_E$  must be 187 years. When the relationship between magnitude and the empirical return period  $T_E$  of each recorded earthquake is plotted in the same manner, the plotted pattern tends to be almost on straight line on one-half of logarithm graph paper, but limited in range of more than magnitude 5. This finding is called the thesis of Gutenberg Richiter or G-R formula. The angle  $b$  of this approximation line represents the difference between the occurrence frequency of big earthquake and that of small earthquake. If the surrounding of Indonesia is divided into some domains, which has consistent condition of seismicity, the above mentioned angle  $b$  must be

particular for each particular domain. If the occurrence of earthquakes is a spatially independent and independent time wise incident Poisson model can be applied to the analysis.

The peak acceleration value of the base rock at a certain point can be calculated utilizing attenuation formula. Attenuation formula is a kind of regression formula by which the peak acceleration value of the base rock is presumed from the magnitude of earthquake source and distance from earthquake source to a certain point.

In this computational procedure previously mentioned each domain must be further divided into small piece by utilizing polar coordinate system. In addition, an implicit method is needed in this procedure because the magnitude of earthquake source, which brings the peak acceleration value in a certain point, must be obtained at a computation step. Therefore a huge amount of the calculation is required in order to carry out this analysis. The computer program "EZFRISK" or "EQRISK" is used in an actual analysis. The peak acceleration value of the base rock at each part of Indonesia was calculated. Figure 3.2.5 shows the results of the above described procedure.

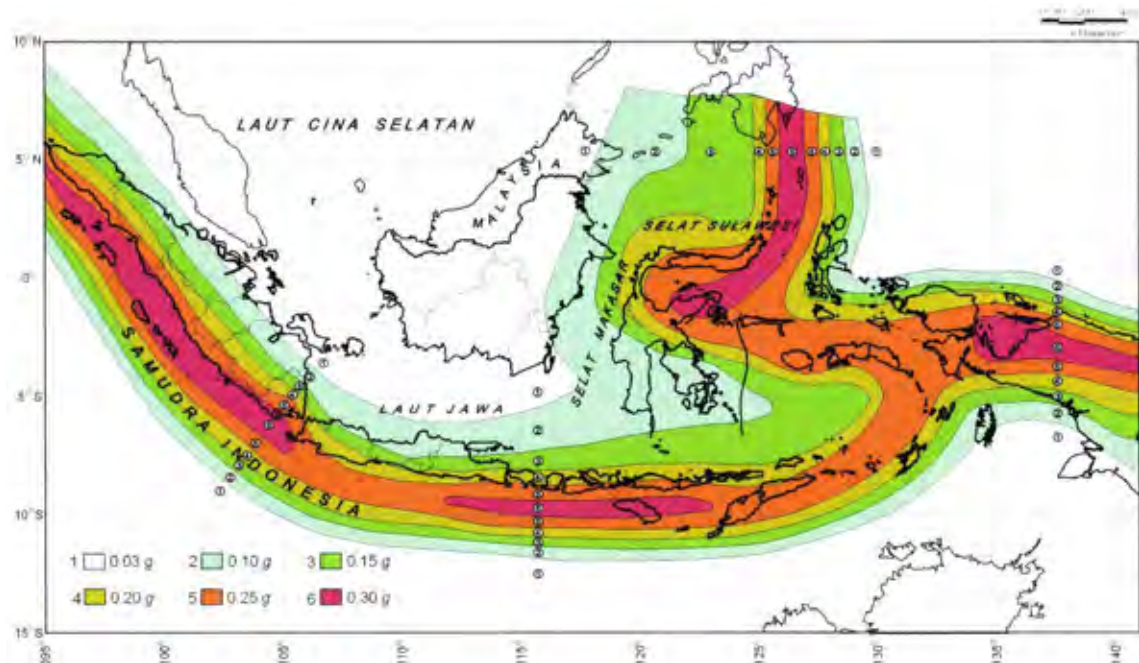


**Figure 3.2.5 Peak Acceleration Value of the Base Rock at Each Part of Indonesia (From SNI 03-1726-2002 the Indonesian code for seismic load)**

Each value shown in Figure 3.2.5 is the peak acceleration value of the base rock at each colored zone and corresponding 500 years of return period. For instance, almost part of Kabupaten Padang Pariaman belongs to Zone 5. Therefore the peak acceleration value of the base rock is 0.25g (the value of 0.25g means 0.25 times acceleration of gravity). Detail of zone around study area is shown in Figure 3.2.6.

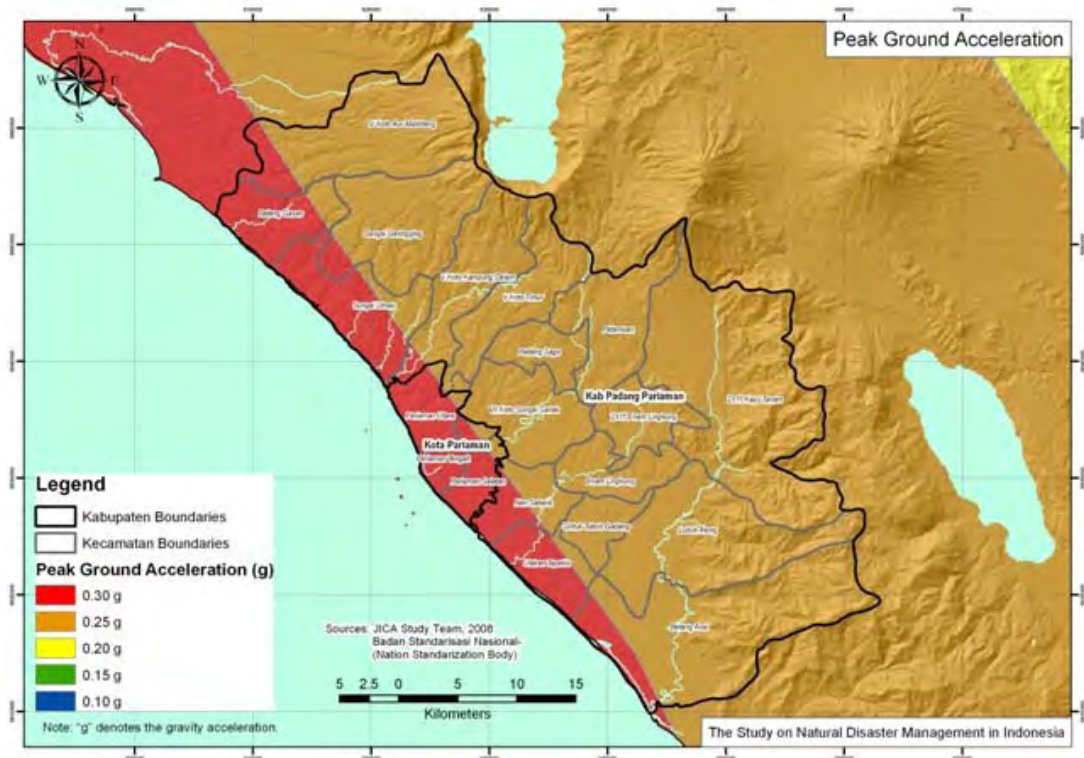


**Figure 3.2.6 PGA Ground Acceleration**

When concretely explaining the 500 years of return period it means that the probability of exceedance is 10% for 50 years. For example, if a structure, which has 50 years of service time, is designed utilizing the design seismic load of 500 years of return period the probability by which the structure will fall due to an unexpectedly large earthquake is 10%. Indeed 90% of incidents are comprised in this category. This setting is almost perfect in realistic meaning because 100% of safety can not be obtained using probability theory.

The above explained value is the peak acceleration value at the base rock that is defined as a base rock layer that is consisted of homogeneous material. The peak acceleration value at the base rock can be estimated utilizing attenuation function. However the value, which is needed for application of hazard map, must be the peak acceleration value at ground surface.

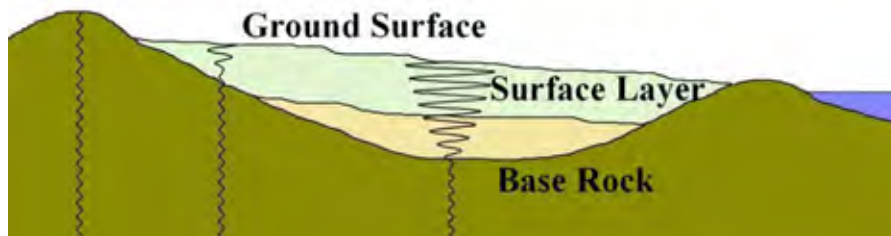


**Figure 3.2.7 Peak Acceleration Value of the Base Rock and Peak Acceleration Value of Ground Surface**

As explained in Figure 3.2.7 the ground tremor is amplified while it is propagated in the surface layer. In fact, the ground tremor at outcrop of base rock is usually small. On the other hand the ground tremor at the soft layer is usually large. Degree of amplification depends on characteristics of surface layer of the ground. Surface layer must be investigated in order to discuss this aspect. Geomorphological feature of surface layer around Kabupaten Padang Pariaman is shown in Figure 3.2.8.

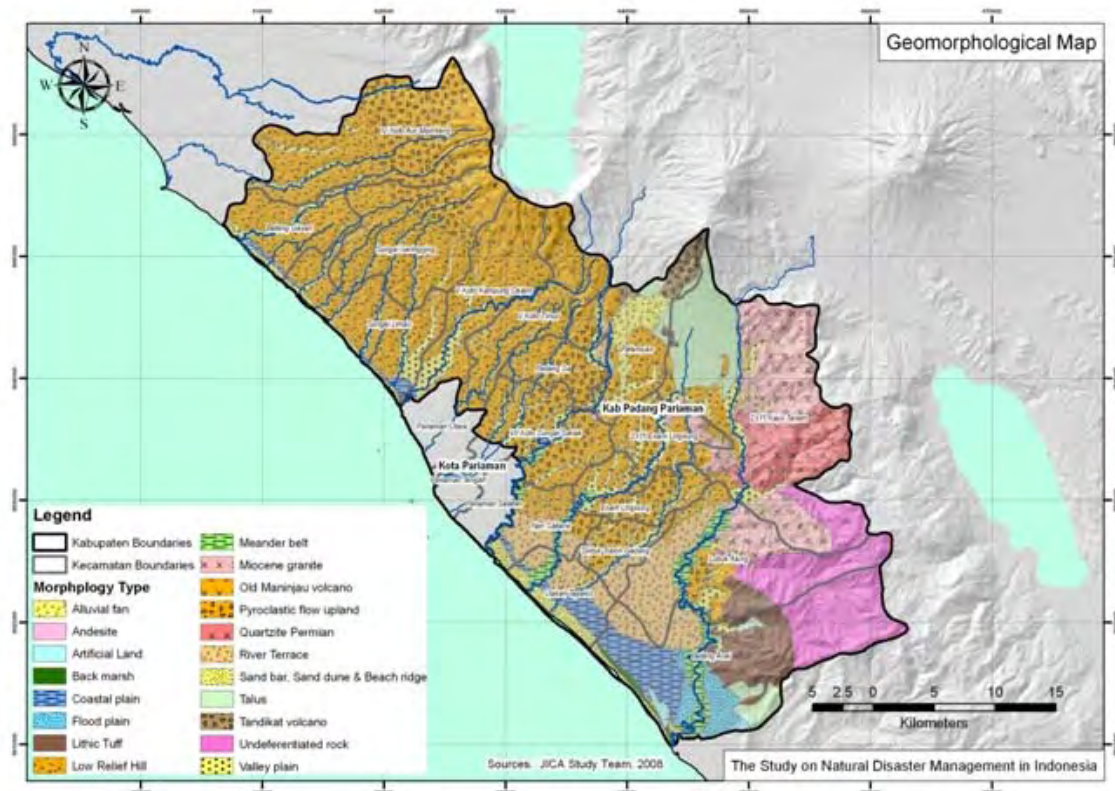


**Figure 3.2.8 Geomorphological Feature of Surface Layer around Kabupaten Padang Pariaman**

Distribution of characteristics of surface layer at each Segment of the study area is shown in Figure 3.2.9.

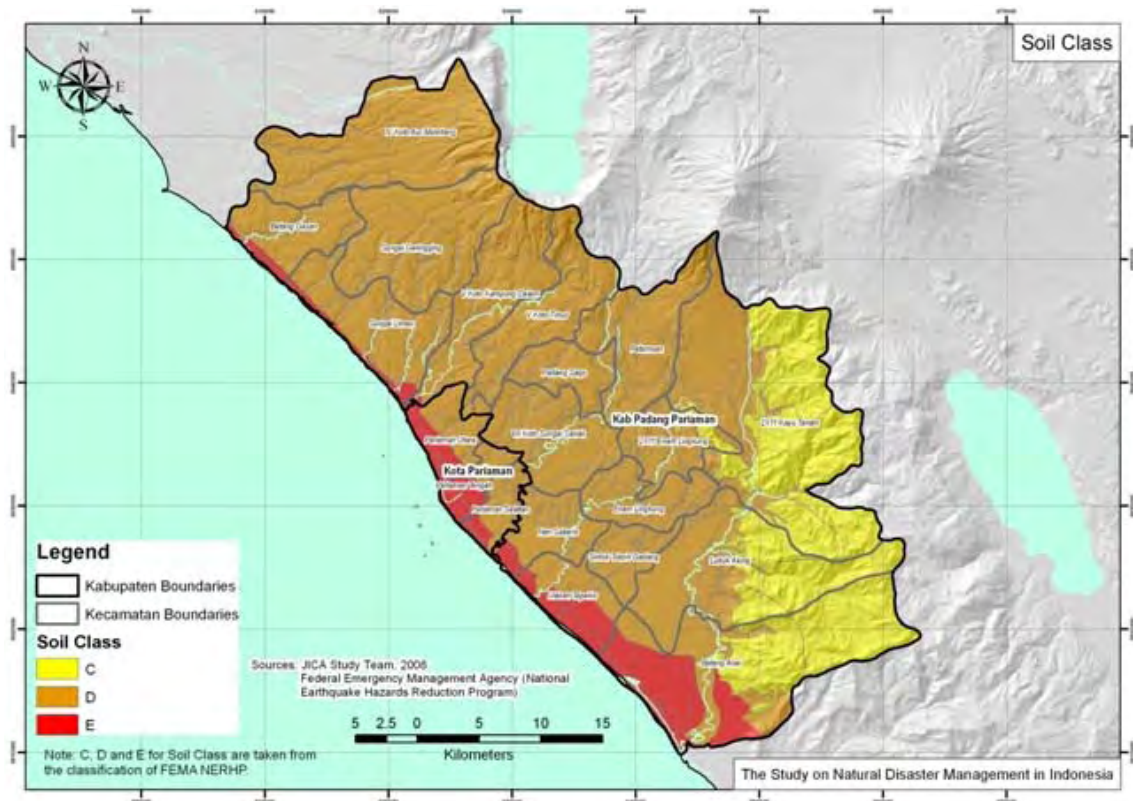


**Figure 3.2.9 Segmentation of Soil Class (classified according to stiffness of surface layer)**

Segmentation of soil class shown in Figure 3.2.9 is classified according to stiffness of surface layer. The classification is based on some speculations on geomorphological feature given by geological map and field survey done by the expert in charge of geological features. However more accurate material that will be given by borehole logging and PS logging must be referred if it is available. Moreover, continuous improving effort shall be made regarding accuracy of hazard mapping.

As explain here, the intensity of the surface ground motion at earthquake is estimated referring the zone classified in SNI 03-1726-2002 and the soil class. The surface ground motion is expressed by PGA and the response spectrum, shown in Figure 3.2.10. The value of vertical axis in the response spectrum means the acceleration response of the SDOF (Single degree of Freedom) model that has the natural period shown in the horizontal axis. Therefore the value on the extreme left correspond to PGA. This value of PGA shall be shown in the hazard map because these values represent the tremor of ground surface.

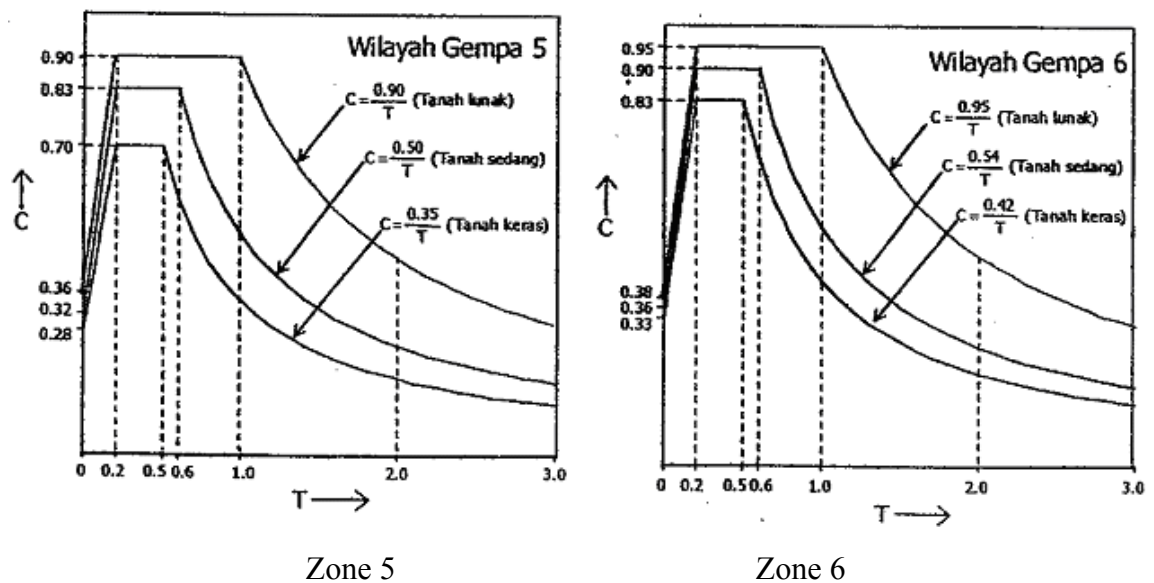


Figure 3.2.10 Response Spectrum Stipulated in 03-1726-2002

## 2) Earthquake Hazard Map in Kabupaten Padang Pariaman

The expected value distribution of the ground surface acceleration intensity is shown in Figure 3.2.11. The ground surface acceleration intensity is described using the title of PGA and MMI. PGA is a value which will be obtained as the maximum value when the quake of the ground level is measured with accelerograph. The modified Mercalli intensity scale (MMI) divides earthquake intensity into 12 stages of evaluation, and each stage is defined by describing the incident through observation and sensing (for example; "Difficult to stand"). Therefore expression of MMI is discrete number originally but one digit below the decimal point is written in this report in order to distinguish a detailed difference. The estimated MMI for Kabupaten Padang Pariaman is from 8 between 8 or more in the MMI display. This level of intensity corresponds to "5 or more" in Japan Meteorological Agency Seismic Intensity Scale (it is called as JMI hereafter). JMI also divides earthquake intensity into 10 stages of evaluation, and each stage is defined by describing the incident through observation and sensing. Some sort of slight damage is found when the earthquake of "5 or more" in JMI occur in Japan but it is thought that considerably more serious damage may be generated by the same level of earthquake in Indonesia because earthquake resistant capacity of Indonesian buildings is poor comparing with that of Japan.

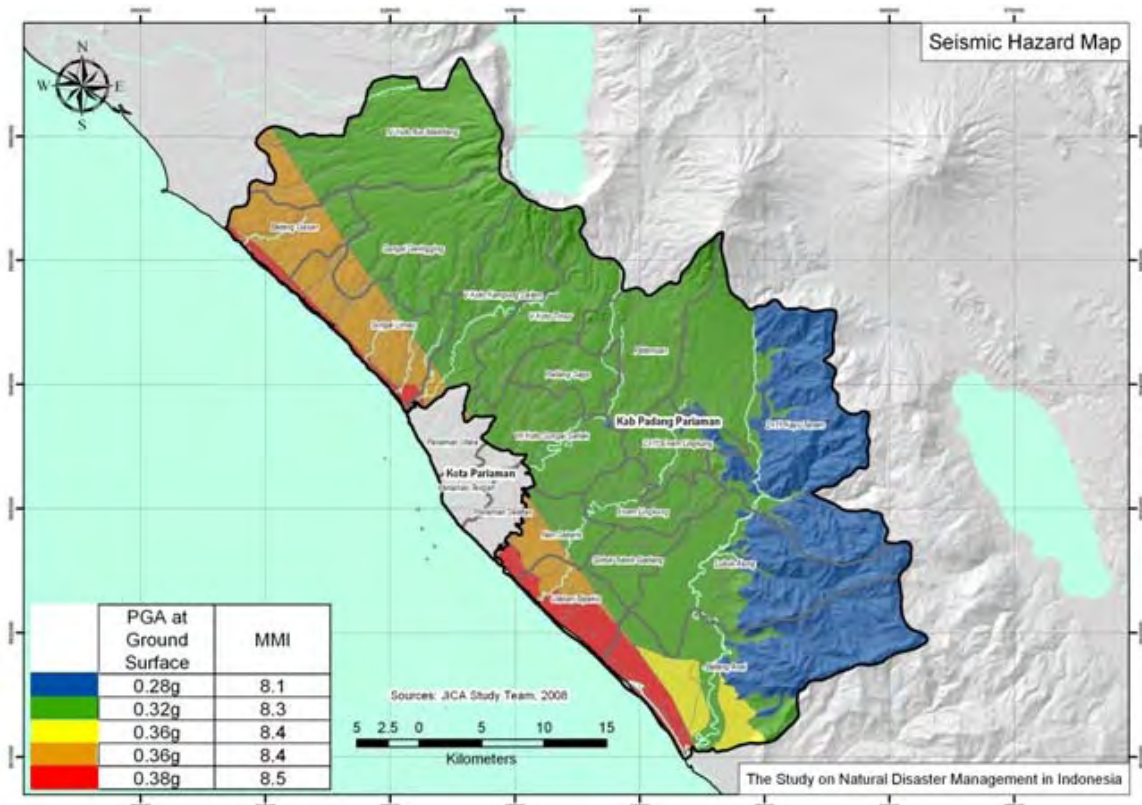
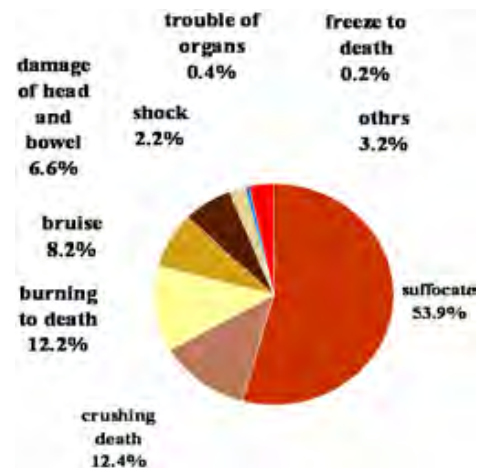


Figure 3.2.11 Expected Value Distribution of Ground Surface Tremor

### 3.2.3 Earthquake Risk Map in Kabupaten Padang Pariaman

#### 1) Basis of Risk Map Creation for Earthquake

Earthquake risk is an abstract concept by itself. So some definition or physical understanding must be supplied. Earthquake disaster risk is the possibility of destruction that can be analyzed as a synergistic result of earthquake hazard and vulnerability of a facility. Every aspect of the magnitude in earthquake disaster, including human loss and economical loss, can be evaluated based on structural destruction. In an actual disaster situation people are not killed by quake of ground but they are killed by collapsing of buildings. As shown in Figure 3.2.12 the majority cause of death in 1995 Great Hanshin Earthquake originated almost always in the collapse of the building. Therefore it can be said that it is indispensable to know how many buildings shall collapse when we discuss the risk of earthquakes.



**Figure 3.2.12 Ratio of the Cause of Death at 1995 Great Hanshin Earthquake**

Therefore Earthquake risk is defined as the damage ratio  $P$  under the condition of assumed ground motion and characteristics of the buildings. The damage ratio  $P$  is defined by Eq. 3.4.

$$P = \frac{N_D}{N_T} \quad (\text{Eq. 3.4})$$

Where,

$N_D$  : Number of damaged building

$N_T$  : Total number of existing building

In this context damaged buildings means the buildings that suffer equal or more “large damage” defined by Architectural Institute of Japan (AIJ). The damage grade “large damage” is strictly defined from the viewpoint of structure engineering. Generally, dead and injured are generated in the buildings that suffer equal or more “large damage”. That is why this grade was chosen for the target of this evaluation. This grade is also similar to “Grade 4 Very Heavy Damage” of European Macroseismic Scale (EMS).

The damage ratio  $P$  is assessed by utilizing the fragility function. The outline of the fragility function analysis utilized in this study is shown in Figure 3.2.13.

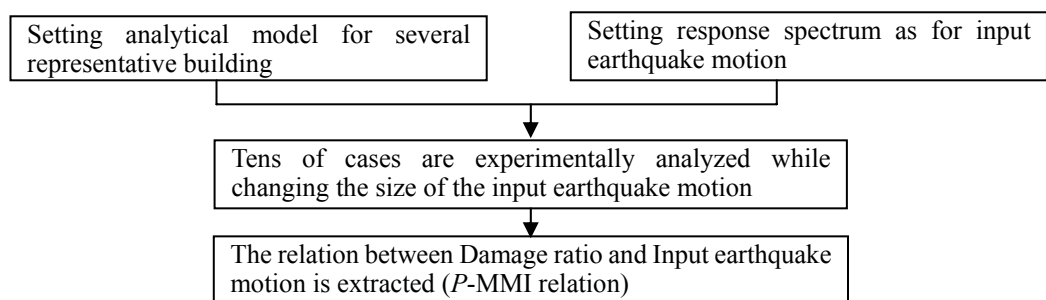


**Figure 3.2.13 Outline of Fragility Function Analysis**

The fragility function mainly depends on the characteristics of building structure. Therefore the buildings in the study area are divided into several building types and the typical building of each building type is modeled. Outline of building model is shown in Figure 3.2.14

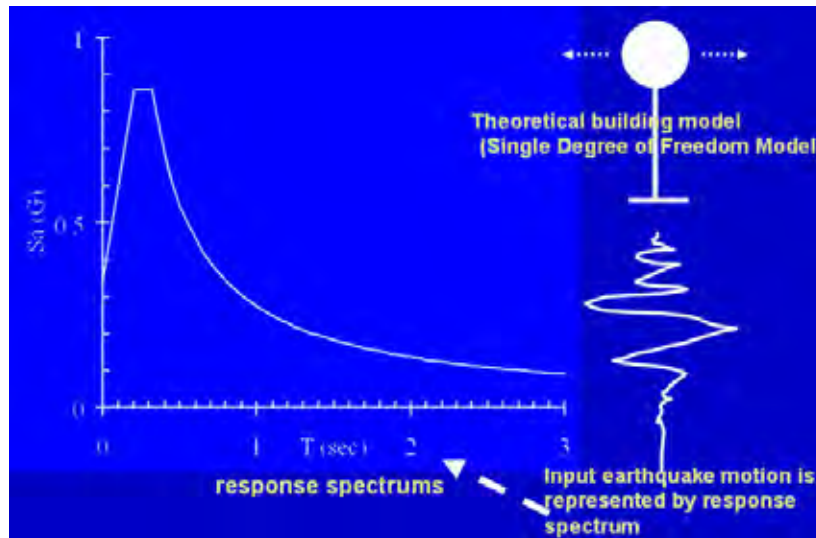


**Figure 3.2.14 Outline of Building Model**

Then a simplified dynamic analysis is carried out applying increasing earthquake input motion step by step. Then the relationship between MMI and the damage ratio  $P$  is obtained as a fragility function. The procedure to generate the relationship between MMI and the damage ratio  $P$  is common to the procedure done by committee of Japanese government and US Project “HAZUS” (see Appendix of this report).

A highly probable result can not be obtained when the sensitivity of the fragility function does not fit real earthquake resistance of the buildings in a corresponding study area. In this study some steps of calibration were carried out applying consideration through the research report of past earthquake disasters that occurred near the study area. The example of Yogyakarta city (i.e, 27 May 2006 Yogya Earthquake  $M_w6.5$ ) was a effective material to apply because a Japanese reconnaissance team reported the intensity of surface ground motion investigated through interview intended for the residents and some observation on damage state of the building in disaster area (Shiro Takada et. al “Strong Ground Motion and Lifeline Damage during the Java Jogjakarta Earthquake”).

The obtained relationship between MMI and the damage ratio  $P$  is shown in Figure 3.2.15. The fragility function is generated for each building type.

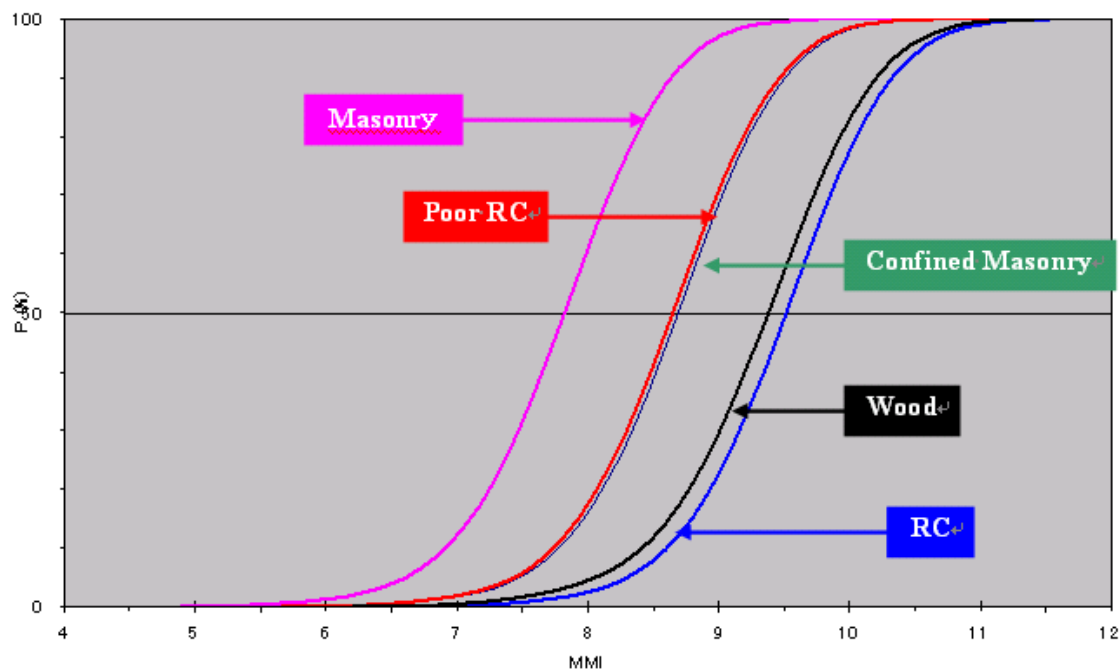


**Figure 3.2.15 Fragility Function (Relationship between MMI and the damage ratio P)**

On the other hand the damage example observed in Sumatra Island also needs to be referred. Therefore some report about 2004 Andaman earthquake and 2007 Solok earthquake were referred and it was confirmed that these observations do not contradict the fragility function.

In this report the hazard map shows the expected surface ground motion intensity of each point by MMI. So the value of the damage ratio  $P$  can be obtained by applying the fragility function and referring the value of MMI. By using a database and that indicates the number of each building type, the expected number of damaged buildings can be calculated by multiplying existing building number and the damage ratio  $P$ .

If above estimation is carried out based on enough grounds

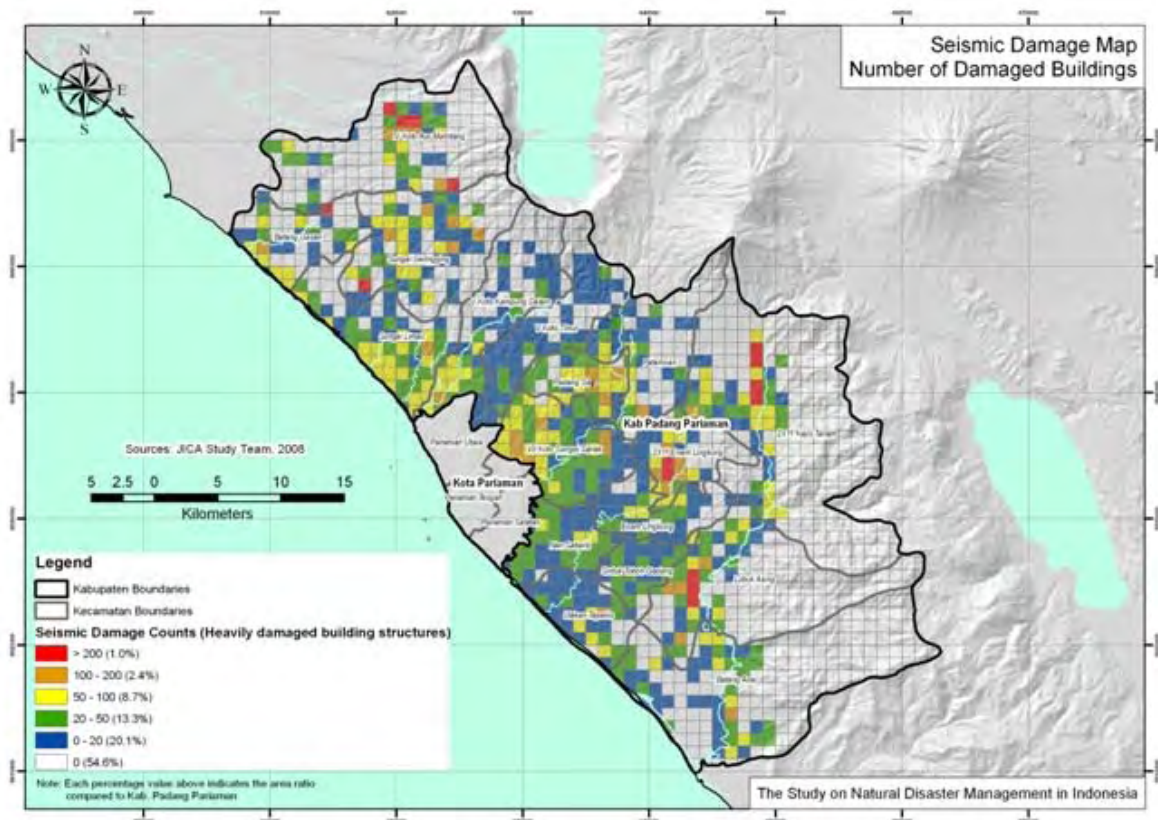
- It can be known how large project of building strengthening is needed for disaster mitigation view point
- Expected number of dead and injured at earthquake can be estimated and
- Scale of preparedness required for emergency aid can be estimated

However in this study, gaps in the database had to be filled by referring to some survey results and rough considerations because the database which was obtained now did not offer detailed information. The responsible Agency in Kabupaten Padang Pariaman has to implement the building census from the structural viewpoint and improve the database in the future.

## 2) Earthquake Risk Map in Kabupaten Padang Pariaman

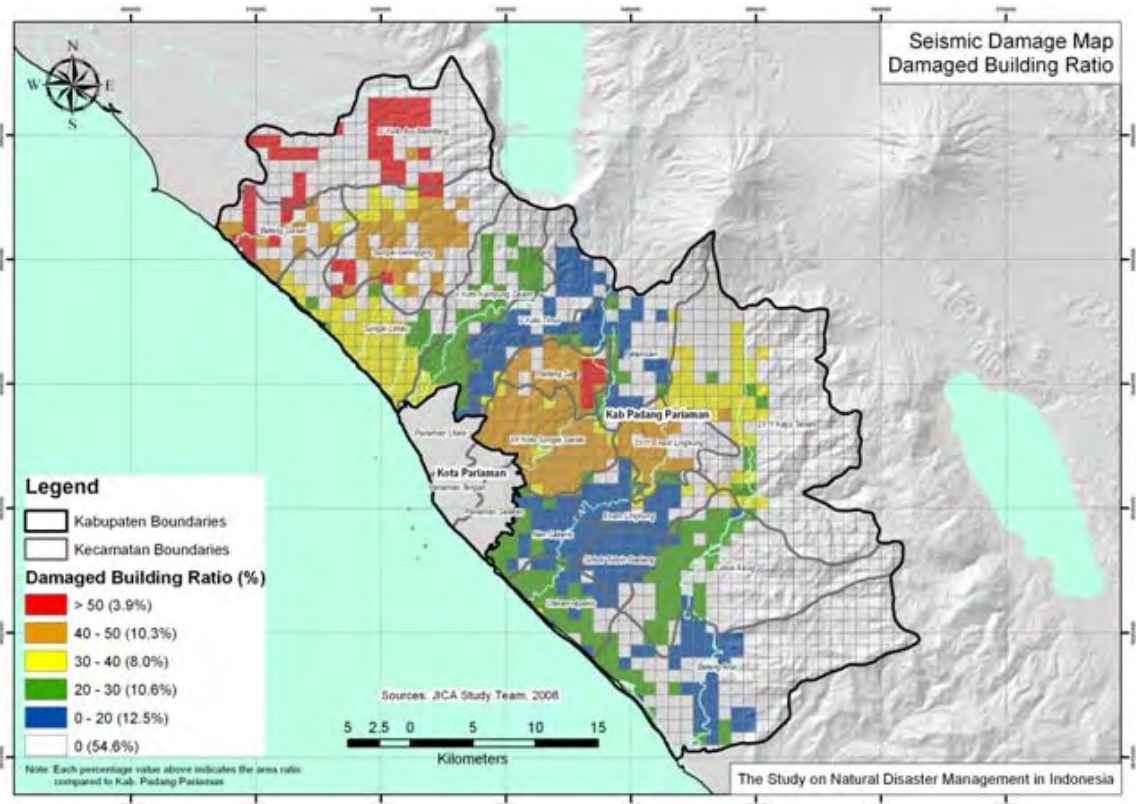
The intensity of surface ground motion differs according to the location. The vulnerability of the building also differs according to the building type. For instance the reinforced concrete building, which was designed and constructed through modern design concepts, is sustainable with 10% or less of damage ratio even if the intensity of surface ground motion is equal to MMI 8 or more, but the unreinforced masonry building may suffer damage with near to 90% of damage ratio. There is some difficulty to wrap up the risk map to only one figure because of above situation.

Figure 3.2.16 shows the expected number of damaged buildings that are located in each grid square of 1km × 1km. The tendency of the distribution of damaged buildings that depends on vulnerability of existing buildings is shown. In a word there is high risk at the location where vulnerable buildings exist.



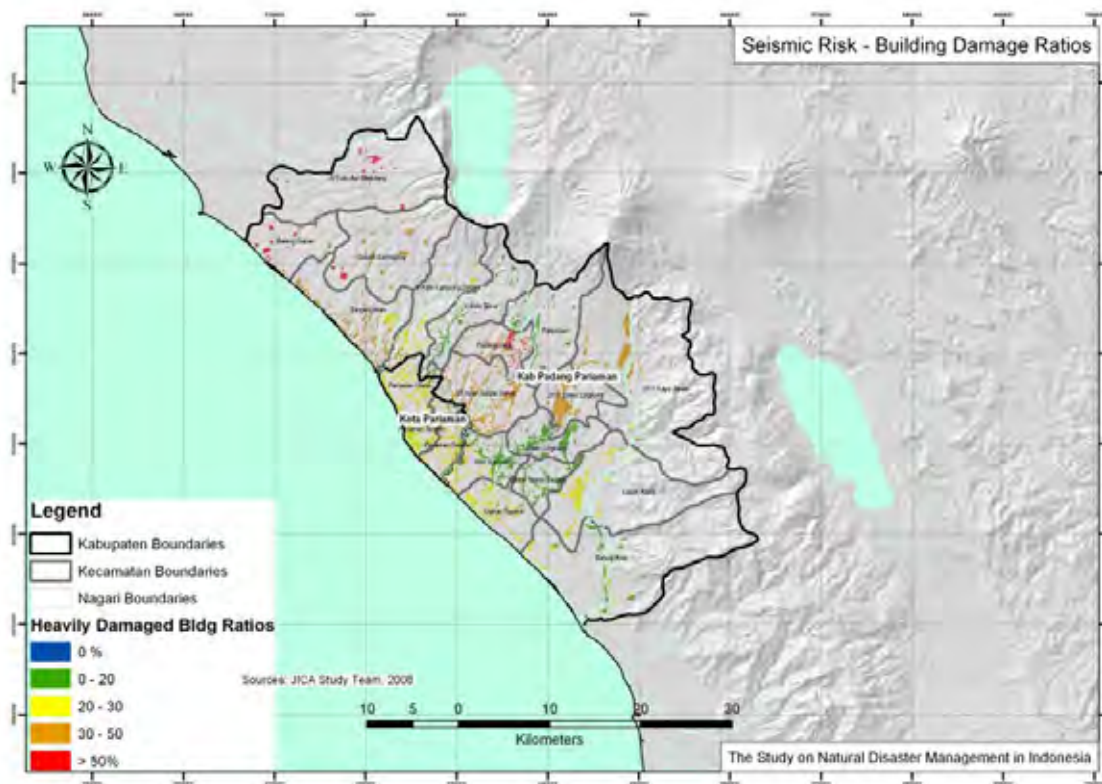
**Figure 3.2.16 Building Damage Per Grid**

Figure 3.2.17 shows the value of the expected number of damaged buildings divided by the total number of existing buildings that is located in each grid of 1km × 1km. This indicates the average damage ratio for each grid and thus it shows the tendency more clearly than previous Figure 3.2.16.



**Figure 3.2.17 Building Damage Ratio Per Grid**

Figure 3.2.18 also shows average damage ratio at each built up area not regarding the grid. This figure was made because the specific situation of this study area, that most buildings are concentrated at very limited area and other areas are less-populated, was considered. However additional careful consideration is needed when information is made public.



**Figure 3.2.18 Building Damage Ratio**

It is felt strongly that the accuracy of building database is very important for this kind of study because above shown study results indicate that the difference of vulnerability in each building type is a dominant factor of damage distribution. The number of buildings in each grid is shown in Figure 3.2.19. The number of buildings in each survey unit and ratio of each building type is shown in Figure 3.2.20. These figures are shown in order to obtain an overview of the building data. Currently, the area of each survey unit is uneven. Some of them are corresponding to Kecamatan; some of them are corresponding to Nagari. Especially, the most northern survey unit is very large and built up areas are concentrated there. This kind of inconsistency of statistics data may skew the analysis. This is the reason why effort of data collection must be continued and improved.

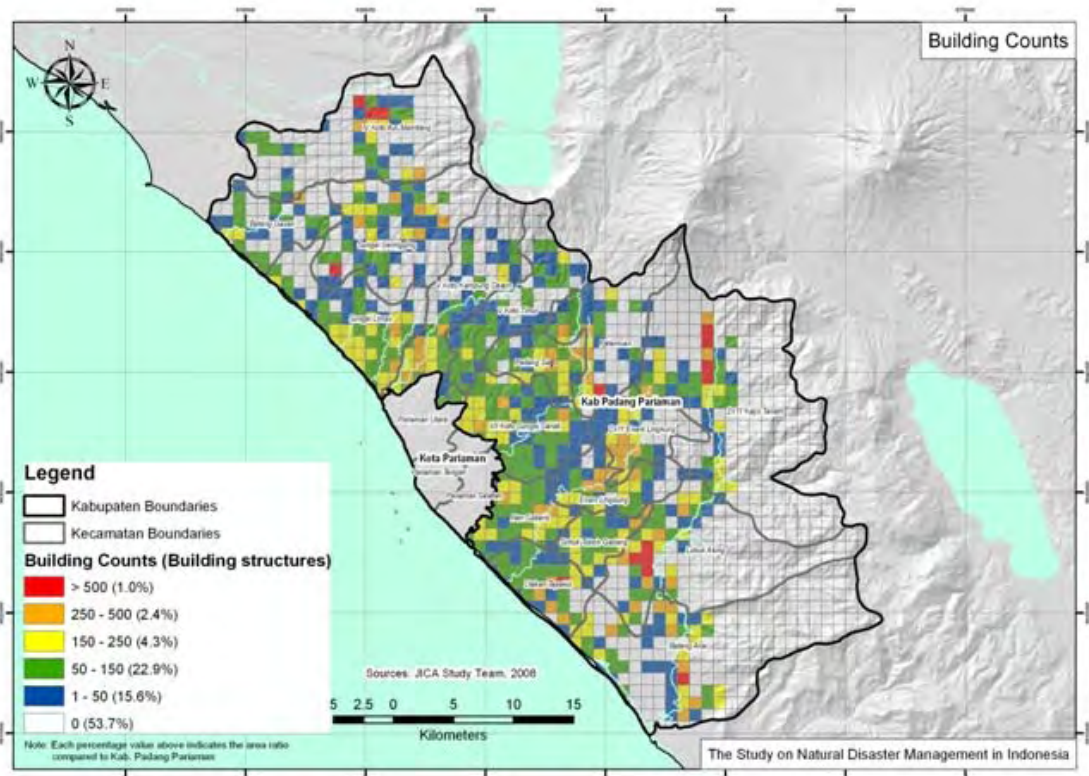


Figure 3.2.19 Number of Buildings in Each Grid

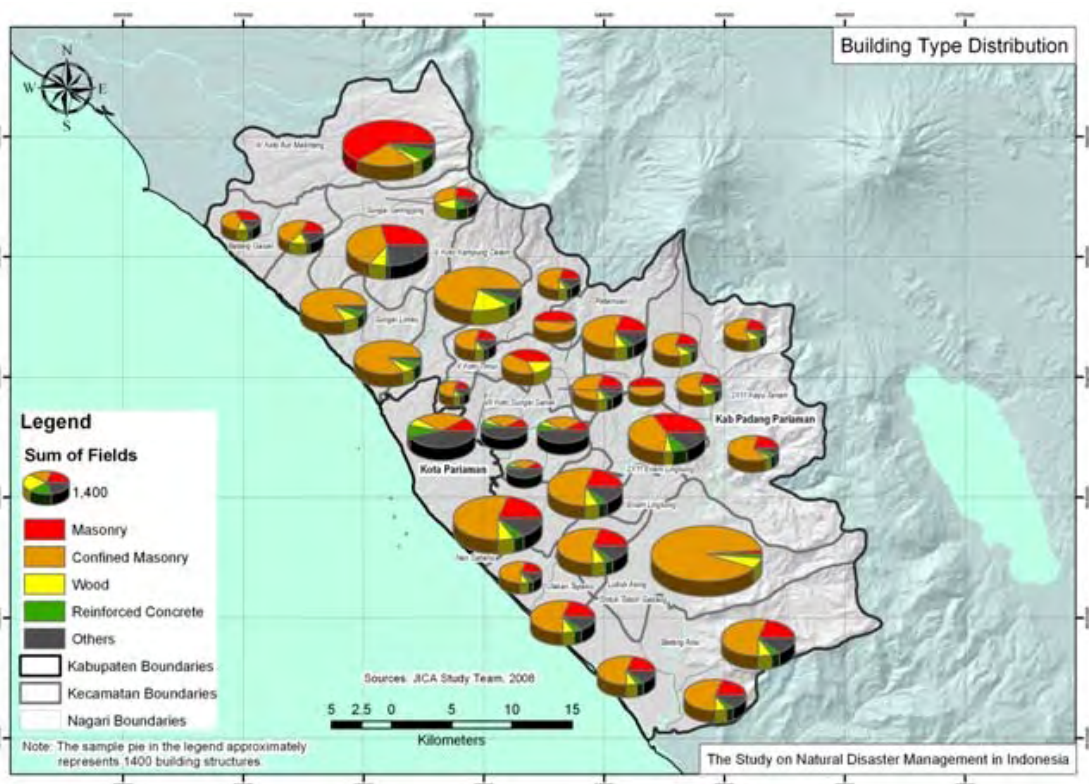


Figure 3.2.20 Number of Buildings in Each Survey Unit and Ratio of Each Building Type

There are some common points of building structure and distribution of building type in Indonesia. Aspect of building construction method and its variety are discussed below.

**(1) Timber made and Bamboo made**

This is a comparatively old type of construction method. There are some 100-year old buildings of this type in study area. Two types of structure are found: one is dressed timber made or elemental bamboo made frame structure, and the other consists of column and wall made of slim wood strings or bamboo strings grouted with lime or mortar. There are several types of structure details according to the region. Earthquake resistant capacity of these buildings is generally better than masonry and Confined masonry, but many examples with badly designed or deteriorated condition are found.



**a)** timber made frame

**b)** column and wall made of slim wood strings or bamboo strings grouted with lime

**Figure 3.2.21 Timber Made and Bamboo Made**

**(2) Brick Masonry**

The bearing wall thickness of most of brick masonry in this area is as much as one brick. Matters which should be obeyed on masonry construction are hardly paid attention to. There are problems of quality of brick and grout in many cases.



**Figure 3.2.22 Brick Masonry**

### (3) Cobble masonry

There are many cobble masonry buildings in the area far from the main street. Earthquake resistant capacity of this type is very poor because of lack in grip effect between each cobble and poor quality of grout.



**Figure 3.2.23 Cobble Masonry**

### (4) Confined masonry

This building type is becoming the major type in recent years. Regarding confined masonry bearing wall itself resists against load. RC made column, beam and lintel only give confinement effect to bearing wall. This is the difference between confined masonry and RC frame. Dimension of RC made members of confined masonry is smaller than that of RC frame. Earthquake resistant capacity of this type is better than unreinforced masonry but considerably poorer than RC frame with modern design concepts.



**Figure 3.2.24 Confined Masonry**

**(5) Reinforced Concrete Moment Resisting Frame**

Buildings of Reinforced Concrete Moment Resisting Frame (RCMRF) resist against load by its frame consisting of column and beam although its appearance is similar to confined masonry. Wall of most RCMRF buildings in this study area are made of brick. This kind of wall can not be a bearing wall, they are partition walls, because brick wall may lose its stiffness when the frame is deformed by inertia force caused by earthquake. Of course the wall can resist against inertia force caused by earthquake if it consists of Reinforced Concrete Shear Wall but effective shear walls can rarely be seen in this study area.



**Figure 3.2.25 Reinforced Concrete Moment Resisting Frame**

**(6) Combination of different kind construction method**

There are many buildings with combination of different kinds construction methods in this study area. Different kind construction methods tend to be applied when the building is extended after some time interval. Serious destruction can start at the boundary of this kind combination when earthquake hits as was seen in examples damaged during 2007 Solok earthquake.



**Figure 3.2.26 Combination of Different Kinds of Construction Methods**

---

The following situation is seen in study area regarding building distribution.

**(1) Building density**

Most buildings are concentrated in very limited area and other area is less-populated. Generally speaking this tendency works advantageously during earthquake damage because interference between neighboring buildings under quake phenomenon does not happen easily. Empty space can be found to use as an urgent support center easily after an earthquake.

**(2) Building Type**

Comparatively modern building types like as RCMRF or confined masonry are dominated in main street; on the other hand, old building type like as masonry, timber made and combination of different kind construction method exceed modern building types in the area far from main street. Especially cobble masonry, which can be seen a lot in the area far from main street, does not have sufficient earthquake resistant capacity.

**(3) Comparatively modern and old**

Confined Masonry building is becoming the major type in recent years. It is thought that this type of construction method can achieve almost sufficient earthquake resistant capacity if it is designed and constructed in a careful manner. At least it has greater capacity than stone masonry or brick unreinforced masonry. It is close to RC building capacity even though it is not equal. Actually some researchers offer the results of experiment and instructional books in order to obtain structural capacity. However there can be found a lot of examples that were constructed without sufficient attention in this study area.

The following points are found frequently:

- Bricks are not soaked in water before piling up (Sufficient water is needed for the hydration reaction of cement in grout)
- Situations in which a building is seen as a whole load path system are not present
- Opening in bearing wall is excessively large
- Dimension of confinement members is not sufficient
- Detail of reinforcing bar is not sufficient
- Compaction of concrete is not sufficient
- Inadequate aggregate (pumice stone)
- Stiffness and bearing capacity of foundation is not sufficient

### **3.2.4 Possible Countermeasures against Earthquake in Kabupaten Padang Pariaman**

#### **1) Structure measure**

Only strengthening of structure done beforehand is effective to mitigate human damage because structural damage due to earthquake occurs quite suddenly, and we can not prepare any effective warning system. Any effort done after earthquake can not be effective to reduce the number of human lives lost. Rescue activity and supporting activity have to be done after earthquake occurrence but those efforts hardly reduce lives lost.

Strengthening measure are as follows:

##### **(1) Consolidate building permission and supervising system**

In many cases, individually owned buildings are not built by a specialist, but rather by inexperienced amateurs or workmen who did not pass professional instruction.

Building permissioning and supervising system was established already but not necessarily all permits were applied for. There have been a lot of application leakages. Even for investigation on structural issues is generally loose. In addition most buildings are usually built without any public supervision. If these defects are not going to be solved, every earthquake with considerable size may cause a large number of casualties.

##### **(2) Consolidate diagnosis system for existing building**

##### **(3) Encourage earthquake strengthening in existing building**

There can not be the concept of “Existing nonqualified building” because building permission and supervising system is not functioning currently. However existing weak buildings have to be reconstructed if they are evaluated as “nonqualified” through the diagnosis. If it is not possible to reconstruct every building the next best thing to do is to strengthen existing buildings. The fundamental principle of strengthening is to specify the weak point of the building and to improve capacity of that weak point. Dominant weak points found in this study area are as follows:

#### **A. Rigidity shortage of roof and floor**

There can be seen many one-story buildings, which do not have any lintel or roof slab, in this study area. As a result that building does not have sufficient rigidity in roof level so collapse because of twisting motion during earthquake is likely. As countermeasures, additional lintel or additional roof slab had better be set up.



**Figure 3.2.27 Building with no Lintel and Roof Slab**

### **B. Capacity shortage of brick masonry wall**

Brick masonry wall is weak to force in an out-of-plane direction.

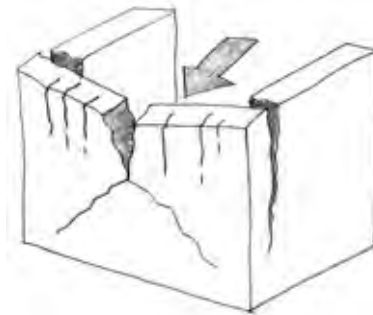


**Figure 3.2.28 Destruction by Force in Out-of-Plane Direction**

Many kind of reinforcement methods are proposed to prevent this type destruction. For instance, it is reported that reinforcement using meshed steel wire and cement mortar is effective as measures. However brick column or brick wall with small cross section can not have sufficient bearing capacity. This kind of member has to be changed to reinforce the concrete member.

### **C. Defect of connection part of combined building**

Serious kind of destruction can start at connection part of combined building.



**Figure 3.2.29 Example of Connection Part**

Even if the different kinds of construction methods are connected, the shape of each single construction part must be completed. However some kind of unfit end tends to be left at the connecting part. That kind of unfit may generate extraordinary concentration of force that causes decay. Demolishing and reconstruction is recommended when the effect of unfit shape is serious.

**(4) Encouragement of rebuilding**

Effort to make a financing system of the earthquake strengthening construction capital should be made for people who have a concrete plan of earthquake strengthening construction.

**(5) Education regarding earthquake resistance of building**

**2) Non structural measures**

It is not possible to reduce human casualties by implementing non structural measures but still it is beneficial to make advance preparations toward emergency rescue, life support and relief. The preparation for that is as follows:

**(1) Securing temporary shelter place**

**(2) Preparing and Stock materials in emergency**

**(3) Mutual support agreement with the administrative organization in the vicinity**

**(4) Establishment Cooperation method with disaster prevention organization of central government**

**(5) Establishment of Post-Earthquake Temporary Risk Evaluation system**

**(6) Educate and hold drills for the organizations and the residents in the region**

### **3.3 Disaster Characteristics of Earthquake and Countermeasures in Kota Pariaman**

#### **3.3.1 Disaster Characteristics of Earthquake in Kota Pariaman**

##### **1) Earthquake Disaster in the past**

A history of previous disasters can offer effective lessons for mitigation because comparatively large earthquake disasters occur periodically. In fact, the earthquake is a phenomenon which happens together with the movement of the lithospheric plate. There is some periodicity in the occurrences of large earthquakes although the movement speed of lithospheric plate is nearly constant. The return period of large earthquakes, which may have a big influence, is considerably long compared to human life (i.e. 200~1000 years). Therefore, even a person who lives in one region for a long time can hardly experience such as large seismic hazard. There are few documented historical facts or study's findings obtained by archaeological survey regarding the earthquake in Indonesia. However, this tendency does not mean that big earthquakes do not occur in that region. Plate tectonic surroundings and the past occurrences of earthquakes needs to be discussed widely to ensure accurate understanding of frequency and magnitude of seismic hazard. Actually, the earthquake hazard in Indonesia is more frequent than that of Japan if we count only the earthquake by which 100 lives or more were lost using "Utsu Database" or "USGS Database". Of course, the total human damage due to the earthquake is discussed here. Damage due to tremor is not discussed separately from damage due to seismic sea wave.

**Table 3.3.1 Earthquake by Which 100 Lives or More were Lost in Indonesia (1/2)**

(Web:[http://iisee.kenken.go.jp/utsu/utsuweq\\_bak.html](http://iisee.kenken.go.jp/utsu/utsuweq_bak.html))

Year	Month	day	Latitude	Longitude	Depth	M	Death	Injured	Remarks
416	9	10	-1.0	120	--	--	many	--	Indonesia(Java/Sumatra)
1674	2	12	-3.5	128.2	--	--	2342	--	Indonesia(Moluccas) Amboina
1792	2	12	--	--	--	--	300	--	Indonesia(Sumatra) Padang
1815	11	27	-8	115.2	--	--	10253	--	Indonesia(Bali)
1820	12	29	-7	119	--	7.5	400	--	Indonesia(Sulawesi) Makassar, Sumbawa
1828	12	29	-2	121	--	--	many	--	Indonesia(Sulawesi) Macassar, Dorelekomba(I=9)
1835	11	1	-3.4	128.1	--	--	149	--	Indonesia(Moluccas) Amboina, Haruku, Saparua(I=9)
1846	2	14	0.5	127.3	--	--	many	--	Indonesia(Moluccas) Ternate, Is.
1856	3	2	3.5	125.5	--	--	3000	--	Indonesia Great Sangir(Volcanic)
1861	2	16	0.5	97.5	--	8.4	great	--	Indonesia(Sumatra) Lagundi, Padang, Batu I, Nias I
1861	3	9	0	98	--	7	750	--	Indonesia(Sumatra) Padang, Batu Is., Simuk D=200
1864	5	23	-3	135	*	--	250	--	Indonesia(Irian Jaya) Geobink, Elay
1867	6	10	-7.8	110.5	--	--	327	--	Indonesia(Java) Djakarta, Soerakarta(I=9)
1871	3	2	0	128	--	--	400	--	Indonesia(Moluccas) Tagulandang, Is., Dubias
1883	8	27	-5.8	106.3	--	--	Several tens of thousands	--	Indonesia Krakatoa
1890	12	12	-6.4	111	--	--	many	--	Indonesia(Java) Djoewana(Japura)(I=8) D=some
1896	4	18	-8.3	126	--	--	250	--	Indonesia(Timor/Alor)(I=8)
1899	9	29	-3	128.5	--	7.4	3864	--	Indonesia(Moluccas) Ceram(south coast) 7.1S
1907	1	4	2	96.3	u	7.8	400	--	Indonesia(Sumatra) Gunung Sibol(Nias) 7.5S
1909	6	3	-2.5	101.5	--	7.5	200	--	Indonesia(Sumatra) Korint, Djambi 7.3S
1914	6	25	-4	102.5	--	8.1	many	--	Indonesia(Sumatra) Benkulen D=11/20 7.6S
1917	1	21	-8	115.4	--	6.5	18000	--	Indonesia(Bali)
1924	11	12	-7.2	109.5	--	--	609	--	Indonesia(Java) Wonosobo D=many/60
1924	12	2	-7.3	109.9	--	--	115	--	Indonesia(Java) Wonosobo
1924	12	22	--	--	--	--	113	--	Indonesia(Java) Wonosobo
1926	6	28	-0.5	100.5	--	6.8	222	--	Indonesia(Sumatra) Padang Highlands 新層
1926	6	29	--	--	--	--	400	--	Indonesia(Sumatra)
1928	8	4	-8.3	121.7	--	--	226	--	Indonesia(Palembang) Is.(Rokatinda Volcano)
1943	7	23	-9.5	110	90	8.1	213	--	Indonesia(Java) Jayakarta 7.6E
1964	1	4	-1.9	102.3	33	6.7	110	479	Indonesia(Sumatra)
1964	4	2	5.8	95.7	132	7	110	479	Indonesia(Sumatra)
1968	8	14	0.16	119.78	23	7.4	392	--	Indonesia(Sulawesi) D=200 7.3S
1969	2	23	-3.12	118.87	13	6.9	600	--	Indonesia(Sulawesi) D=64 H=97
1976	6	25	-4.6	140.09	33	7.1	6000	--	Indonesia(Irian Jaya) D=422
1976	7	14	-8.17	114.89	40	6.5	563	2300	Indonesia(Bali)
1976	10	29	-4.52	139.92	33	7.2	6000	--	Indonesia(Irian Jaya) D=108/133(I=8)
1977	8	19	-11.09	118.46	33	7.9	189	75	Indonesia(Sumbawa Is. IG)
1981	1	19	-4.58	139.23	33	6.7	1300	--	Indonesia(Irian Jaya) Jayawijaya Mts. D=261 6.6W
1989	8	1	-4.51	139.02	14	5.8	120	125	Indonesia(Irian Jaya) Kurima D=90 6.1W
1992	12	12	-8.48	121.9	28	7.5	1740	2144	Indonesia(Flores) Maumere, Babi Is. D=2080 7.7W
1994	2	15	-4.97	104.3	23	7	207	2000	Indonesia(Sumatra) Liew(Lampung Prov.) 6.9W
1994	6	2	-10.48	112.84	18	7.2	277	423	Indonesia(SE coast of Java, Bali)
1996	2	17	-0.89	136.95	33	8.1	166	423	Indonesia(Irian Jaya) Blok Supiori 8.2W
2000	6	4	-4.72	102.09	33	8	103	2585	Indonesia(Sumatra) Bengkulu D=90 I=2174 7.9W
2004	12	26	3.3	95.98	30	8.8	Several tens of thousands	Several tens of thousands	Indonesia(Sumatra)(I=9)landslide,mud volcano 9.0W

**Table 3.3.2 Earthquake by Which 100 Lives or More were Lost in Indonesia (2/2)**

(Web:<http://infotrek.er.usgs.gov/>)

Year	Mnth	Day	Time	Longitude	Latitude	Depth	Magnitude	Tsunami	Death	Injured	Damage	Note
1986	5	28	1327U	-2.91	139.32	85	7.7	-	-	0	limi	Indonesia(Irian Jaya) 7.2E
1986	8	10	0207U	1.42	126.22	33	7.8	T	-	-	limi	Indonesia(Molucca Passage) 7.5S
1986	8	14	2214U	0.16	119.78	23	7.4	T	392	-	seve	Indonesia(Sulawesi) D=200 7.3S
1988	1	30	1029U	4.81	127.44	70	7.9	-	-	-	-	Indonesia(Teleau) 7.1E
1971	1	10	0717U	-3.13	139.7	33	8.1	-	-	-	made	Indonesia(Irian Jaya) Djigapura, Sentani 7.8S
1971	2	4	1333U	0.65	96.84	33	7.1	-	-	-	limi	Indonesia(Sumatra) Nbel, Sibolga, Tarutung, Pasaman
1972	6	11	1841U	3.94	124.32	325	7.5	-	-	-	-	Indonesia(Celebes) Sea 7.4E
1976	6	25	1918U	-4.6	140.09	33	7.1	-	8000	-	seve	Indonesia(Irian Jaya) D=422 Missign 5-8 千 6.8S
1976	10	29	0251U	-4.52	139.92	33	7.2	-	8000	-	cons	Indonesia(Irian Jaya) D=108/133(I=8)
1977	8	19	0808U	-11.09	118.46	33	7.9	T	189	75	made	Indonesia(Sumbawa Is. EQ) 8.1S 8.3W
1979	9	12	0517U	-1.68	136.04	5	7.9	T	15	many	seve	Indonesia(Irian Jaya) Yapan 7.5 7.5W
1984	11	17	0649U	0.2	96.03	33	7.2	-	0	1	limi	Indonesia(Off W. Sumatra) Nias Is. D=1 7.1W
1985	11	17	0940U	-1.64	134.91	10	7.1	-	0	0	limi	Indonesia(Irian Jaya) Mandowai 7.1W
1990	4	18	1339U	1.19	122.86	26	7.4	-	3	25	some	Indonesia(Sulawesi) Bolaang-Garontara area 7.8W
1991	6	20	0518U	1.2	122.79	31	7.?	-	0	-	limi	Indonesia(Sulawesi) Gorontalo(Minahassa Pen.) 7.5W
1992	12	12	0329U	-8.48	121.9	28	7.5	T	1740	2144	seve	Indonesia(Flores) Maumere, Babi Is. D=2080 7.7W
1994	1	21	0224U	1.02	127.73	20	7.2	-	7	40	made	Indonesia(Halmahera) Kou area 7.0W
1994	2	15	1707U	-4.97	104.3	23	7	-	207	2000	cons	Indonesia(Sumatra) Liew(Lampung Prov.) 6.9W
1994	6	2	1817U	-10.48	112.84	18	7.2	T	277	423	cons	Indonesia(SE coast of Java, Bali) Tsunami 7.7W
1995	3	19	2353U	-4.18	135.11	33	7.1	-	0	0	limi	Indonesia(Irian Jaya) Ayam, Fakrak, Nabire 6.9W
1996	1	10	083U	0.73	119.93	24	7.6	T	10	-	some	Indonesia(Sulawesi) Minahasa Pen. 7.9W
1996	2	17	0559U	-0.89	136.95	33	8.1	T	186	423	cons	Indonesia(Irian Jaya) Blok Supiori 8.2W
1996	2	17	1459U	-0.89	136.95	33	8.1	T	0	0	D1	Indonesia Chichijima 103m, Shionomisaki 96cm 8.2W
1998	11	29	1410U	-2.07	124.89	33	7.7	-	41	181	cons	Indonesia(Ceram Sea) Mangale, Telabu, Manado 7.7W
2000	5	4	0421U	-1.11	123.57	26	7.5	T	46	264	cons	Indonesia(Sulawesi) Luwuk, Banggai, Padang 7.8W
2000	6	4	1828U	-4.72	102.09	33	8	-	103	2585	cons	Indonesia(Sumatra) Bengkulu D=90 I=2174 7.9W
2002	10	10	050U	-1.76	134.3	10	7.7	T	8	8	cons	Indonesia(Irian Jaya) Fault, Slope Failure 7.5W
2002	11	20	128U	2.82	96.09	30	7.6	-	3	85	made	Indonesia(Simeulu) 7.4W
2003	5	26	1923U	2.35	128.85	31	7.1	-	1	7	limi	Indonesia(Halmahera) Erebere 7.0W

Frequency and magnitude of earthquake must be discussed observing the characteristics of surrounding plate structure and past occurrence of big earthquakes. Indonesia has a plate boundary in southern part of Sumatra and Java Island. The oceanic plate subducts towards the bottom of the island. The subduction zone is located in Sunda Trench. A very big earthquake caused by reverse fault occurs in this subduction zone.

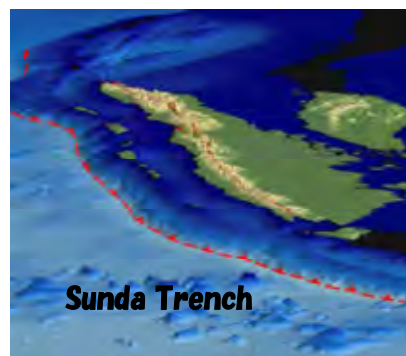


**Figure 3.3.1 Sunda Trench**

Recent impressive earthquakes generated in this zone are Andaman earthquake 26 Dec. 2004 M<sub>w</sub>9.1 and Bengkulu earthquake 12 Sep. 2007 M<sub>w</sub>8.4. Structure damage caused by tremor of this earthquake tend to be considered less serious because damage caused by seismic sea wave is so dominant. Certainly, the surface ground motion at these disaster areas is less than the value estimated considering magnitude of earthquake source. Two factors contribute to this tendency: one is rupture speed of these fault which is comparatively slow and the other is hypocentral distance from population concentration area which is long. However large damage is usually caused even by not so large earthquake motion because earthquake resistant capacity of residential buildings in this area is quite low.

Another dominant earthquake source is The Great Sumatran Fault that is located through the Sumatra Island. Mechanics of this fault are dextral strike-slip fault. Magnitude of earthquakes generated at this fault is slightly smaller than that of subduction zone, but the surface ground motion and damage can be seriously large if population concentration area is located near to the fault.



**Figure 3.3.2 The Great Sumatran Fault**

Recent impressive earthquakes generated in this fault are Solok earthquake 6 March 2007 6.4, and Mw6.3. Two particular earthquakes were generated during 2 hours at south east side of Singkalak lake and north west side of it.

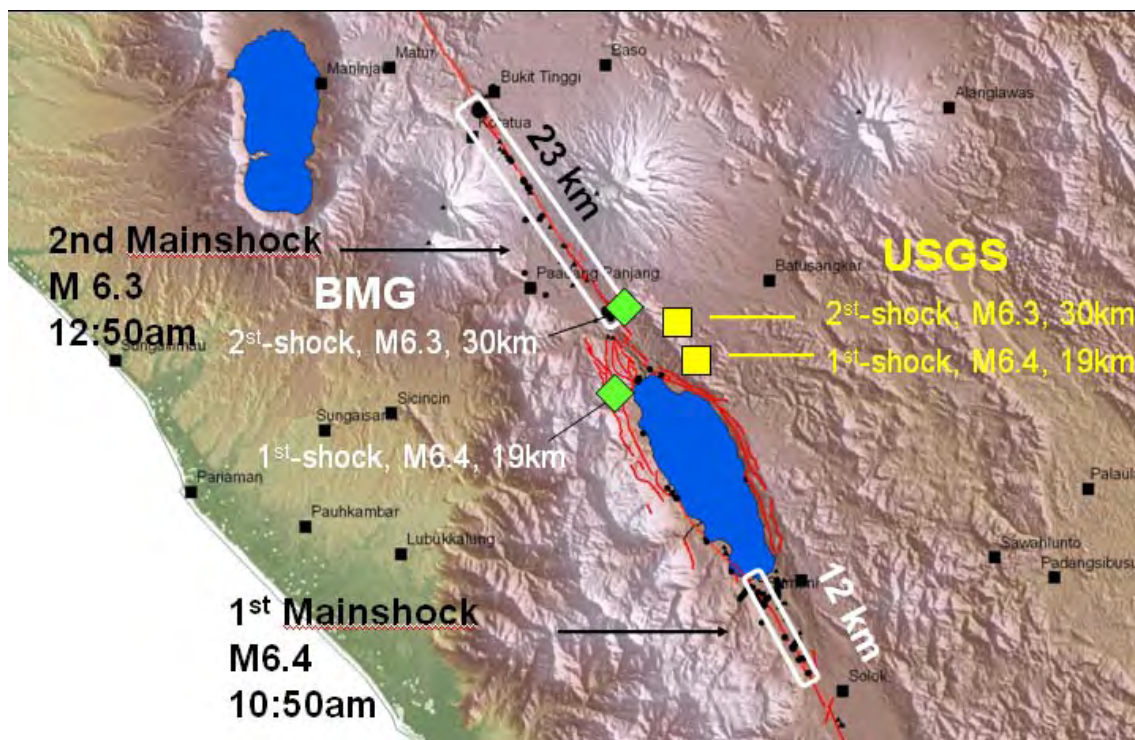


**Figure 3.3.3 Fault of Solok Earthquake 6 March 2007**

Source: (DANNY HILMAN NATAWIDJAJA, ADRIN TOHARI, EKO SUBOWO, AND MUDRIK R. DARYONO : A Review On The Sumatran Fault Zone And The 6 March 2007 Events (M 6.4 & 6.3) In Singkarak Lake, Central Sumatra, APRU/AEARU Research Symposium on Earthquake Hazards around the Pacific Rim June 21-22, Nikko Hotel, Jakarta, Indonesia) Geoteknologi LIPI

There was another example of near-field earthquake at Yogyakarta city (i.e, 27 May 2006 Yogya Earthquake  $M_w$  6.5). The relationship between damage and surface ground motion intensity in Kabupaten Bantul was referred to as a benchmark of the vulnerability function in this report.

The above-mentioned seismic circumstance is also very similar to Japanese circumstance, so Japan experiences regarding earthquake hazard needs to be used.

## 2) Factors for Damages due to Earthquake

Damage of earthquake disaster is divided into following three aspects:

1. Structure damage due to ground tremor
2. Damage due to capacity shortage of ground such as slope failure or liquefaction
3. Damage due to seismic sea wave

It is pointed that the aspects of above 1 and 2 tend to be forgotten after earthquake because the damage due to seismic sea wave gives overwhelming impression to victims. The aspects of above 1 and 2 are absolutely different from the sea wave because we can have some leeway to mitigate damage due to seismic the sea wave. However structural damage due to ground tremor occurs quite suddenly. Any warning can not be effective. Only strengthening of structure done beforehand is effective to mitigate damage. Any effort done after earthquake can not be effective to reduce the number of human lives lost.

### 3.3.2 Earthquake Hazard Map in Kota Pariaman

#### 1) Basis of Hazard Map Creation for Earthquake

The meaning of the word “Hazard” is defined as the cause of disaster. Therefore, regarding earthquake, only the distribution of the ground surface acceleration intensity must be shown in “Hazard Map”. No other aspect is necessary for Hazard Map for the above definition.

The ground surface acceleration intensity is described at each part of mesh in study area using the title of “Peak Ground Acceleration” (it is called as PGA here in after) or “Modified Mercalli Intensity scale” (it is called as MMI here in after).

Next topic, which is discussed in this chapter, is how to define the target value of the ground surface acceleration intensity. Generally there is a steady tendency of the relationship between the magnitude of earthquake and frequency of occurrence. So this means that small earthquake can occur frequently, but large earthquake rarely occur so frequently.

Figure 3.3.4 shows the relationship between the magnitude of earthquake and frequency of occurrence regarding earthquakes that occurred from 1629 to 2004 in Indonesia

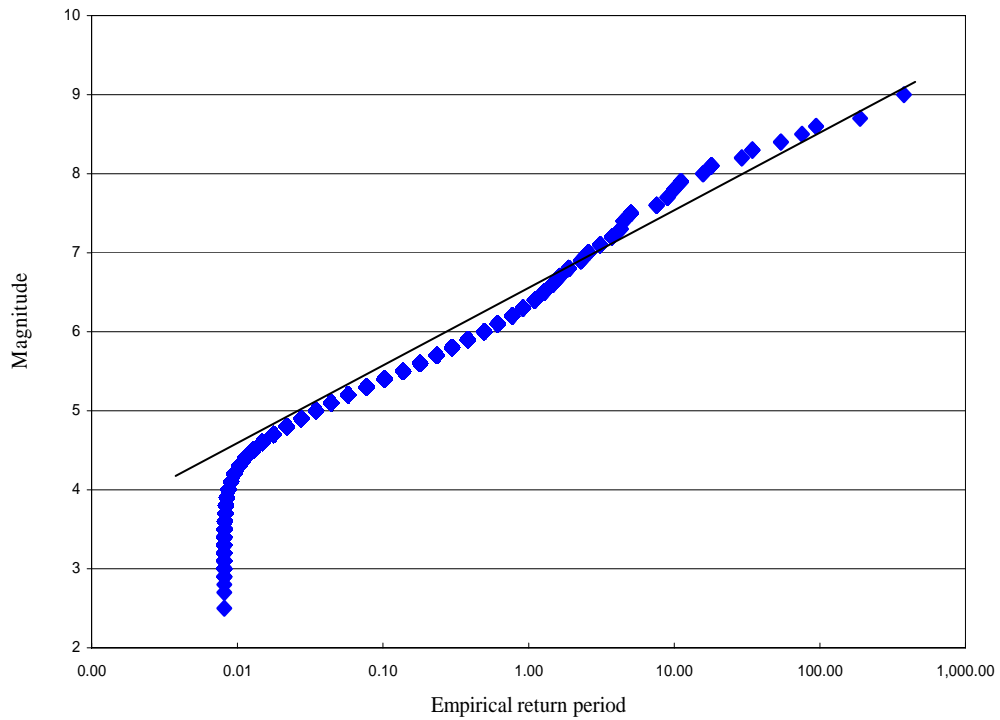


**Figure 3.3.4 Relation between Magnitude and Return Period**

Y axis means magnitude of the earthquake, and X axis means empirical return period  $T_E$ .

$$T_E = \frac{T_S}{m} \tag{Eq.3.5}$$

Where

$T_E$  : Empirical return period

$T_S$  : Sampling term

$m$  : Order when the sample is arranged in magnitude order

For example, the largest earthquake generated in this area is the 2004 earthquake with magnitude 9, then order  $m$  is the first, Sampling term  $T_S$  is 2004 minus 1629 equal to 375, Empirical return period  $T_E$  must be 375 years. The large one in second is the 1833 earthquake with magnitude 8.7, then order  $m$  is the second, Sampling term  $T_S$  is 375 years divided 2 equal to 187, Empirical return period  $T_E$  must be 187 years. When the relationship between magnitude and the empirical return period  $T_E$  of each recorded earthquake is plotted in the same manner, the plotted pattern tends to be almost on straight line on one-half of logarithm graph paper, but limited in range of more than magnitude 5. This finding is called the thesis of Gutenberg Richter or G-R formula. The angle  $b$  of this approximation line represents the difference between the occurrence frequency of big earthquake and that of small earthquake. If the surrounding of Indonesia is divided into some domains, which has consistent condition of seismicity, the above mentioned angle  $b$  must be

particular for each particular domain. If the occurrence of earthquakes is a spatially independent and independent time wise incident Poisson model can be applied to the analysis.

The peak acceleration value of the base rock at a certain point can be calculated utilizing attenuation formula. Attenuation formula is a kind of regression formula by which the peak acceleration value of the base rock is presumed from the magnitude of earthquake source and distance from earthquake source to a certain point.

In this computational procedure previously mentioned each domain must be further divided into small piece by utilizing polar coordinate system. In addition, an implicit method is needed in this procedure because the magnitude of earthquake source, which brings the peak acceleration value in a certain point, must be obtained at a computation step. Therefore a huge amount of the calculation is required in order to carry out this analysis. The computer program "EZFRISK" or "EQRISK" is used in an actual analysis. The peak acceleration value of the base rock at each part of Indonesia was calculated. Figure 3.3.5 shows the results of the above described procedure.

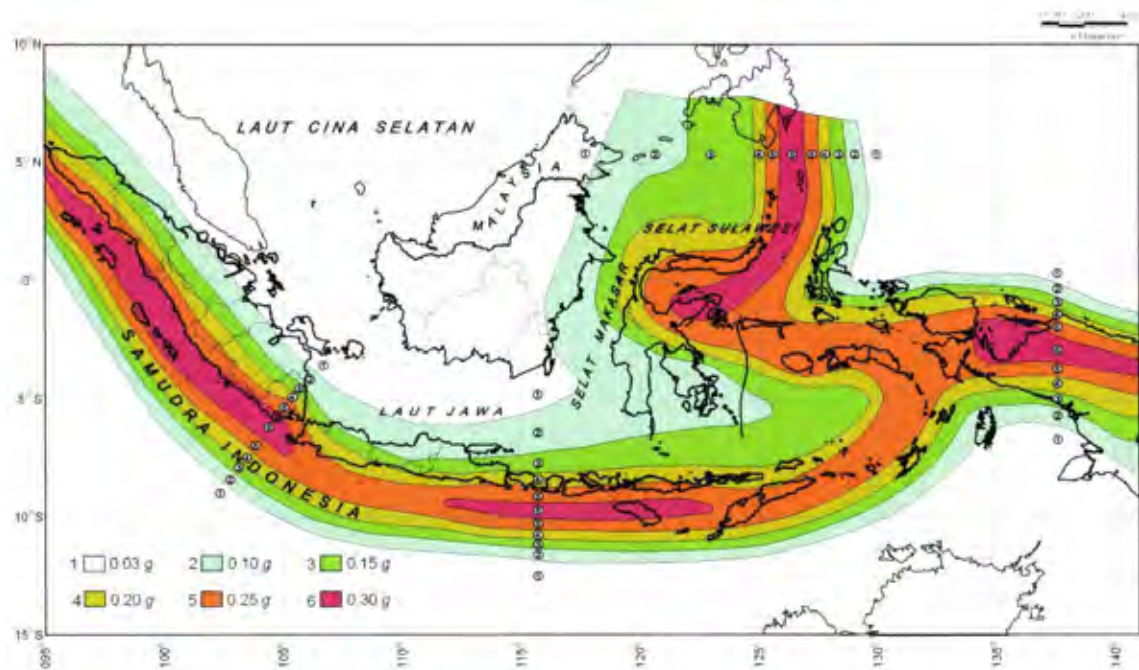


**Figure 3.3.5 Peak Acceleration Value of the Base Rock at Each Part of Indonesia (From SNI 03-1726-2002 the Indonesian code for seismic load)**

Each value shown in Figure 3.3.6 is the peak acceleration value of the base rock at each colored zone and corresponding 500 years of return period. For instance, almost part of Kota Pariaman belong to Zone 6. Therefore the peak acceleration value of the base rock is 0.3g (the value of 0.3g means 0.3 times acceleration of gravity). Detail of zone around study area is shown in Figure 3.3.7.

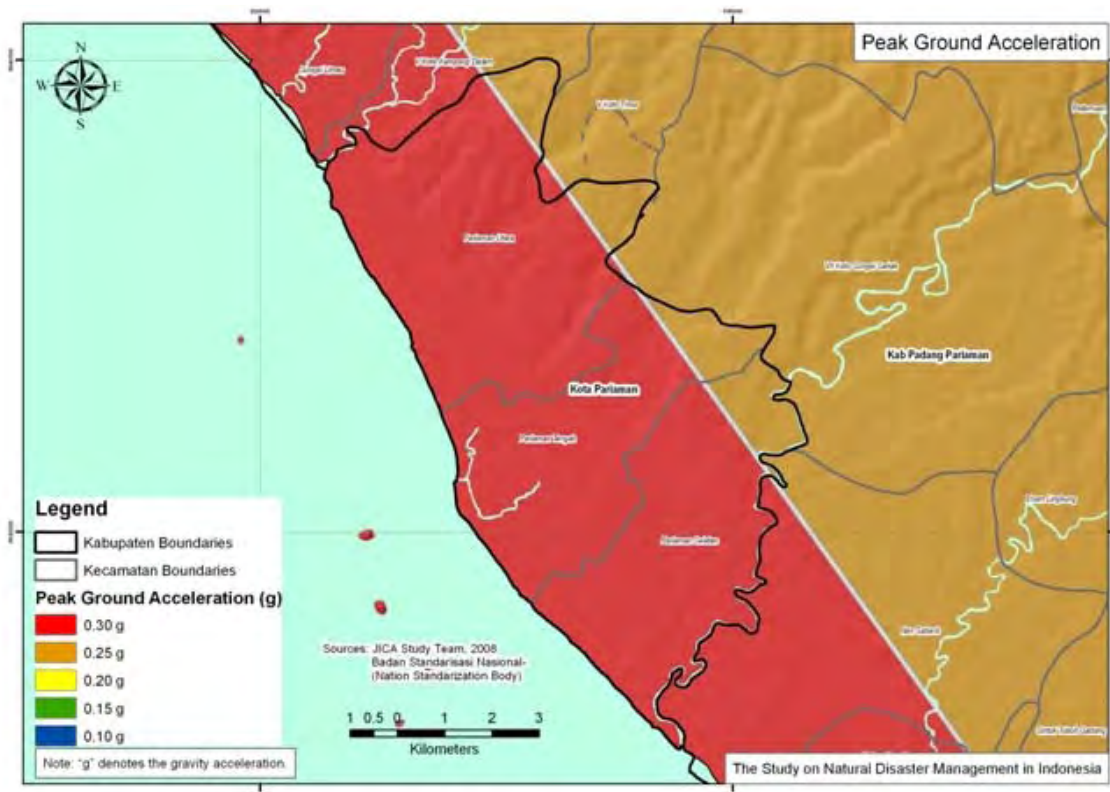


**Figure 3.3.6 PGA Ground Acceleration**

When concretely explaining the 500 years of return period it means that the probability of exceedance is 10% for 50 years. For example, if a structure, which has 50 years of service time, is designed utilizing the design seismic load of 500 years of return period the probability by which the structure will fall due to an unexpectedly large earthquake is 10%. Indeed 90% of incidents are comprised in this category. This setting is almost perfect in realistic meaning because 100% of safety can not be obtained using probability theory.

The above explained value is the peak acceleration value at the base rock that is defined as a base rock layer that is consisted of homogeneous material. The peak acceleration value at the base rock can be estimated utilizing attenuation function. However the value, which is needed for application of hazard map, must be the peak acceleration value at ground surface.

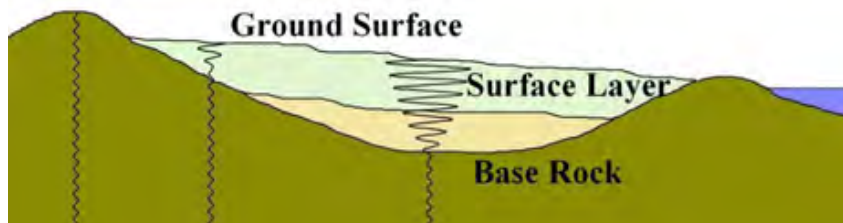


**Figure 3.3.7 Peak Acceleration Value of the Base Rock and Peak Acceleration Value of Ground Surface**

As explained in Figure 3.3.7 the ground tremor is amplified while it is propagated in the surface layer. In fact, the ground tremor at outcrop of base rock is usually small. On the other hand the ground tremor at the soft layer is usually large. Degree of amplification depends on characteristics of surface layer of the ground. Surface layer must be investigated in order to discuss this aspect. Geomorphological feature of surface layer around Kota Pariaman is shown in Figure 3.3.8.

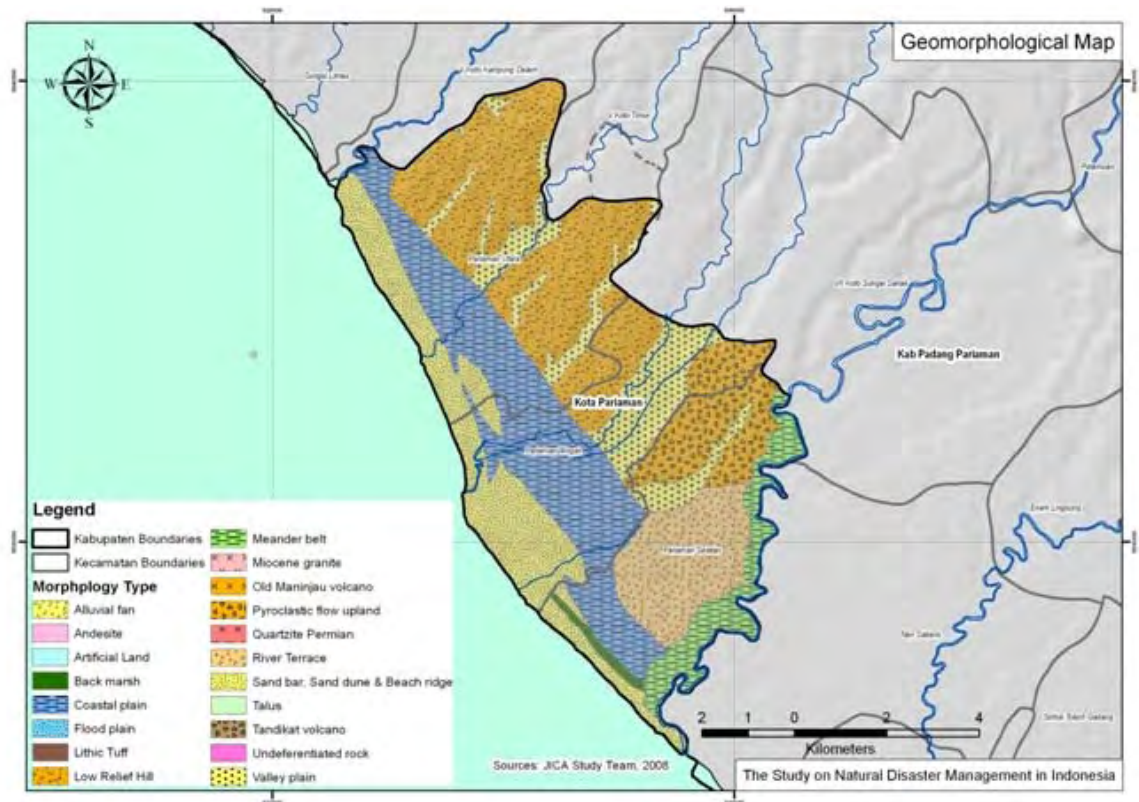


**Figure 3.3.8 Geomorphological Feature of Surface Layer around Kota Pariaman**

Distribution of characteristics of surface layer at each Segment of the study area is shown in Figure 3.3.9.

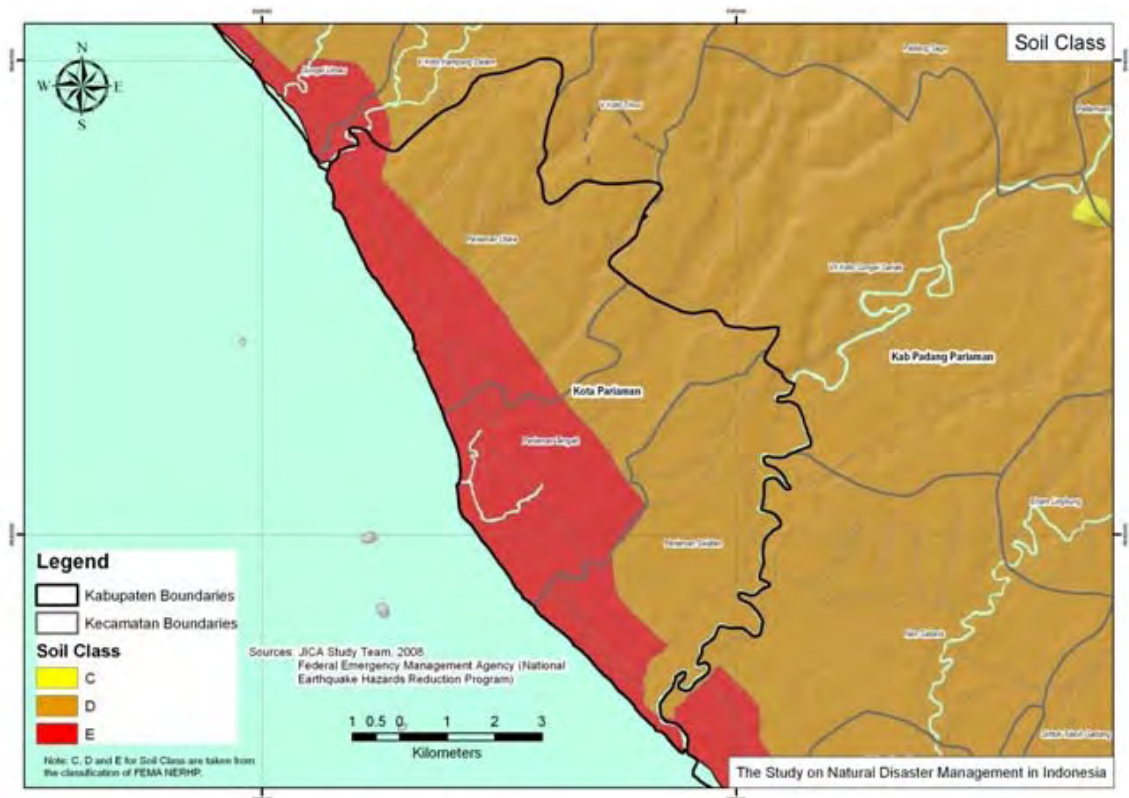


**Figure 3.3.9 Segmentation of Soil Class (classified according to stiffness of surface layer)**

Segmentation of soil class shown in Figure 3.3.9 is classified according to stiffness of surface layer. The classification is based on some speculations on geomorphological feature given by geological map and field survey done by the expert in charge of geological features. However more accurate material that will given by borehole logging and PS logging must be referred if it is available. Moreover, continuous improving effort shall be made regarding accuracy of hazard mapping.

As explain here, the intensity of the surface ground motion at earthquake is estimated referring the zone classified in SNI 03-1726-2002 and the soil class. The surface ground motion is expressed by PGA and the response spectrum shown in Figure 3.3.10. The value of vertical axis in the response spectrum means the acceleration response of the SDOF (Single degree of Freedom) model that has the natural period shown in the horizontal axis. Therefore the value on the extreme left correspond to PGA. This value of PGA shall be shown in the hazard map because these values represent the tremor of ground surface.

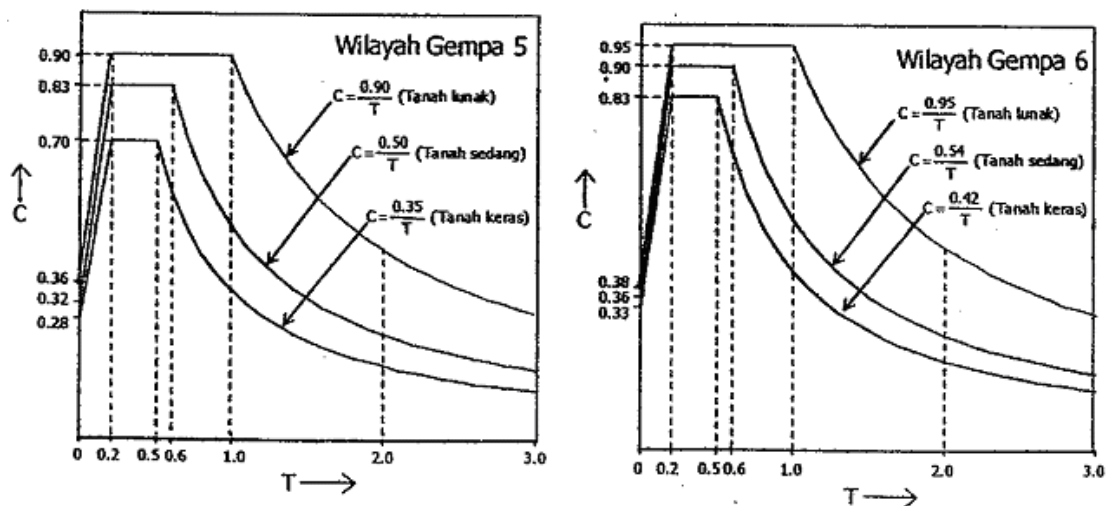


Figure 3.3.10 Response Spectrum Stipulated in 03-1726-2002

## 2) Earthquake Hazard Map in Kota Pariaman

The expected value distribution of the ground surface acceleration intensity is shown in Figure 3.3.11. The ground surface acceleration intensity is described using the title of PGA and MMI. PGA is a value which will be obtained as the maximum value when the quake of the ground level is measured with accelerograph. The modified Mercalli intensity scale (MMI) divides earthquake intensity into 12 stages of evaluation, and each stage is defined by describing the incident through observation and sensing (for example; "Difficult to stand"). Therefore expression of MMI is discrete number originally but one digit below the decimal point is written in this report in order to distinguish a detailed difference. The estimated MMI for Kota Pariaman is 8 or more in the MMI display. This level of intensity corresponds to "5 or more" in Japan Meteorological Agency Seismic Intensity Scale (it is called as JMI hereafter). JMI also divides earthquake intensity into 10 stages of evaluation, and each stage is defined by describing the incident through observation and sensing. Some sort of slight damage is found when the earthquake of "5 or more" in JMI occur in Japan but it is thought that considerably more serious damage may be generated by the same level of earthquake in Indonesia because earthquake resistant capacity of Indonesian buildings is poor comparing with that of Japan.

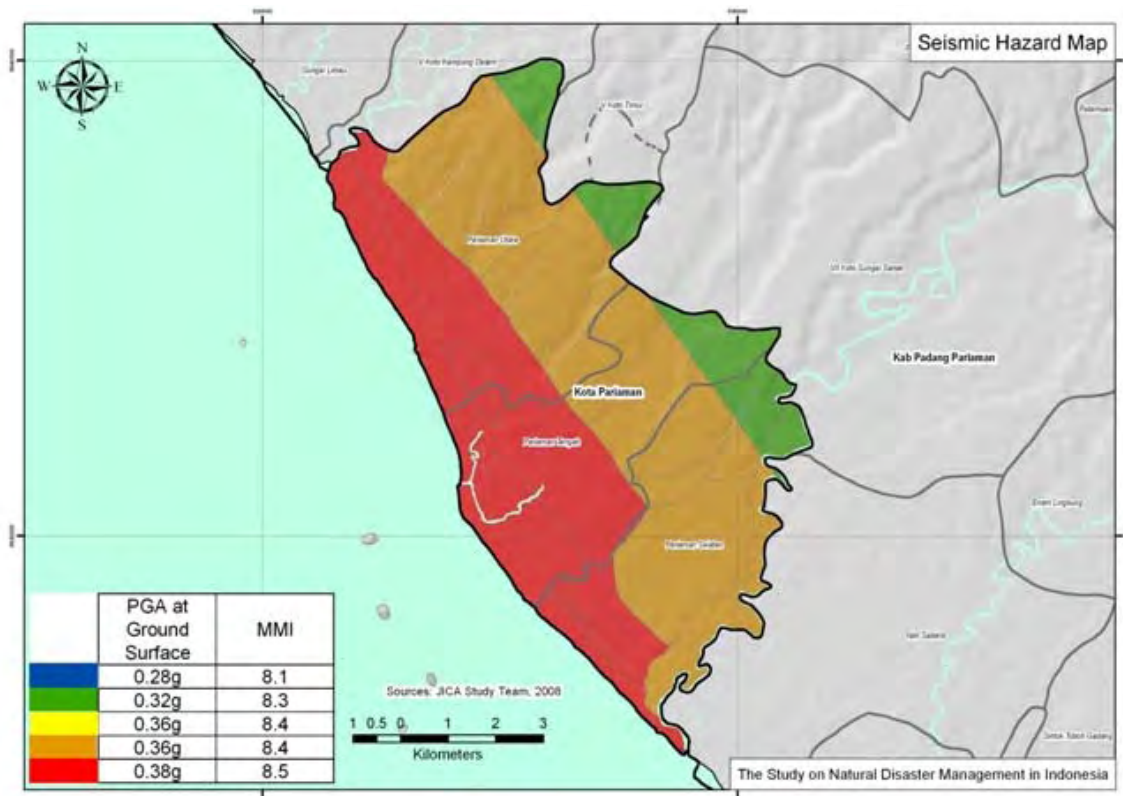
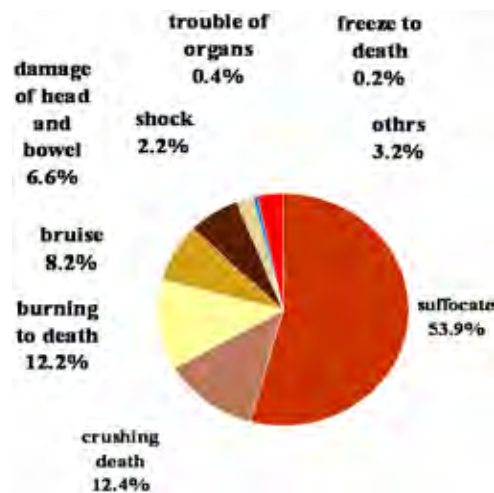


Figure 3.3.11 Expected Value Distribution of Ground Surface Tremor

### 3.3.3 Earthquake Risk Map in Kota Pariaman

#### 1) Basis of Risk Map Creation for Earthquake

Earthquake risk is an abstract concept by itself. So some definition or physical understanding must be supplied. Earthquake disaster risk is the possibility of destruction that can be analyzed as a synergistic result of earthquake hazard and vulnerability of a facility. Every aspect of the magnitude in earthquake disaster, including human loss and economical loss, can be evaluated based on structural destruction. In an actual disaster situation people are not killed by quake of ground but they are killed by collapsing of buildings. As shown in Figure 3.3.12 the majority cause of death in 1995 Great Hanshin Earthquake originated almost always in the collapse of the building. Therefore it can be said that it is indispensable to know how many buildings shall collapse when we discuss the risk of earthquakes.



**Figure 3.3.12 Ratio of the Cause of Death at 1995 Great Hanshin Earthquake**

Therefore Earthquake risk is defined as the damage ratio  $P$  under the condition of assumed ground motion and characteristics of the buildings. The damage ratio  $P$  is defined by Eq. 3.6.

$$P = \frac{N_D}{N_T} \quad (\text{Eq. 3.6})$$

Where,

$N_D$  : Number of damaged building

$N_T$  : Total number of existing building

In this context damaged buildings means the buildings that suffer equal or more “large damage” defined by Architectural Institute of Japan (AIJ). The damage grade “large damage” is strictly defined from the viewpoint of structure engineering. Generally dead and injured are generated in the buildings that suffer equal or more “large damage”. That is why this grade was chosen for the target of this evaluation. This grade is also similar to “Grade 4 Very Heavy Damage” of European Macroseismic Scale (EMS).

The damage ratio  $P$  is assessed by utilizing the fragility function. The outline of the fragility function analysis utilized in this study is shown in Figure 3.3.13.

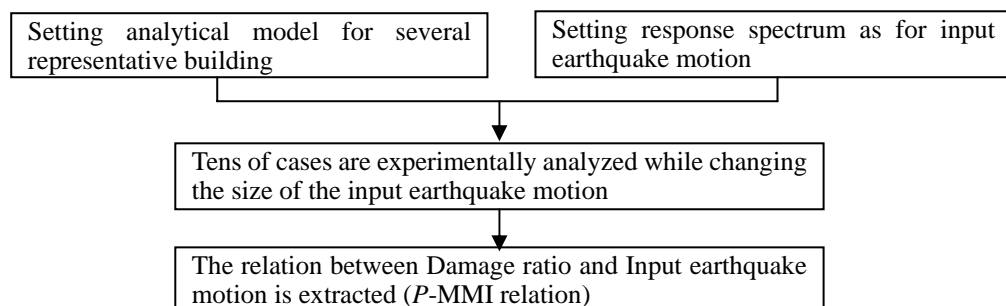


**Figure 3.3.13 Outline of Fragility Function Analysis**

The fragility function mainly depends on the characteristics of building structure. Therefore the buildings in the study area are divided into several building types and the typical building of each building type is modeled. Outline of building model is shown in Figure 3.3.14.

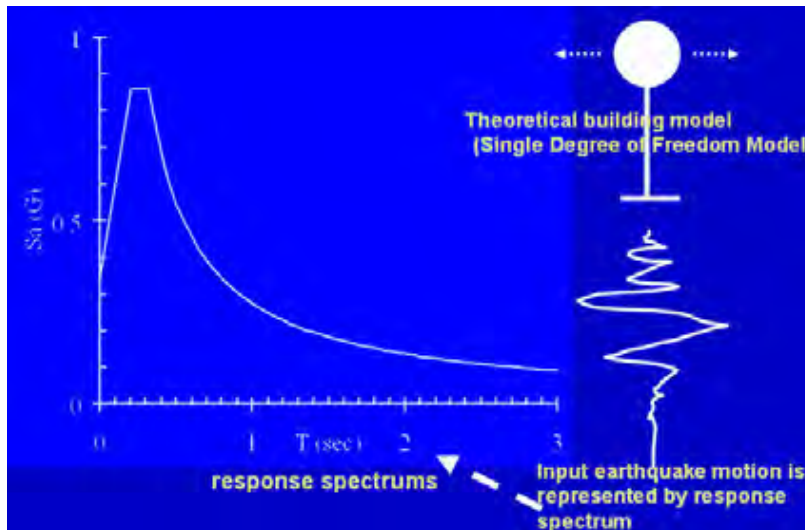


**Figure 3.3.14 Outline of Building Model**

Then a simplified dynamic analysis is carried out applying increasing earthquake input motion step by step. Then the relationship between MMI and the damage ratio  $P$  is obtained as a fragility function. The procedure to generate the relationship between MMI and the damage ratio  $P$  is common to the procedure done by committee of Japanese government and US Project “HAZUS” (see Appendix of this report).

The highly probable result can not be obtained when the sensitivity of the fragility function does not fit real earthquake resistance of the buildings in a corresponding study area. In this study some steps of calibration were carried out applying consideration through the research report of past earthquake disasters that occurred near the study area. The example of Yogyakarta city (i.e, 27 May 2006 Yogya Earthquake  $M_w$  6.5) was a effective material to apply because a Japanese reconnaissance team reported the intensity of surface ground motion investigated through interview intended for the resident and some observation on damage state of the building in disaster area (Shiro Takada et. al “Strong Ground Motion and Lifeline Damage during the Java Jogjakarta Earthquake”).

The obtained relationship between MMI and the damage ratio  $P$  is shown in Figure 3.3.15. The fragility function is generated for each building type.

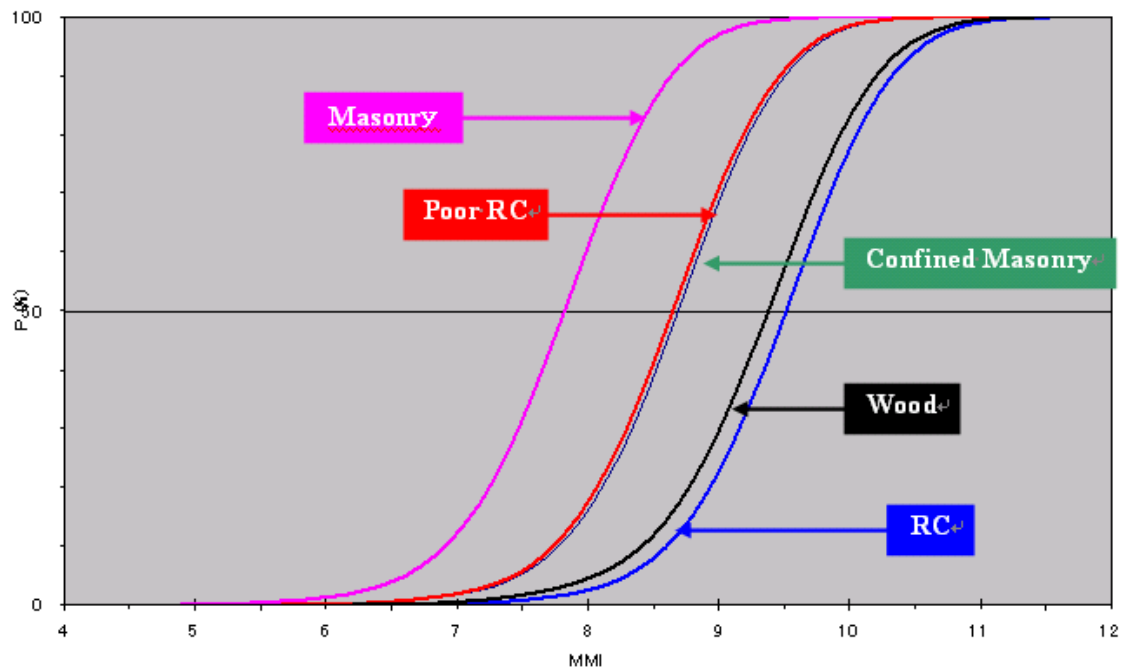


**Figure 3.3.15 Fragility Function (Relationship between MMI and the damage ratio P)**

On the other hand the damage example observed in Sumatra Island also needs to be referred. Therefore some report about 2004 Andaman earthquake and 2007 Solok earthquake were referred and it was confirmed that these observations do not contradict the fragility function.

In this report the hazard map shows the expected surface ground motion intensity of each point by MMI. So the value of the damage ratio  $P$  can be obtained by applying the fragility function and referring the value of MMI. By using a database and that indicates the number of each building type the expected number of damaged buildings can be calculated by multiplying existing building number and the damage ratio  $P$ .

If above estimation is carried out based on enough grounds

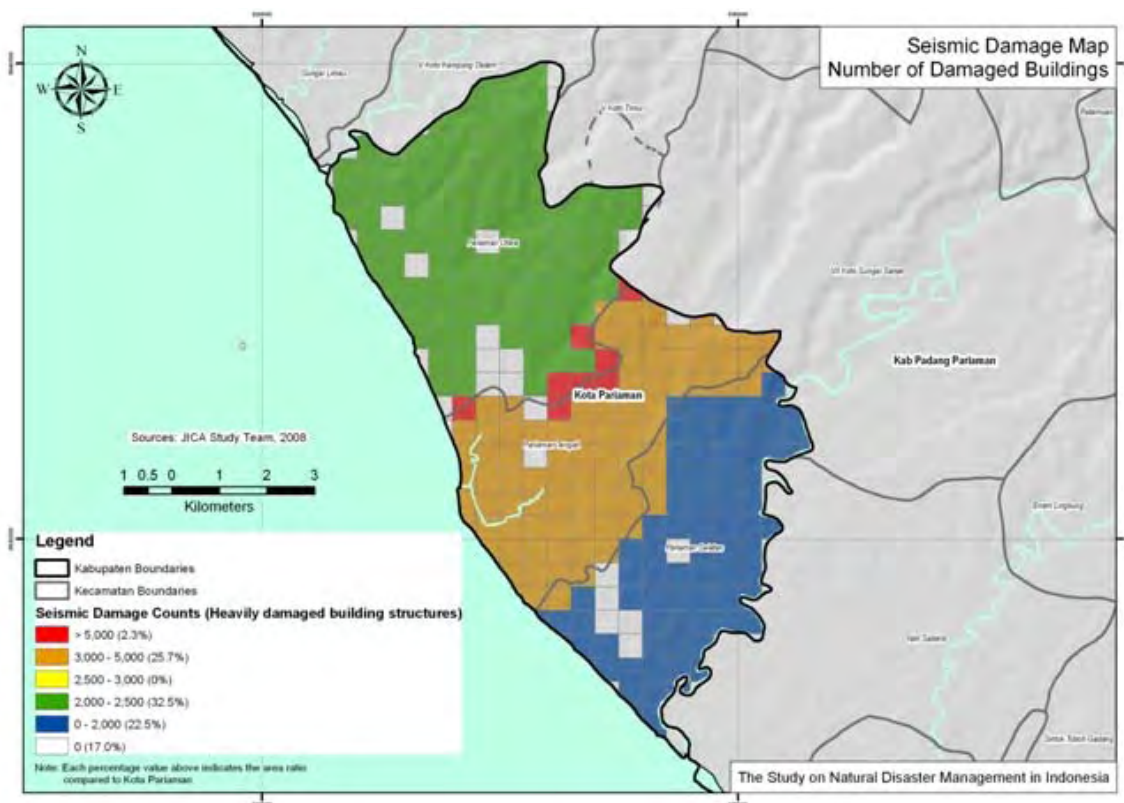
- It can be known how large project of building strengthening is needed for disaster mitigation view point
- Expected number of dead and injured at earthquake can be estimated and
- Scale of preparedness required for emergency aid can be estimated

However in this study, gaps in the database had to be filled by referring to some survey results and rough considerations because the database which was obtained now did not offer detailed information. The responsible Agency in Kota Pariaman has to implement the building census from the structural viewpoint and improve the database in the future.

## 2) Earthquake Risk Map in Kota Pariaman

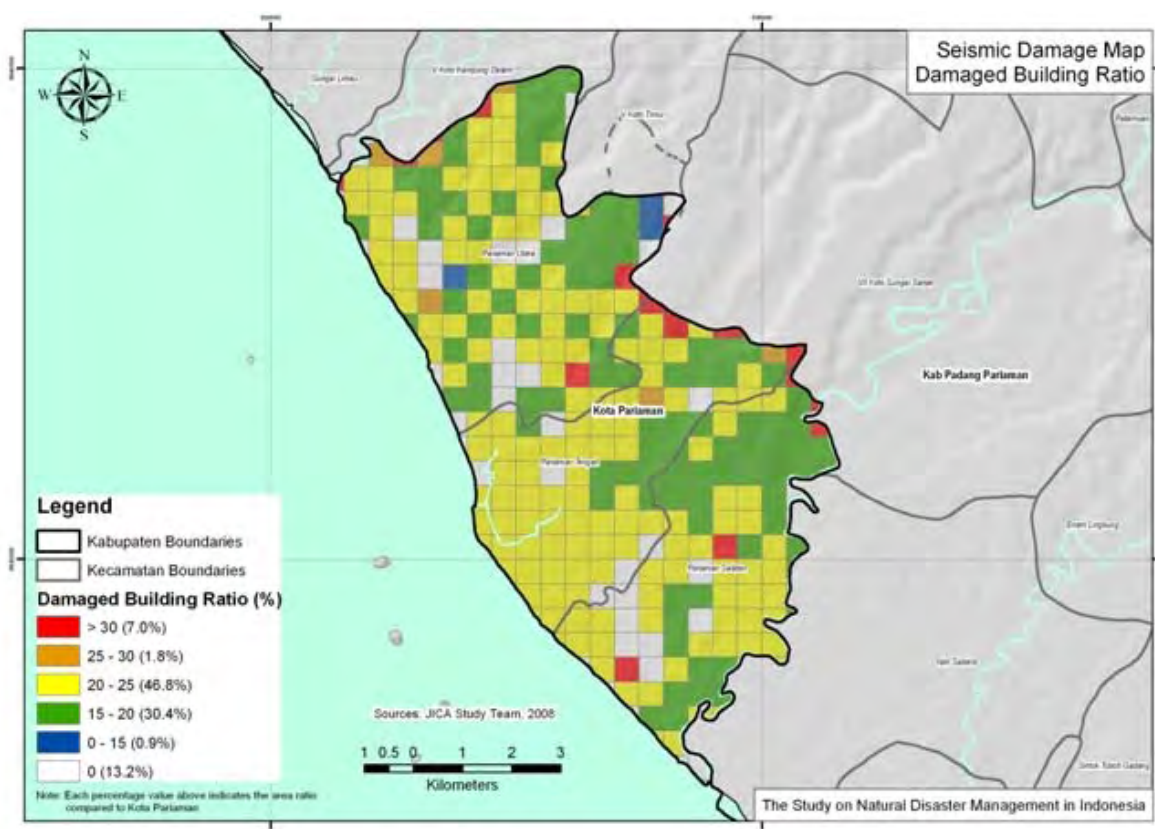
The intensity of surface ground motion differs according to the location. The vulnerability of the building also differs according to the building type. For instance the reinforced concrete building, which was designed and constructed through modern design concepts, is sustainable with 10% or less of damage ratio even if the intensity of surface ground motion is equal to MMI 8 or more but the unreinforced masonry building may suffer damage with near to 90% of damage ratio. There is some difficulty to wrap up the risk map to only one figure because of above situation.

Figure 3.3.16 shows the expected number of damaged buildings that are located in each grid square of 1km × 1km. The tendency of the distribution of damaged buildings that depends on vulnerability of existing buildings is shown. In a word there is high risk at the location where vulnerable buildings exist.



**Figure 3.3.16 Building Damage Per Grid**

Figure 3.3.17 shows the value of the expected number of damaged buildings divided by the total number of existing buildings that is located in each grid of 1km × 1km. This indicates the average damage ratio for each grid and thus it shows the tendency more clearly than previous Figure 3.3.16.



**Figure 3.3.17 Building Damage Ratio Per Grid**

It is felt strongly that the accuracy of building database is very important for this kind of study because above shown study results indicate that the difference of vulnerability in each building type is a dominant factor of damage distribution. The number of buildings in each grid is shown in Figure 3.3.18. The number of buildings in each survey unit and ratio of each building type is shown in Figure 3.3.19. These figures are presented in order to obtain an overview of the building data. Currently, the area of each survey unit is uneven. Some of them are corresponding to Kecamatan; some of them are corresponding to Nagari. Especially, the most northern survey unit is very large and built up areas are concentrated there. This kind of inconsistency of statistics data may skew the analysis. This is the reason why effort of data collection must be continued and improved.

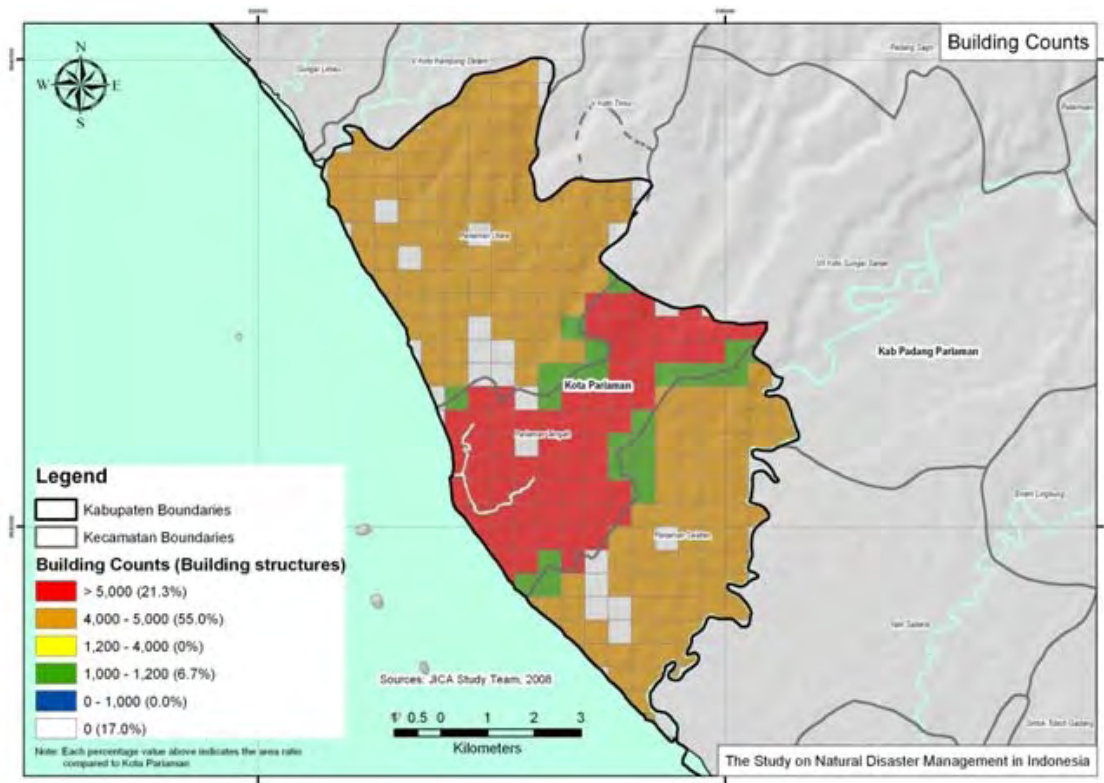


Figure 3.3.18 Number of Buildings in Each Grid

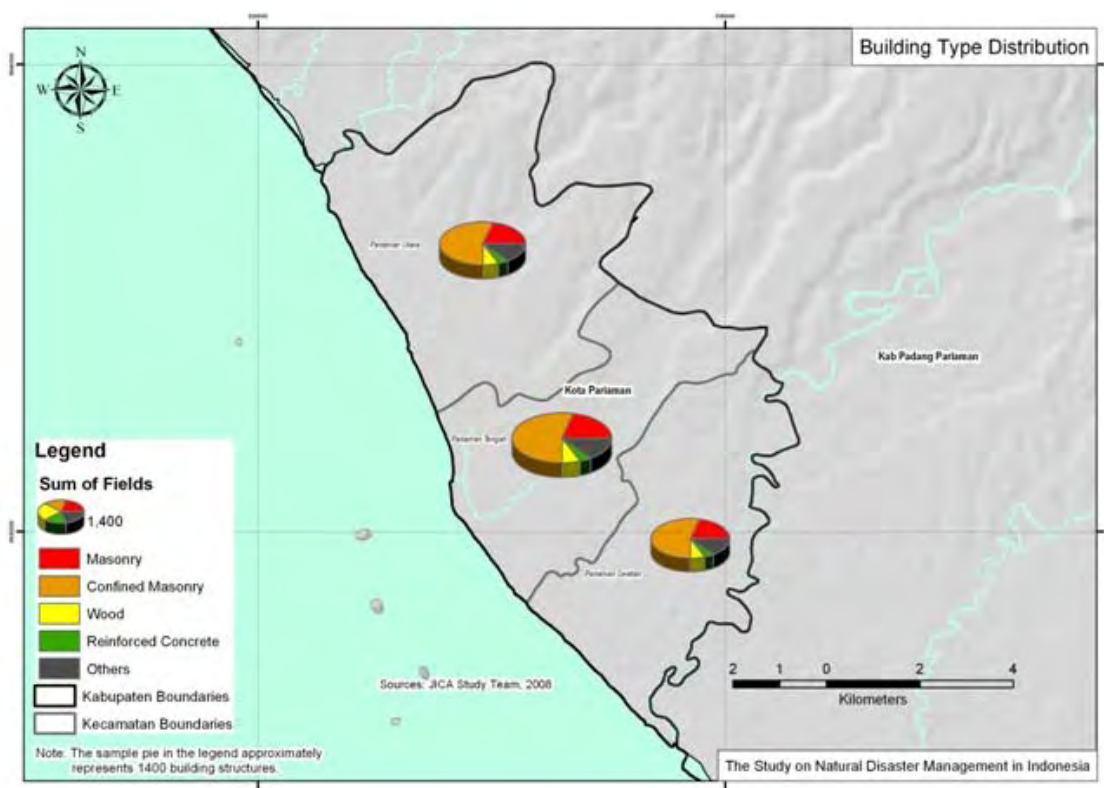


Figure 3.3.19 Number of Buildings in Each Survey Unit and Ratio of Each Building Type

There are some common points of building structure and distribution of building type in Indonesia. Aspect of building construction method and its variety are discussed below.

**(1) Timber made and Bamboo made**

This is a comparatively old type of construction method. There are some 100-year old buildings of this type in study area. Two types of structure are found: one is dressed timber made or elemental bamboo made frame structure, and the other consists of column and wall made of slim wood strings or bamboo strings grouted with lime or mortar. There are several types of structure detail according to the region. Earthquake resistant capacity of these buildings is generally better than masonry and Confined masonry but many examples with badly designed or deteriorated condition are found.



**a)** timber made frame

**b)** column and wall made of slim wood strings or bamboo strings grouted with lime

**Figure 3.3.20 Timber Made and Bamboo Made**

**(2) Brick Masonry**

The bearing wall thickness of most of brick masonry in this area is as much as one brick. Matters which should be obeyed on masonry construction are hardly paid attention to. There are problem of quality of brick and grout in many cases.



**Figure 3.3.21 Brick Masonry**

**(3) Cobble masonry**

There are many cobble masonry buildings in the area far from the main street. Earthquake resistant capacity of this type is very poor because of lack in grip effect between each cobble and poor quality of grout.



**Figure 3.3.22 Cobble Masonry**

**(4) Confined masonry**

This building type is becoming the major type in recent years. Regarding confined masonry bearing wall itself resists against load. RC made column, beam and lintel only give confinement effect to bearing wall. This is the difference between confined masonry and RC frame. Dimension of RC made members of confined masonry is smaller than that of RC frame. Earthquake resistant capacity of this type is better than unreinforced masonry but considerably poorer than RC frame with modern design concepts.



**Figure 3.3.23 Confined Masonry**

**(5) Reinforced Concrete Moment Resisting Frame**

Buildings of Reinforced Concrete Moment Resisting Frame (RCMRF) resist against load by its frame consisting of column and beam although its appearance is similar to confined masonry.

Wall of most RCMRF buildings in this study area are made of brick. This kind of wall can not be a bearing wall, they are partition walls, because brick wall may lose its stiffness when the frame is deformed by inertia force caused by earthquake. Of course the wall can resist against inertia force caused by earthquake if it consists of Reinforced Concrete Shear Wall but effective shear walls can rarely be seen in this study area.



**Figure 3.3.24 Reinforced Concrete Moment Resisting Frame**

**(6) Combination of different kind construction method**

There are many buildings with combination of different kinds construction methods in this study area. Different kind construction methods tend to be applied when the building is extended after some time interval. Serious destruction can start at the boundary of this kind combination when earthquake hits as was seen in examples damaged during 2007 Solok earthquake.



**Figure 3.3.25 Combination of Different Kinds of Construction Methods**

The following situation is seen in study area regarding building distribution.

**(1) Building density**

Most buildings are concentrated in very limited area and other area is less-populated. Generally speaking this tendency works advantageously during earthquake damage because interference between neighboring buildings under quake phenomenon does not happen easily. Empty space can be found to use as an urgent support center easily after an earthquake.

**(2) Building Type**

Comparatively modern building types like as RCMRF or confined masonry are dominated in main street, on the other hand, old building type like as masonry, timber made and combination of different kind construction method exceed modern building types in the area far from main street. Especially cobble masonry, which can be seen a lot in the area far from main street does not have sufficient earthquake resistant capacity.

**(3) Comparatively modern and old**

Confined Masonry building is becoming the major type in recent years. It is thought that this type of construction method can achieve almost sufficient earthquake resistant capacity if it is designed and constructed in a careful manner. At least it has greater capacity than stone masonry or brick unreinforced masonry. It is close to RC building capacity even though it is not equal. Actually some researchers offer the results of experiment and instructional books in order to obtain structural capacity. However there can be found a lot of examples that were constructed without sufficient attention in this study area.

The following points are found frequently:

- Bricks are not soaked in water before piling up (Sufficient water is needed for the hydration reaction of cement in grout)
- Situations in which a building is seen as a whole load path system are not present
- Opening in bearing wall is excessively large
- Dimension of confinement members is not sufficient
- Detail of reinforcing bar is not sufficient
- Compaction of concrete is not sufficient
- Inadequate aggregate (pumice stone)
- Stiffness and bearing capacity of foundation is not sufficient

### 3.3.4 Possible Countermeasures against Earthquake in Kota Pariaman

#### 1) Structure measure

Only strengthening of structure done beforehand is effective to mitigate human damage because structural damage due to earthquake occurs quite suddenly, and we can not prepare any effective warning system. Any effort done after earthquake can not be effective to reduce the number of human lives lost. Rescue activity and supporting activity have to be done after earthquake occurrence but those efforts hardly reduce lives lost.

Strengthening measure are as follows:

#### (4) Consolidate building permission and supervising system

In many cases individually owned buildings are not built by a specialist, but rather by inexperienced amateurs or workmen who did not pass professional instruction.

Building permitting and supervising system was established already but not necessarily all permits were applied for. There have been a lot of application leakages. Even for investigation on structural issues is generally loose. In addition most buildings are usually built without any public supervision. If these defects are not going to be solved, every earthquake with considerable size may cause a large number of casualties.

#### (5) Consolidate diagnosis system for existing building

#### (6) Encourage earthquake strengthening in existing building

There can not be the concept of “Existing nonqualified building” because building permission and supervising system is not functioning currently. However existing weak buildings have to be reconstructed if they are evaluated as “nonqualified” through the diagnosis. If it is not possible to reconstruct every building the next best thing to do is to strengthen existing buildings. The fundamental principle of strengthening is to specify the weak point of the building and to improve capacity of that weak point. Dominant weak points found in this study area are as follows:

#### A. Rigidity shortage of roof and floor

There can be seen many one story buildings, which do not have any lintel or roof slab, in this study area. As a result that building does not have sufficient rigidity in roof level so collapse because of twisting motion during earthquake is likely. As countermeasures, additional lintel or additional roof slab had better be set up.



**Figure 3.3.26 Building with no Lintel and Roof Slab**

**B. Capacity shortage of brick masonry wall**

Brick masonry wall is weak to force in an out-of-plane direction.

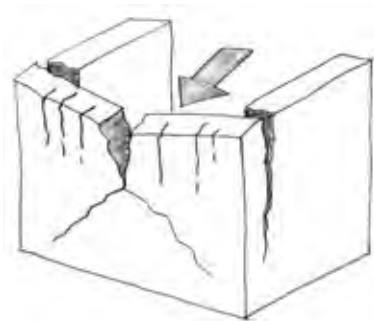


**Figure 3.3.27 Destruction by Force in Out-of-Plane Direction**

Many kind of reinforcement methods are proposed to prevent this type destruction. For instance, it is reported that reinforcement using meshed steel wire and cement mortar is effective as measures. However brick column or brick wall with small cross section can not have sufficient bearing capacity. This kind of member have to be changed to reinforce the concrete member.

**C. Defect of connection part of combined building**

Serious kind of destruction can start at connection part of combined building.



**Figure 3.3.28 Example of Connection Part**

Even if the different kinds of construction method are connected, the shape of each single construction part must be completed. However some kind of unfit end tends to be left at the connecting part. That kind of unfit may generate extraordinary concentration of force that causes decay. Demolishing and reconstruction is recommended when the effect of unfit shape is serious.

**(7) Encouragement of rebuilding**

Effort to make a financing system of the earthquake strengthening construction capital should be made for people who have a concrete plan of earthquake strengthening construction.

**(8) Education regarding earthquake resistance of building**

**2) Non structural measure**

It is not possible to reduce human casualties by implementing non structural measures but still it is beneficial to make advance preparations toward emergency rescue, life support and relief. The preparation for that is as follows:

- (1) Securing temporary shelter place**
- (2) Preparing and Stock materials in emergency**
- (3) Mutual support agreement with the administrative organization in the vicinity**
- (4) Establishment Cooperation method with disaster prevention organization of central government**
- (5) Establishment of Post-Earthquake Temporary Risk Evaluation system**
- (6) Educate and hold drills for the organizations and the residents in the region**

**【Chapter 3 Appendix】**

# **Fragility Function**

# Table of Contents

CHAPTER 1	OUTLINE.....	1
1.1	SIGNIFICANCE OF FRAGILITY FUNCTION.....	1
1.2	HOW TO APPLY THE RESULT OF FRAGILITY FUNCTION.....	1
CHAPTER 2	METHODOLOGY .....	2
2.1	FRAGILITY FUNCTION BASED ON SPECTRAL DISPLACEMENT .....	2
2.1.1	Basic formula.....	2
2.1.2	Spectral Displacement Sd .....	4
2.1.3	Threshold Value .....	8
2.2	RELATIONSHIP BETWEEN RESPONSE SPECTRUM INTENSITY AND MMI..	8
CHAPTER 3	PARAMETER SETTING.....	9
3.1	BASIC POLICY .....	9
3.1.1	Basic procedure.....	9
3.1.2	Procedure of Calibration .....	9
3.2	PARAMETER AND CALIBRATION.....	9
3.2.1	Response spectrum .....	9
3.2.2	Parameter .....	12
3.3	CALIBRATION.....	13
CHAPTER 4	FRAGILITY FUNCTION FOR DAMAGE ESTIMATION.....	15
Table 3.2.1	Parameters set for each individual building type .....	12
Table 3.3.1	Assessed IJMA.....	13
Table 3.3.2	Control Points Set for Calibration.....	14
Figure 2.1.1	Multi Degrees-of-Freedom Model .....	4
Figure 2.1.2	Schematic Drawing of Capacity Spectrum .....	5
Figure 3.2.1	Response Spectrums of Indonesian Standard concerning Seismic Load SNI 03-1726-2002.....	10
Figure 3.2.2	Zone Map Corresponding each Response Spectrum.....	11
Figure 3.3.1	Survey point .....	13
Figure 3.3.2	Result of Calibration .....	15
Figure 4.1.1	Fragility Function for Damage Estimation.....	15

## CHAPTER 1 OUTLINE

### 1.1 Significance of Fragility Function

First of all, explaining in this paragraph is logic concerning the seismic damage. Specific attention must be paid if the logic in this paragraph is applied to the disasters other than the seismic damage.

In general, it is abundant learning to the experience of the person who lives long in the region and the experience can be basic to think about disaster prevention. However this principle does not often consist about the earthquake disaster because the return period of the earthquake is longer than the length of person's life, it is dissatisfied only with experience in the limited region. Systematic result observed for a longer period and consideration on plate tectonics can become effective to take the place of experience in limited generation.

For the next step of understanding, it is demanded to know the level of damage caused by predicted earthquake motion. It is necessary to know whether our towns are strong enough from the viewpoint of the earthquake disaster prevention. If our towns are not strong enough, next question is what happens because of the predicted earthquake motion. The fragility function is the tool that can answer this demand. We can estimate how many buildings may be destructed and their damage level.

From the viewpoint of emergency assistance, it is necessary to know the total amount of urgent support after the earthquake has happened. If the number of collapsing buildings is presumed we can assess the number of death the number of people, who need urgent medical treatments, the number of people, who need material mobilization, and the number of needed shelter. If the total amount of urgent support exceeds the urgent support ability of related administrative body it is necessary to perform the effort to shorten the difference between them.

### 1.2 How to Apply the Result of Fragility Function

The Fragility Function is expressed as “Relation between damage ratio  $P$  and earthquake motion strength  $MMI$ ” in the main report. The damage rate  $P$  is given in Eq. (1.2.1).

$$P = \frac{N_D}{N_T} \quad (1.2.1)$$

Where,

$N_D$  : Number of damaged buildings in corresponding area

$N_T$  : Total number of buildings in corresponding area

The targeted damage grade in this paragraph is the damage grade, which exceeds the damage grade defined as “Very Heavy Damage” by Architectural Institute of Japan (AIJ). AIJ strictly defines the damage grade from a structural engineering viewpoint.<sup>1</sup> Casualties are generated in the building

---

<sup>1</sup> “Very Heavy Damage” defined by AIJ is similar to G4 defined by European Macroseismic Scale (EMS)

where the destruction of this damage grade or more is caused. This is the reason why this damage grade is targeted in this study.

Damage ratio  $P$  is evaluated for divided each building type.

Modified Mercalli Intensity MMI is a international expression of the earthquake motion strength at ground surface. This seismic intensity scale was defined as 12 stage evaluation referring incident, which the people observed and felt at quake induced field (“Difficult to stand” etc.). In this study the MMI map is shown as a hazard map. Therefore damage level at each area of Jember can be recognized when MMI value of corresponding area is referred and damage ratio  $P$  is read from fragility function.

The number of damaged building in each area can be calculated by multiplying the number of each building type and the value of damage ratio  $P$  if a database, in which the number of each building type in that area, is prepared. However that kind of database was not obtained in Jember. The execution of Building Census is a task which the administrative body of Jember should be going to do in the future.

Operation scale of building strengthening needed from the view point of disaster mitigation and the total amount of urgent support after the earthquake is clarified when above calculation is carried out.

## CHAPTER 2 METHODOLOGY

### 2.1 Fragility Function Based on Spectral Displacement

#### 2.1.1 Basic formula

It was described that the *Fragility Function* is expressed as Relation between damage ratio  $P$  and earthquake motion strength MMI in the main report. However this relationship can not be clarified directly. It is necessary to execute several step of structural engineering deduction work in order to obtain it. The first step of deduction work is to define fragility function based on spectral displacement.

Damage ratio  $P$  is given as the cumulative lognormal distribution in which the spectral displacement is assumed to be a probability variable. Basic formula is shown in Eq. (2.1.1).

$$P[D \geq d_s S_d] = \Phi \left[ \frac{\ln S_d - \lambda}{\beta_{ds}} \right] \quad (2.1.1)$$

Where,

$P[D \geq d_s S_d]$  : It means probability of that the damage state of the building  $D$  corresponds to under  $d_s$  when paying attention to spectral displacement  $S_d$

$S_d$  : Spectral displacement

$\lambda$  : Logarithm of median of displacement  $S_d$  to damage state  $d_s$  (It is defined in Eq. (2.1.1) )

$$\lambda = \ln(S_{dm}) \quad (2.1.2)$$

$S_{dm}$  : Median of spectral displacement  $S_d$  to damage state  $d_s$   
(Median is defined as the value in which the probability of exceedence becomes equal with non-exceeding probability i.e. cumulative distribution equal with 50%)

$\beta_{ds}$  : Standard deviation of logarithm of the spectral displacement  $S_d$  to damage state  $d_s$ .

$\Phi$  : Operational calculus for obtaining the cumulative standard normal distribution

According to above definition, damage ratio  $P$  is obtained by substituting the spectral displacement  $S_d$  to Eq. (2.1.1). The spectral displacement  $S_d$  is calculated utilizing a building model explained in the next section. The value of  $S_{dm}$  and  $\beta_{ds}$  are also explained in following section.

The calculation expressed as a operational calculus of  $\Phi$  is explained as follows.

When the variables included in the contents of operational calculus  $\left[ \frac{\ln S_d - \lambda}{\beta_{ds}} \right]$  are converted as follows standardization variable  $z$  is given by Eq. (2.1.3).

$$\begin{aligned} \ln S_d &\rightarrow x \\ \lambda &\rightarrow \bar{x} \\ \beta_{ds} &\rightarrow \sigma \\ z &= \frac{x - \bar{x}}{\sigma} \end{aligned} \quad (2.1.3)$$

The cumulative distribution  $P(x)$  is defined as Eq. (2.1.4).

$$P(x) = \frac{1}{\sqrt{2\pi}} \int_{-\infty}^{\frac{x-\bar{x}}{\sigma}} \exp\left\{-\frac{z^2}{2}\right\} dz \quad (2.1.4)$$

Where,

$P(x)$  : Cumulative distribution

$\bar{x}$  : Average

$\sigma$  : Standard deviation

Then the cumulative distribution can not be obtained by computation on paper because that needs integration from  $-\infty$  to corresponding  $x$ . However a complementary error function is prepared as a intrinsic function in the computer software EXCEL and some programming tool (Fortran compiler

etc.). If these functions are used, the cumulative distribution is operated in the business without trouble.

## 2.1.2 Spectral Displacement $S_d$

### 1) Building Model

The spectral displacement  $S_d$  can be obtained when the dynamic analysis model is set and the response spectrum is utilized. Then, a multi degrees-of-freedom model shown in Figure 2.1.1 is set for each building type as a dynamic analysis model.

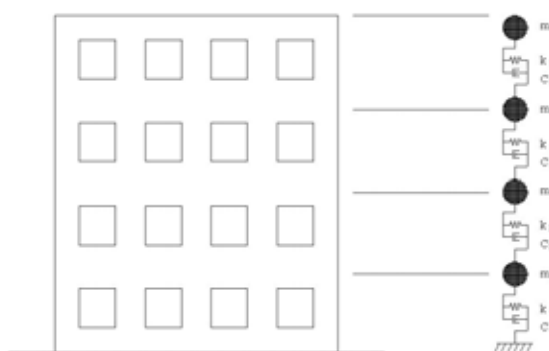


**Figure 2.1.1 Multi Degrees-of-Freedom Model**

This kind of model is usually set as a dynamic analysis model for building earthquake resistance design and represents the mass and stiffness of each floor in a building (This model is not necessary for single story building but it is indispensable when a multi story building is discussed).

Eigenvalue (ie. fundamental period and eigen vector) is obtained by carrying out eigenvalue analysis using the building model. Eigenvalue is solutions, which satisfy Eq. (2.1.5) and of the same number as degrees-of-freedom of the model.

$$([K] - \omega^2 [M])\{\phi\} = \{0\} \quad (2.1.5)$$

Where,

$[K]$  : Stiffness matrix composed by the stiffness of each story in the model

$[M]$  : Mass matrix composed by the mass of each story in the model

$\{\phi\}$  : Eigen vector

$\omega$  : Angular velocity defined in Eq. (2.1.6)

$$\omega = 2\pi f = \frac{2\pi}{T} \quad (2.1.6)$$

$f$  : Natural frequency

$T$  : Natural period

For the above defined stiffness matrix, the following assumption is set.

In general, dimension of the columns in lower story is larger than that of the columns in upper story so that the stiffness of the columns becomes going below stiff.

Then, it is assumed that the stiffness of  $N^{\text{th}}$  story from top of the model building is calculated by Eq. (2.1.7).

$$k_N = N^I \cdot k_1 \quad (2.1.7)$$

Where,

$K_N$  : Stiffness of  $N^{\text{th}}$  story from top of the model building

$N$  : Total number of stories

$I$  : Index

When  $I$  is 0.0, the stiffness of the each story becomes equal.

When  $I$  is 1.0, the story drift induced by inertia force distributed evenly over each story becomes equal

0.5 is applied for  $I$  value in this study.

$K_1$  : Stiffness of the top story

## 2) Capacity Spectrum

### (1) Concept of Capacity Spectrum

The building model explained in the foregoing section is replaced with the capacity spectrum shown in Figure 2.1.2.

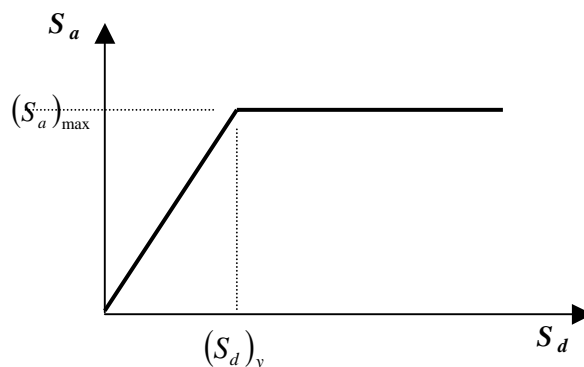


**Figure 2.1.2 Schematic Drawing of Capacity Spectrum**

The capacity spectrum express characteristics of single degree of freedom (SDOF) model (ie. dynamic analysis model). Therefore it represents a component, which affects the fundamental mode of the multi degrees-of-freedom model. The vertical axis of the capacity spectrum shows spectral acceleration  $S_a$ , the horizontal axis shows spectral displacement  $S_d$ . it is assumed that characteristics keeps elastic behavior before yield displacement  $(S_d)_y$ , and it keeps flat line of capacity acceleration  $(S_a)_{\text{max}}$  after  $(S_d)_y$ .

**(2) Capacity Acceleration ( $S_a$ ) max**

The capacity acceleration  $(S_a)_{max}$  is given by Eq. (2.1.8).

$$(S_a)_{max} = \left( \frac{V}{W} \right) \cdot \frac{G}{\alpha_1} \quad (2.1.8)$$

Where,

$(S_a)_{max}$  : Capacity acceleration

$\left( \frac{V}{W} \right)$  : Ratio of horizontal seismic load to weight

$G$  : Acceleration of gravity

$\alpha_1$  : Effective mass ratio of fundamental mode

Effective mass ratio of fundamental mode  $\alpha_1$  is given by Eq. (2.1.9) (The value of  $\alpha_1$  for single story building is 1.0).

$$\alpha_1 = \frac{M_{x1}}{\sum m_n} \quad (2.1.9)$$

Where,

$M_{x1}$  : Effective mass of fundamental mode

$\sum m_n$  : Total mass

The ratio of horizontal seismic load to weight  $\left( \frac{V}{W} \right)$  is given by Eq. (2.1.10).

$$\left( \frac{V}{W} \right)_i = C_i \cdot \gamma_i \cdot \lambda_i \quad (2.1.10)$$

Where,

$C_i$  : Design coefficient of earthquake intensity

$\gamma_i$  : Over strength factor relating “true” yield strength to design strength

$\lambda_i$  : Over strength factor relating “ultimate” strength to yield strength

(Subscript represents building type.)

$C_i$  corresponds to the coefficient called *base shear coefficient* in general analysis of building design. Over strength factor is set  $\gamma_i=1.5$ ,  $\lambda_i=3.0$  in this study according to technological consideration. The value of  $C_i$  is set for the building type thought that design with frame analysis was done. The value of  $\left( \frac{V}{W} \right)$  is set for the building type thought that conventional design

without modern analysis was done. In addition, some calibration is needed while referring to some past observations of real earthquake disaster.

**(3) Yield Displacement ( $S_d$ )<sub>y</sub> is given by Eq. (2.1.11).**

$$(S_d)_y = \frac{D_y}{F_p \cdot \frac{\phi_{top}}{\sum H}} \quad (2.1.11)$$

Where,

$D_y$  : Yield story drift ratio

$\phi_{top}$  : Eigen vector of building top

$\sum H$  : Total height of building

$F_p$  : Participation factor of first mode

**(4) Spectral Displacement  $S_d$**

When the acceleration response spectrum is prepared as a condition of input earthquake motion the *spectral acceleration* ( $S_a$ )<sub>l</sub> can be read on the value of vertical axis corresponds to the horizontal axis  $T$  of that spectrum. Pseudo-displacement ( $S_d$ )<sub>l</sub> is given by Eq. (2.1.12).

$$(S_d)_l = (S_a)_l \cdot \left( \frac{T}{2\pi} \right)^2 \quad (2.1.12)$$

Where,

( $S_a$ )<sub>l</sub> : Spectral acceleration depending on the elasticity assumption

( $S_d$ )<sub>l</sub> : Spectral displacement depending on the elasticity assumption

$T$  : Fundamental period of the capacity spectrum given by Eq. (2.1.13)

$$T = 2\pi \sqrt{\frac{(S_d)_y}{(S_a)_{\max}}} \quad (2.1.13)$$

Spectral displacement  $S_d$  is given by Eq. (2.1.14) as a elasto-plastic solution.

$$\left. \begin{aligned} S_d &= (S_d)_l && \text{when } (S_d)_l \leq (S_d)_y \\ S_d &= \frac{(S_d)_l^2 + (S_d)_y^2}{2(S_d)_y} && \text{when } (S_d)_l > (S_d)_y \end{aligned} \right\} \quad (2.1.14)$$

Where,

( $S_d$ )<sub>l</sub> : Spectral displacement depending on the elasticity assumption

( $S_d$ )<sub>y</sub> : Spectral yield Displacement

### 2.1.3 Threshold Value

Damage which building suffers is evaluated by comparing the *Spectral displacement*  $S_d$  and the *Median of spectral displacement*  $S_d$  corresponds damage state  $d_s$   $S_{dm}$ . The value of  $S_{dm}$  is called the threshold value. The each specific value of  $S_{dm}$  is given for each building type. The value of  $S_{dm}$  is given by Eq. (2.1.15) based on the story drift in the building.

$$S_{dm} = \frac{D_s}{F_p \cdot \left[ \frac{\phi_j - \phi_{j+1}}{H_j} \right]_{\max}} \quad (2.1.15)$$

Where,

$D_s$  : Story drift ratio corresponds damage state  $d_s$  “*Very Heavy Damage*”

$F_p$  : Participation factor of fundamental mode

$\phi_j$  : Eigen vector of  $j^{\text{th}}$  story

$H_j$  : Height of  $j^{\text{th}}$  story

## 2.2 Relationship between Response Spectrum Intensity and MMI

The relationship between the damage ratio  $P$  and the spectral displacement  $S_d$  was clarified in 2.1.1. then the damage ratio  $P$  can be given as a function which assumes the seismic intensity MMI to be a explanation variable.

Six pairs of the response spectrums of Indonesian standard concerning seismic load SNI 03-1726-2002 were used as input earthquake motion in this study. In general, response spectrum intensity at *fundamental period*  $T=0$  sec corresponds to maximum value of the acceleration (PGA ) of surface of the ground.

On the other hand the relationship between PGA and MMI is given by the regression formula shown in Eq. (2.2.1). Therefore relationship between the damage ratio  $P$  and MMI is related through PGA.

$$\log a = 0.014 + 0.3(MMI) \quad (2.2.1)$$

Where,

$a$  : maximum value of the acceleration (PGA ) of surface of the ground

The relationship between PGA and  $I_{JMA}$  (Japan Meteorological Agency Seismic Intensity Scale) is given by the regression formula shown in Eq. (2.2.2). Therefore relationship between the damage ratio  $P$  and  $I_{JMA}$  is related through PGA.

$$I_{JMA} = 0.55 + 1.90 \log(a) \quad (I = 4 \text{ to } 7) \quad (2.2.2)$$

## CHAPTER 3 PARAMETER SETTING

### 3.1 Basic policy

#### 3.1.1 Basic procedure

The following parameters are set to set fragility function based on the spectral displacement,.

- *Ratio of horizontal seismic load to weight*  $\left(\frac{V}{W}\right)$ , or a combination of *Design coefficient of earthquake intensity*  $C_i$  and *over strength factor*  $\gamma_i, \lambda_i$ .
- *Yield story drift ratio*  $D_y$
- *Height of each stories*  $H_j$
- *Story drift ratio corresponds damage state “Very Heavy Damage”*  $D_s$

Capacity Spectrum is generated utilizing the above parameters through the procedure described at 2.1.22). The spectral displacement  $S_d$  is calculated utilizing the Capacity Spectrum and the response spectrum. *Damage ratio*  $P$  is given through the relationship between the spectral displacement  $S_d$  and the threshold of “Very Heavy Damage”.

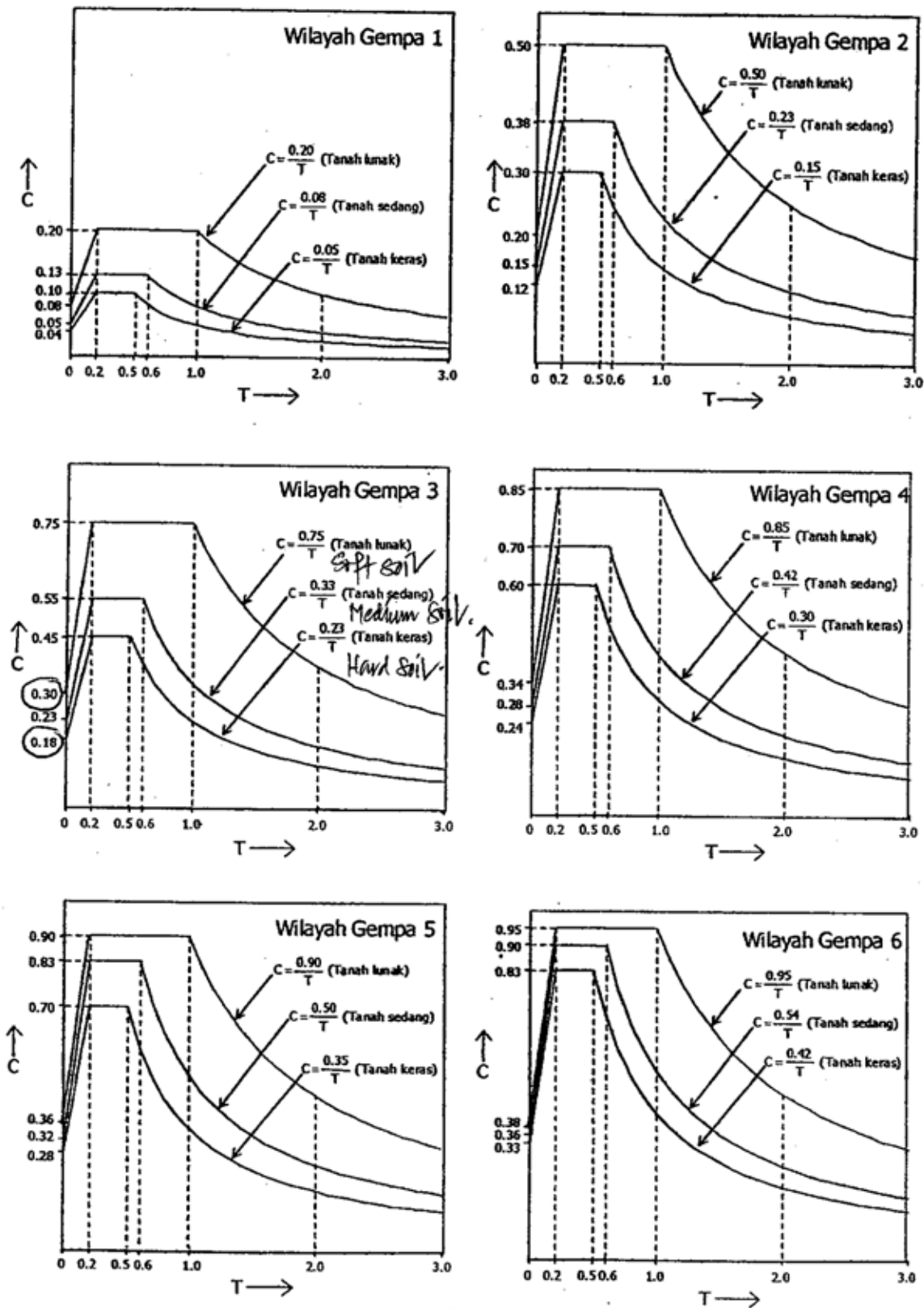
#### 3.1.2 Procedure of Calibration

Fragility Function is necessary to calibrated referring to the observation of the damage situation in the past earthquake disaster. However the earthquake disaster case in the past is not necessarily assessed with strict unit of earthquake motion. So refer to the summary here as a relation between  $I_{JMA}$  and the *damage ratio*  $P$ . The *damage ratio*  $P$  is calculated utilizing the procedure described in 3.1.1 while gradually changing the value of  $I_{JMA}$ . Previously assumed parameters are calibrated reoffering above result and the observation of the damage situation in the past earthquake disaster.

### 3.2 Parameter and Calibration

#### 3.2.1 Response spectrum

Six pairs of the response spectrums of Indonesian standard concerning seismic load SNI 03-1726-2002 were shown in . The zone map corresponding each response spectrum is shown in .



Gambar 2 Respons spektrum gempa rencana

Figure 3.2.1 Response Spectrums of Indonesian Standard concerning Seismic Load SNI 03-1726-2002

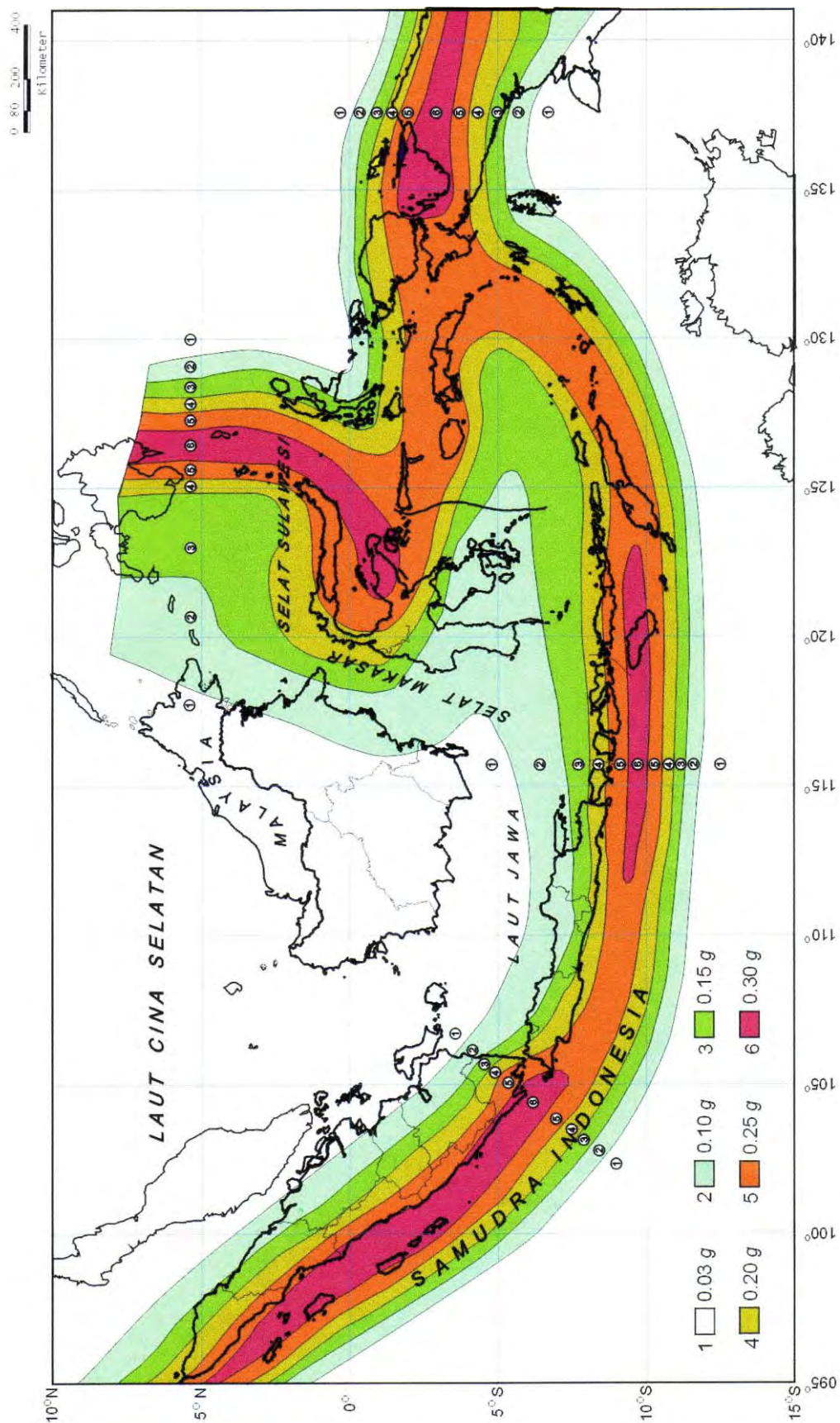


Figure 3.2.2 Zone Map Corresponding each Response Spectrum

The response spectrum in Figure 3.2.1 is composed of the following principle.

PGA value indicated in Figure 3.2.2 is maximum acceleration value at the surface of base rock of the deep underground. The acceleration is amplified by the surface layer and reaches the maximum value of the acceleration (PGA) of surface of the ground.

In general, response spectrum intensity at *fundamental period*  $T=0$  sec corresponds to the maximum value of the acceleration (PGA) of surface of the ground.

As shown in Figure 3.2.2 Jember is located in Zone 4. The maximum value of the acceleration (PGA) of surface of the ground is 0.24g for Hard Soil, 0.28g for Medium Soil and 0.34g for Soft Soil.

The response spectrum intensity between  $T = 0$  sec to  $T = 0.2$  sec is given as a value proportional at the fundamental period  $T$ .

The response spectrum intensity longer than  $T = 0.2$  sec is constant for a while. The maximum value 2.5 times PGA is indicated.

The response spectrum intensity in comparatively long period is given as a value in inverse proportion at the fundamental period  $T$ .

Considering the above mentioned principle a similar in principle a response spectrum form is set and the *damage ratio*  $P$  is calculated utilizing the procedure described in 3.1.1 while gradually changing the value of  $I_{MA}$ .

#### Parameter

The parameters set for each individual building type is shown in Table 3.2.1.

**Table 3.2.1 Parameters set for each individual building type**

Building Type	C	$\gamma$	$\lambda$	V/W	$D_y$	$H_i$ (m)	Fundamental Period (sec)	$D_s$
Confined Masonry	0.071	1.5	3.0	0.3195	1/400	2.25	0.266	1/66
Un-reinforced Masonry	0.039	1.5	3.0	0.1755	1/400	2.25	0.359	1/66
RC	0.1255	1.5	3.0	0.56475	1/400	2.25	0.200	1/66
Conventional RC	0.069	1.5	3.0	0.3105	1/400	2.25	0.270	1/66
Wood Bamboo	0.134	1.5	3.0	0.603	1/300	2.25	0.224	1/66



**Table 3.3.2 Control Points Set for Calibrationa**

		Good Quality		Poor Quality	
		JMAI	P	JMAI	P
Yogyakarta	Confined Masonry	5.5	45.0		
	Masonry	5.5	90		
	RC	5.1829298	2.2750132	5.5	50
	Wood	5.5	15.8655254		
	Bamboo	5.5			

Above control points are composed of the following principle.

- Damage ratio  $P$  of confined masonry to be 50% or less for  $I_{JMA} = 5.5$  assuming the description of Report No. 18900001 to be grounds.
- Damage ratio  $P$  of Masonry to be 90% for  $I_{JMA} = 5.5$  referring to the description that almost of masonry house buildings collapsed though it is in a limited area.
- Damage ratio  $P$  of Reinforced concrete to be 2.28% for  $I_{JMA} = 5.18$  because it is thought that the excellent one satisfies the building code, which is effective in a pertinent region.

As for above-mentioned grounds,

It is thought that  $I_{JMA}$  which will be set when designing corresponds to 5.18 because the PGA value 0.28g, which is read on the response spectrum for medium soil in the Zone 4 at  $T=0$  sec.

When *Index of Reliability*  $\beta$  is assumed to be 2.0, the cumulative failure probability of the structure which receives the seismic load equal with the design earthquake motion becomes 2.28%.

- Damage ratio  $P$  of RC buildings that quality is low was assumed as 50% in  $I_{JMA} 5.5$  which was the representative value of Jogjakarta area. It is thought that earthquake-resistances of RC buildings that quality is low is lower than that of Confined Masonry.

(The Story drift ratio corresponds damage state “Very Heavy Damage”  $D_s$  about above mentioned type was assumed as **1/400**.)

- Damage ratio  $P$  of Wood buildings was assumed as 15.9% in  $I_{JMA} 5.5$  which was the representative value of Jogjakarta area referring to the description that almost of wood house buildings did not collapse even if it is in a severely shaken area.
- When *Index of Reliability*  $\beta$  is assumed to be 1.0, the cumulative failure probability of the structure which receives the seismic load equal with the  $I_{JMA} 5.5$  which was the representative value of Jogjakarta becomes 15.9%. In a word, a value of  $\beta$ , which is reliability different from that of a building type with modern construction method, was set in wood buildings.

(The Story drift ratio corresponds damage state “Very Heavy Damage”  $D_s$  about wood buildings was assumed as **1/300**.)

Relation between damage ratio  $P$  and  $I_{JMA}$  obtained by the calculation which uses the control point and the control point itself is compared in Figure 3.3.2.

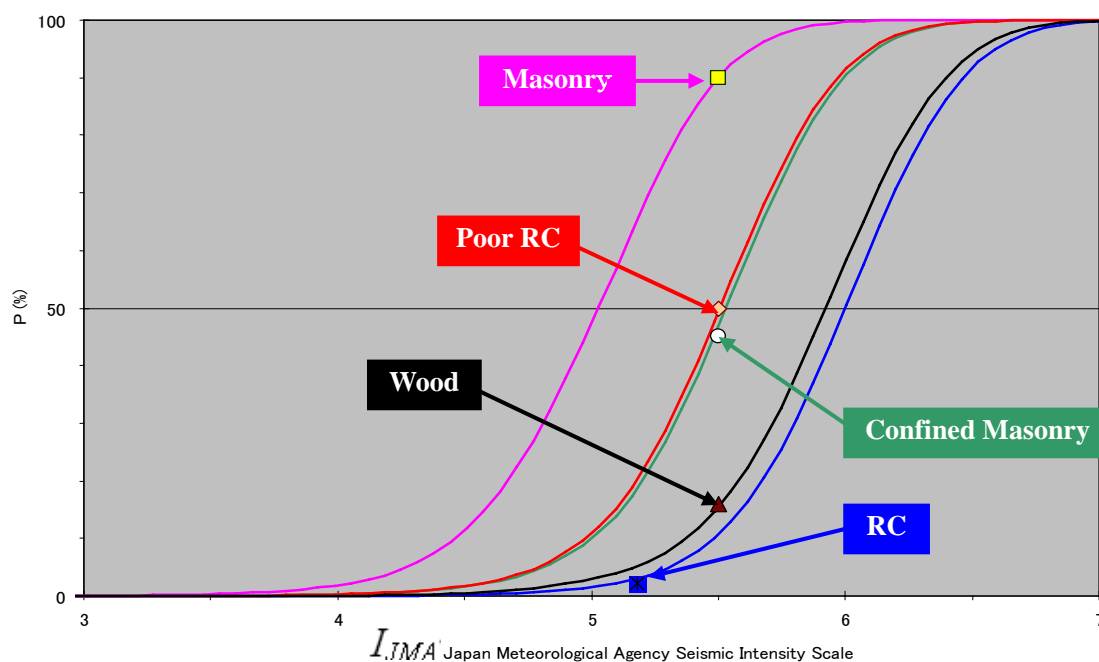


Figure 3.3.2 Result of Calibration

## CHAPTER 4 FRAGILITY FUNCTION FOR DAMAGE ESTIMATION

Relation between damage ratio  $P$  and MMI obtained by the calculation is shown in Figure 4.1.1.

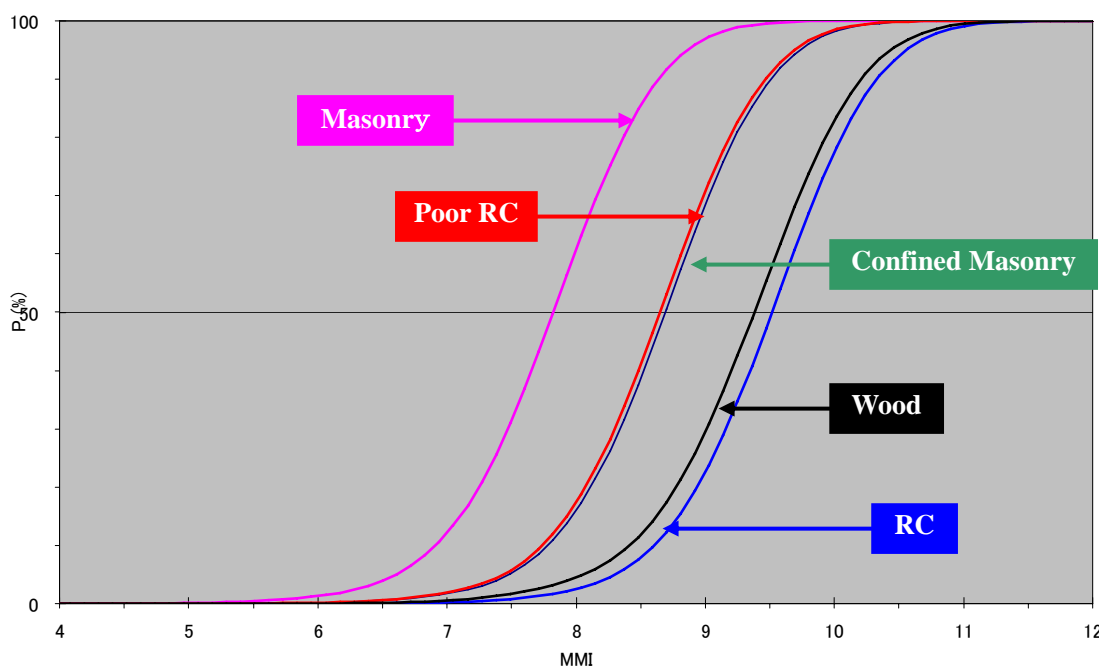


Figure 4.1.1 Fragility Function for Damage Estimation